Rellevància del TNF i l'esfingomielinasa àcida en la fibrogènesi hepàtica

Núria Tarrats Font

DEPARTAMENT DE MORT I PROLIFERACIÓ CEL·LULAR, IIBB-CSIC

UNIVERSITAT DE BARCELONA

RELLEVÀNCIA DEL TNF i L'ESFINGOMIELINASA ÀCIDA EN LA FIBROGÈNESI HEPÀTICA

Núria Tarrats Font

Barcelona 2012

OBJECTIUS

La fibrosi hepàtica és una afectació mèdica greu causada per l'acumulació excessiva de matriu extracel·lular. Els principals estímuls que condueixen a una fibrosi hepàtica són, entre d'altres, la infecció pels virus de l'hepatitis, el consum crònic d'alcohol o l'obstrucció biliar. Aquest dany, a través de múltiples vies, segons la etiologia, desencadenarà l'activació de vies de senyalització que conduiran cap a l'activació de les cèl·lules estrellades hepàtiques, la degeneració dels hepatòcits, i a la deposició de fibres de col·lagen que conduiran a un malfuncionament de l'òrgan.
El TNF és un dels mediadors inflamatoris més importants del nostre organisme, i és per això que és una de les principals citocines involucrades en la resposta al dany hepàtic. Altres citocines com el PDGF o el TGF-β, també implicades en la fibrosi hepàtica, estan ben caracteritzades. En el cas del TNF i els seus receptors, però, encara no s'ha descrit quin paper desenvolupen en el procés d'activació de les CEH i en el seu potencial fibrogènic tan *in vitro* com *in vivo*. Per aquest motiu, i perquè el rol anti- o pro-fibrogènic del TNF encara és un tema controvertit, el nostre primer objectiu va ser el següent:

OBJECTIU 1:

- Determinar el paper de TNF i els seus receptors, TNFR1 i TNFR2, en el procés de transdiferenciació de les CEH i quin paper desenvolupen en la fibrogènesi hepàtica.

L'esfingomielinasa àcida és la responsable de la hidròlisi d'esfingomielina per produir ceramida, un reconegut mediador de mort cel·lular, entre d'altres. A més, l'ASMasa ha estat implicada en varis processos cel·lulars, i s'ha descrit que TNF és capaç d'activar-la. Com que anteriorment al nostre grup s'havien relacionat les catepsines amb la fibrosi hepàtica, vam voler estudiar si l'esfingomielinasa àcida jugava algun paper important en el procés de transdiferenciació de les CEH i fibrogènesi a través de les catepsines. Per altre banda, està ben establert que la manca d'activitat ASMasa deguda a una mutació en el gen SPMD1 condueix a la malaltia de Niemann-Pick, que es caracteritza per una neurodegeneració primerenca i malaltia hepàtica principalment. Com que havíem establert una

relació directe entre l'ASMasa i la CtsB/D en la fibrosi hepàtica, vam voler estudiar si la inhibició d'aquesta via de senyalització podia contribuir a una millora en la malaltia hepàtica que pateixen els pacients d'aquesta malaltia. Per aquest motiu el següent objectiu plantejat va ser:

OBJECTIU 2:

- Estudiar la implicació de l'ASMasa en el procés de transdiferenciació de les CEH i la fibrogènesi hepàtica així com el seu paper en la malaltia hepàtica d'un fenotip Niemann-Pick tipus A.

RESULTATS

Els resultats obtinguts durant aquests quatre anys d'estudis pre-doctorals han donat lloc a tres articles, publicats en revistes internacionals indexades, dels quals sóc primera autora en dos d'ells, i segona firmant en un tercer. Els articles publicats com a conseqüència d'aquesta tesis són els següents:

Objectiu 1:

Tarrats N, Moles A, Morales A, García-Ruiz C, Fernández-Checa JC, Marí M**. Critical role of TNF-receptor 1 but not 2 in hepatic stellate cell proliferation, extracellular matrix remodelling and liver fibrogenesis**. *Hepatology* 2011 Jul; 54(1p319-27. IF: 10.88

Objectiu 2:

Moles A, **Tarrats N**, Morales A, Dominguez M, Bataller R, Caballeria J, Garcia-Ruiz C, Fernández-Checa JC, Marí M. **Acid Sphingomyelinase promotes Hepatic Stellate Cell activation and liver fibrosis via Cathepsins B induction**. *American Journal of Pathology* 2010 Sep; 177(3p1214-24. IF: 5.224

Moles A*, **Tarrats N***, Fernández-Checa JC, Marí M**. Cathepsin B overexpresion due to acidic sphingomyelinase ablation promotes liver fibrosis in Niemann-Pick disease**. (*compartint autoriap *Journal of Biological Chemistry* 2012 Jan 6;287(2p1178-88p IF: 5.328

El resum dels quals i la publicació corresponent s'adjunten a continuació.

OBJECTIU 1

Article derivat:

Tarrats N, et al. **Critical role of TNF-receptor 1 but not 2 in hepatic stellate cell proliferation, extracellular matrix remodelling and liver fibrogenesis**. *Hepatology* 2011 Jul; 54(1p319-27.

Resum:

- Per tal d'avaluar la participació dels receptors de TNF en l'activació de les CEH, es van aïllar CEH i es va estudiar el seu procés d'activació. Les CEH procedents de ratolins deficients en els dos receptors de TNF (TNFR-DKOpi de ratolins deficients en el receptor TNFR1, o TNFR1-KO, expressen de manera basal menor quantitat de pro-col·lagen tipus 1, mentre que no mostren diferències en l'expressió de TGF-β o α-SMA. Això indicaria que l'expressió de TNFR1 és necessària en les CEH per l'expressió òptima del pro-col·lagen tipus 1.

- Durant la seva transdiferenciació, les CEH TNFR-DKO mostren una menor taxa de proliferació respecte les CEH control. Per aquest motiu, varem voler analitzar si el TNF-α era capaç d'induir la proliferació de les CEH. Després d'incubar amb TNF les LX2 (línia cel·lular de CEH humanesp, vam poder observar que el TNF per si sol no induïa la proliferació de les CEH, i ni tan sols potenciava els efectes mitogènics de PDGF.

- Donat que PDGF és el mitògen més potent per a les CEH, varem voler avaluar si els receptors de TNF eren necessaris per una senyalització òptima de PDGF. El que observàrem va ser que les CEH TNFR-DKO i les TNFR1-KO pràcticament no responen a l'estímul proliferatiu de PDGF i que aquesta menor proliferació ve acompanyada d'una manca o baixa activació d'AKT. Les CEH control i TNFR2-KO sí responen a PDGF i fosforilen AKT de manera normal, demostrant-se així que es requereix TNFR1 per a la proliferació i activació de la via d'AKT.

- El remodelat de la matriu extracel·lular és una de les facetes més crítiques de la fibrosi hepàtica, i també és conseqüència de l'activació de les CEH, per això varem voler determinar el paper dels receptors de TNF en l'expressió de les metal·loproteases MMP2 i MMP-9 i de l'inhibidor de metal·loproteases TIMP-1. Les CEH TNFR-DKO expressen de forma basal una menor quantitat de MMP-9 respecte les cèl·lules control. Quan aquestes cèl·lules són estimulades amb TNF, les CEH procedents de ratolins salvatges mostren una clara inducció de l'expressió de MMP-9, a nivell d'RNAm i de proteïna. Vam observar el mateix en les CEH de ratolins TNFR2-KO, mentre que en les CEH TNFR-DKO i TNFR1-KO no observàvem aquesta inducció. Vèiem el mateix patró amb l'expressió de TIMP-1, mentre que la presència i inducció de MMP-2 no estava regulada per TNF. Aquests resultats mostren que TNFR1 és essencial per a l'expressió de MMP-9 i TIMP-1, factors importants per a la remodelació de la matriu extracel·lular.

- Els resultats anteriors es van confirmar en la línia cel·lular LX2 (Xu et al. 2005p i addicionalment varem poder determinar que la inducció de MMP-9 depenia de l'activació de NF-κB.

- Per avaluar la relació causal entre dany hepàtic i fibrogènesi vam avaluar la fibrosi *in vivo* usant el model de fibrosi de lligadura del conducte biliar (LCBp en ratolins salvatges, TNFR-DKO, TNFR1-KO i TNFR2-KO. Els ratolins TNFR-DKO i TNFR1-KO, com era d'esperar, mostren una millora en el dany hepàtic respecte els animals control i TNFR2-KO, i també mostren una reduïda expressió de gens pro-fibrogènics com TNF hepàtic, MMP-9, TIMP-1, α-SMA, o pro-col·lagen tipus I. De fet s'observa una correlació entre els valors de TNF i MMP-9, TIMP-1 i pro-col·lagen tipus I. Aquests resultats *in vivo* recapitulen els efectes observats *in vitro*, i mostren la dependència de la senyalització via TNFR1 per induir els canvis en la remodelació de la MEC durant la fibrogènesi primerenca.

Critical Role of Tumor Necrosis Factor Receptor 1, but not 2, in Hepatic Stellate Cell Proliferation, Extracellular Matrix Remodeling, and Liver Fibrogenesis

Núria Tarrats,[1] Anna Moles,[1] Albert Morales,[1] Carmen García-Ruiz,[1] José C. Fernández-Checa,[1,2*] and Montserrat Marí[1*]

Tumor necrosis factor (TNF) has been implicated in the progression of many chronic liver diseases leading to fibrosis; however, the role of TNF in fibrogenesis is controversial and the specific contribution of TNF receptors to hepatic stellate cell (HSC) activation remains to be established. Using HSCs from wild-type, TNF-receptor-1 (TNFR1) knockout, TNF-receptor-2 (TNFR2) knockout, or TNFR1/R2 double-knockout (TNFR-DKO) mice, we show that loss of both TNF receptors reduced procollagen-α1(I) expression, slowed down HSC proliferation, and impaired platelet-derived growth factor (PDGF)-induced promitogenic signaling in HSCs. TNFR-DKO HSCs exhibited decreased AKT phosphorylation and *in vitro* proliferation in response to PDGF. These effects were reproduced in TNFR1 knockout, but not TNFR2 knockout, HSCs. In addition, matrix metalloproteinase 9 (MMP-9) expression was dependent on TNF binding to TNFR1 in primary mouse HSCs. These results were validated in the human HSC cell line, LX2, using neutralizing antibodies against TNFR1 and TNFR2. Moreover, *in vivo* liver damage and fibrogenesis after bile-duct ligation were reduced in TNFR-DKO and TNFR1 knockout mice, compared to wild-type or TNFR2 knockout mice. *Conclusion:* TNF regulates HSC biology through its binding to TNFR1, which is required for HSC proliferation and MMP-9 expression. These data indicate a regulatory role for TNF in extracellular matrix remodeling and liver fibrosis, suggesting that targeting TNFR1 may be of benefit to attenuate liver fibrogenesis. (HEPATOLOGY 2011;54:319-327)

Tumor necrosis factor (TNF) is an inflammatory cytokine produced by macrophages/monocytes during acute inflammation and is responsible for a diverse range of signaling events within cells. TNF exerts its biological functions by interactions with two members of the TNF receptor (TNFR) superfamily, namely TNFR1 and TNFR2. The cytoplasmic tail of TNFR1 contains a death

Abbreviations: α-SMA, alpha-smooth muscle actin; BDL, bile-duct ligation; CCl_4, carbon tetrachloride; DTT, dithiothreitol; ECL, enhanced chemiluminescense; EDTA, ethylenediamine tetraacetic acid; ECM, extracellular matrix; EGTA, ethylene glycol tetraacetic acid; ERK, extracellular signal-related protein kinase; FBS, fetal bovine serum; H&E, hematoxylin and eosin; HSC, hepatic stellate cells; HRP, horseradish peroxidase; IL-1α, interleukin-1 alpha; JAK, Janus kinase; LPS, lipopolysaccharide; mRNA, messenger RNA; MMP, matrix metalloproteinase; NF-κB, nuclear factor kappa light-chain enhancer of activated B cells; PDGF, platelet-derived growth factor; RT-PCR, reverse-transcription polymerase chain reaction; siRNA, short interfering RNA; TCA, trichloroacetic acid; TGF-β, transforming growth factor beta; TIMP-1, tissue inhibitor of metalloproteinase-1; TNF, tumor necrosis factor; TNFR, TNF-receptor; TNFR-DKO, TNFR1/R2 double knockout.

From the [1]IDIBAPS, Liver Unit-Hospital Clínic, CIBEREHD, and Department of Cell Death and Proliferation, IIBB-CSIC, Barcelona, Spain; and the [2]Research Center for Alcoholic Liver and Pancreatic Diseases, Keck School of Medicine of the University of Southern California, Los Angeles, CA.

Received September 29, 2010; accepted April 13, 2011.

The work was supported by grants PI09/00056, PI10/02114 (Instituto de Salud Carlos III), 2008-02199, and 2009-11417 (Plan Nacional de I+D), Spain; and P50-AA-11999 (Research Center for Liver and Pancreatic Diseases, National Institute on Alcohol Abuse and Alcoholism, National Institutes of Health).

**These authors share senior authorship.*

Address reprint requests to: José C. Fernández-Checa, Ph.D., or Montserrat Marí, Ph.D., Liver Unit, Hospital Clinic, C/Villarroel 170, 08036 Barcelona, Spain. E-mail: checa229@yahoo.com or monmari@clinic.ub.es; fax: 34-93-363-8301.

View this article online at wileyonlinelibrary.com.

DOI 10.1002/hep.24388

Potential conflict of interest: Nothing to report.

Additional Supporting Information may be found in the online version of this article.

domain, which is essential for the induction of apoptosis. However, this motif is missing in TNFR2 and the function of this latter receptor is poorly understood.[1,2] In the liver, TNF functions as a double-edged sword through TNFR1, being required for normal hepatocyte proliferation during liver regeneration[3,4] and induction of nuclear factor kappa light-chain enhancer of activated B cells (NF-κB), which is essential to elicit antiapoptotic defense and in the control of the immune response. Yet, on the other hand, TNF is the mediator of hepatotoxicity and inflammation in many animal models and has also been implicated as an important pathogenic player in patients with alcoholic liver disease, nonalcoholic steatohepatitis, or viral hepatitis.[5,6] Human and animal studies suggest that hepatocellular injury, followed by inflammation and activation of the innate immune system, leads to early-stage liver fibrosis, ultimately resulting in hepatic stellate cell (HSC) activation and extracellular matrix (ECM) deposition.[7,8] Although the contribution of TNF to hepatocellular injury and inflammation has been widely studied,[5,6,9,10] its specific contribution to HSC activation and liver fibrogenesis remains controversial. In this sense, experimental studies performed with knockout mice after carbon tetrachloride (CCl_4) administration have shown that the absence of either TNFR1[11] or TNFR1/R2 double-knockout (TNFR-DKO)[12] mice inhibit liver fibrosis accompanied by reduced expression of procollagen-α1(I) messenger RNA (mRNA), without effect on hepatic injury, suggesting a profibrogenic role for TNF. In contrast, a recent study showed that the inhibition of TNF processing via TNF-alpha–converting enzyme attenuated liver injury and inflammation after CCl_4 administration, but increased collagen deposition, effects reproduced in the TNFR-DKO mice.[13] Moreover, several reports using cultured HSCs point to an antifibrogenic role of TNF via the inhibition of *procollagen-α1(I)* gene expression[14-17] due, in part, to glutathione depletion.[18]

Hence, although TNF has been implicated in the progression of many chronic liver diseases leading to fibrosis, the specific involvement of TNF or its receptors, TNFR1 and TNFR2, in HSC activation remains to be established. The morphological and metabolic changes associated with HSC activation, reproduced by culturing isolated HSCs on plastic,[19,20] were studied in HSCs from wild-type, TNFR-DKO, TNFR1, and TNFR2 knockout mice to evaluate the impact of TNF signaling and thus its potential direct contribution to liver fibrosis. The results, validated *in vitro* in human activated LX2 cells and *in vivo* using a bile-duct ligation (BDL) mice model, led us to underscore the contribution of TNFR1 in liver fibrosis, and suggest that the blockage of specific TNF receptors may be effective to reduce hepatic deterioration during fibrogenesis.

Materials and Methods

Animals and HSC Isolation. Wild-type, TNFR1 knockout mice, TNFR2 knockout mice, and TNFR-DKO mice (10-18 weeks old) (C57BL/6 strain), a generous gift of Dr. Bluethmann (Discovery Technologies, Hoffmann-La Roche Ltd., Basel, Switzerland), were obtained by the propagation of homozygous pairs. The animals had free access to water and standard purified rodent diet throughout the study. All animals received humane care according to the criteria outlined in the *Guide for the Care and Use of Laboratory Animals* published by the National Institutes of Health (Bethesda, MD). HSCs were isolated by perfusion with collagenase and cultured as described.[21]

Cell Lines and Culture. In addition to primary mouse HSCs, we used the human HSC cell line, LX2. Cells were cultured in Dulbecco's modified Eagle medium (DMEM) plus 10% fetal bovine serum (FBS), and antibiotics were cultured at 37°C in a humidified atmosphere of 95% air and 5% CO_2. Cells were serum-starved with 0.5% FBS before using TNF-α, PDGF-BB, interleukin-1 alpha (IL-1α), and IL-1β (PreproTech EC, London, UK) or lipopolysaccharide (LPS) (from *Escherichia coli* serotype 0128:B12; Sigma-Aldrich Quimica SA, Madrid, Spain). Neutralizing antibodies against human TNFR1 and TNFR2 (R&D Systems, Minneapolis, MN) were used at a concentration of 10 μg/mL. *In vitro* short interfering RNA (siRNA) transfection was performed using commercially available siRNA (Santa Cruz Biotechnology, Heidelberg, Germany) as previously described.[21] Unless otherwise stated, all reagents were from Sigma-Aldrich.

Real-time RT-PCR and Primer Sequences. Total RNA from HSCs, mouse tissue, or LX2 cells was isolated with TRIzol reagent (Invitrogen, Paisley, UK). Real-time reverse-transcription polymerase chain reaction (RT-PCR) was performed with the iScript One-Step reverse transcription (RT)-PCR kit with SYBR Green (Bio-Rad Laboratories SA, Madrid, Spain). Primer sequences were designed based on published sequences (Table 1).

[^{3}H] Thymidine Incorporation. Proliferation was estimated as the amount of [^{3}H]-thymidine incorporated into trichloroacetic acid (TCA)-precipitable material, as previously described.[21]

Table 1. Primers Used in Quantitative Real-Time RT-PCR

	5′ primer	3′ primer
Target gene (mouse)		
β-actin [NM_007393]	GACGGCCAGGTCATCACTAT	CGGATGTCAACGTCACACTT
α-SMA [NM_007392]	ACTACTGCCGAGCGTGAGAT	AAGGTAGACAGCGAAGCCAA
TIMP-1 [NM_001044384]	CATGGAAAGCCTCTGTGGAT	CTCAGAGTACGCCAGGGAAC
MMP-2 [NM_008610]	ACCTGAAGCTGGAGAACCAA	CACATCCTTCACCTGGTGTG
MMP-9 [NM_013599]	CAAATTCTTCTGGCGTGTGA	CGGTTGAAGCAAAGAAGGAG
TGF-β [NM_011577]	GTCAGACATTCGGGAAGCAG	GCGTATCAGTGGGGGTCA
Procollagen α1(I) [NM_007742]	GAGCGGAGAGTACTGGATCG	GTTCGGGCTGATGTACCAGT
TNF [NM_013693]	CTGAACTTCGGGGTGATCGGT	ACGTGGGCTACAGGCTTGTCA
Target gene (human)		
β-actin [NM_001101]	GGACTTCGAGCAAGAGATGG	AGGAAGGAAGGCTGGAAGAG
α-SMA [NM_001613]	CCGACCGAATGCAGAAGG	ACAGAGTATTTGCGCTCCGGA
TIMP-1 [NM_003254]	AGTGGCACTCATTGCTTGTG	GCAGGATTCAGGCTATCTGG
MMP-2 [NM_004530]	ACGACCGCGACAAGAAGTAT	ATTTGTTGCCCAGGAAAGTG
MMP-9 [NM_004994]	GACAAGCTCTTCGGCTTCTG	CTCGCTGGTACAGGTCGAGT

Sodium Dodecyl Sulfate Polyacrylamide Gel Electrophoresis and Immunoblot Analysis. Total cell lysates were incubated, after transferring to nitrocellulose membranes, with rabbit anti-phospho-Akt (1:250), anti-AKT (1:200), anti-MMP-9 (1:200; Santa Cruz Biotechnology), anti-phospho-ERK1/2, anti-ERK (extracellular signal-related protein kinase), anti-phospho-JAK2 (Janus kinase 2), anti-JAK2 (1:2,000; Cell Signaling Technology, Danvers, MA), or mouse anti-α-SMA (alpha-smooth muscle actin; 1:1000) and anti-β-actin (1:5000), followed by incubation with horseradish peroxidase (HRP)-conjugated secondary antibody anti-rabbit (1:20,000) or anti-mouse (1:20,000), and developed in enhanced chemiluminescent (ECL) substrate (Pierce, Rockford, IL).

Histochemical Staining. Liver tissue was fixed in 10% formalin/phosphate-buffered saline, dehydrated in alcohols, incubated in xylene, and embedded in paraffin. Then, 7-μm-thick tissue sections were cut and stained with hematoxylin and eosin (H&E), according to the manufacturer's protocols.

Gelatin Zymography. Medium from cultured HSCs was treated with sample buffer without 2-mercaptoethanol and loaded onto sodium dodecyl sulfate gel, containing 0.1% gelatin. After electrophoresis, the gel was washed twice with 2.5% Triton X-100 for 15 minutes and incubated overnight in developing buffer (50 mmol/L Tris-HCl, pH 7.4, 0.2 mol/L NaCl, 10 mmol/L $CaCl_2$, and 0.002% sodium azide) at 37°C. After, the gel was stained with a solution containing 0.5% Coomassie Brilliant Blue, 40% methanol, and 7% acetic acid and destained. Bands were visualized using a Gel-Doc analyzer (Bio-Rad).

Nuclear Extract Isolation. Briefly, 2×10^6 HSC or LX2 cells were scraped in Buffer A (10 mmol/L Hepes, 10 mmol/L KCl, 0.1 mmol/L ethylenediaminetetraacetic acid [EDTA], 0.1 mmol/L ethylene glycol tetraacetic acid [EGTA], 1 mmol/L dithiothreitol [DTT], and 0.5 mmol/L phenylmethylsulfonyl fluoride [PMSF]), kept on ice for 15 minutes, and lysed by the addition of 1/20 (vol/vol) 10% Igepal and vortexed for 10 seconds. Nuclei were pelleted (12,000*g*, 30 seconds), resuspended in Buffer C (20 mmol/L Hepes, 0.4 mol/L NaCl, 1 mmol/L EDTA, 1 mmol/L EGTA, 1 mmol/L DTT, and 1 mmol/L PMSF), and incubated for 15 minutes on ice with gentle mixing. After, nuclear extracts were obtained by centrifuging at 4°C, 12,000*g* for 5 minutes.

In Vivo Liver Fibrosis After BDL. BDL was performed as previously described.[22]

Statistical Analysis. Results were routinely expressed as mean ± standard deviation, with the number of individual experiments detailed in figure legends. Statistical significance of the mean values was established by the Student *t* test.

Results

Loss of TNFR1/TNFR2 Reduces Procollagen-α1(I) mRNA Expression. To evaluate the participation of TNF receptors on the activation of HSC, we isolated HSC from wild-type and TNFR-DKO mice and plated them on plastic with medium containing 10% FBS to allow their activation. As expected, though TNFR-DKO HSCs did not respond to TNF, as shown by the lack of NF-κB activation after TNF challenge, represented as the translocation of p65 to the nucleus, they were able to activate NF-κB in response to other stimuli, such as LPS addition (Fig. 1A). The expression of α-SMA was followed at different time points along the activation of HSCs. α-SMA protein expression increased during the time of culture

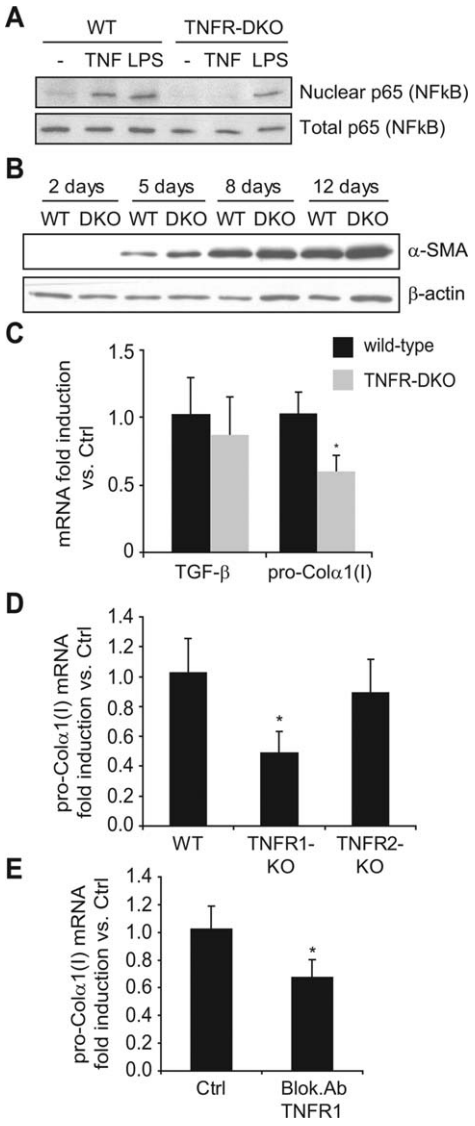

Fig. 1. Expression pattern of wild-type (WT) and TNFR-DKO HSC. (A) p65 subunit of NF-κB translocation to nuclei in HSC after TNF (10 ng/mL) or LPS (50 ng/mL) challenge for 30 minutes. (B) Time course of α-SMA protein expression by western blot. (C) TGF-β and procollagen-α1(I) mRNA expression. Procollagen-α1(I) mRNA expression in TNFR1-KO and TNFR2-KO HSCs (D) or in LX2 cells (E) after incubation with blocking antibody (Ab) anti-TNFR1 (10 μg/mL, 24 hours). Data are mean ± standard deviation; in (C,D,E), $n \geq 3$ and $^*P \leq 0.05$ versus WT HSC.

and its levels were similar among wild-type and TNFR-DKO HSCs (Fig. 1B). Moreover, paralleling the effects on α-SMA, transforming growth factor beta (TGF-β) mRNA levels were comparable in wild-type and TNFR-DKO HSCs, after 7 days of culture. However, procollagen-α1(I) mRNA levels were significantly decreased in TNFR-DKO HSCs during *in vitro* activation (Fig. 1C) and also in TNFR1-KO HSCs, but not in TNFR2-KO (Fig. 1D). In addition, LX2 cells incubated with neutralizing antibody against TNFR1 receptor displayed a significant decrease in procollagen-α1(I) mRNA expression (Fig. 1E), thus indicating that the expression of TNFR1 is necessary in HSCs for optimal expression of procollagen-α1(I).

TNFR1 Is Required for PDGF-Induced AKT Phosphorylation and HSC Proliferation. Next, we assessed whether a lack of TNF signaling would affect HSC proliferation. HSCs from TNFR-DKO displayed a reduced proliferation rate, compared to wild-type HSCs, during their transdifferentiation into myofibroblast-like cells (Fig. 2A). To further evaluate the potential mechanisms involved, we first addressed whether the decreased proliferation of HSCs was due to a reduced ability of TNF to stimulate proliferation. TNF itself did not stimulate the proliferation of HSCs (Fig. 2B). Moreover, because PDGF is a potent mitogenic stimulus for HSCs, we next examined whether TNF would potentiate PDGF signaling and stimulation of cell proliferation. Although PDGF stimulated wild-type HSC cell proliferation, this effect was not enhanced in the presence of TNF, thus discarding a direct role of TNF in HSC proliferation (Fig. 2B). Moreover, to examine whether TNF receptors were required for optimal PDGF signaling, we addressed the effect of PDGF in TNFR-DKO HSCs. As shown, the proliferating effect of PDGF was markedly reduced in TNFR-DKO HSCs (Fig. 2C) due to impaired AKT phosphorylation (Fig. 2D).

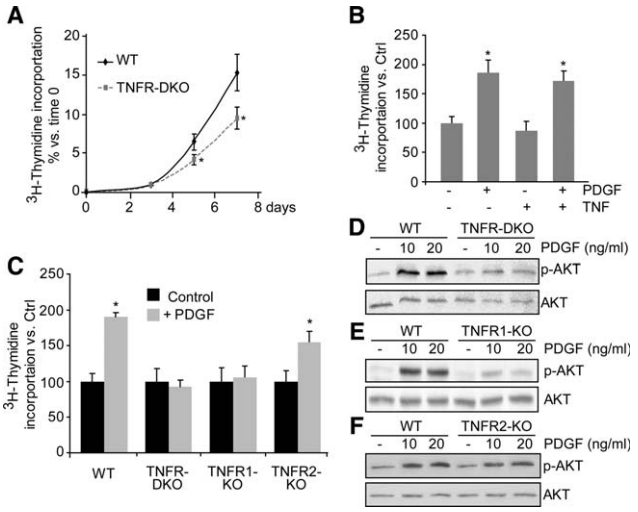

Fig. 2. Lack of TNF receptors affects HSC proliferation. (A) Wild-type and TNFR-DKO HSC proliferation. (B) LX2 proliferation after 24 hours of PDGF (20 ng/mL) and/or TNF (50 ng/mL) challenge. (C) Wild-type, TNFR-DKO, TNFR1-KO, and TNFR2-KO proliferation after 24 hours of PDGF (20 ng/mL) challenge. AKT phosphorylation induced by PDGF (10 or 20 ng/mL) for 15 minutes in wild-type versus TNFR-DKO (D), TNFR1-KO (E), or TNFR2-KO (F) HSCs. Data are mean ± standard deviation in (A) and (C), $n = 3$ and $^*P \leq 0.05$ versus wild-type HSCs; in (B), $^*P \leq 0.05$ versus PDGF untreated cells.

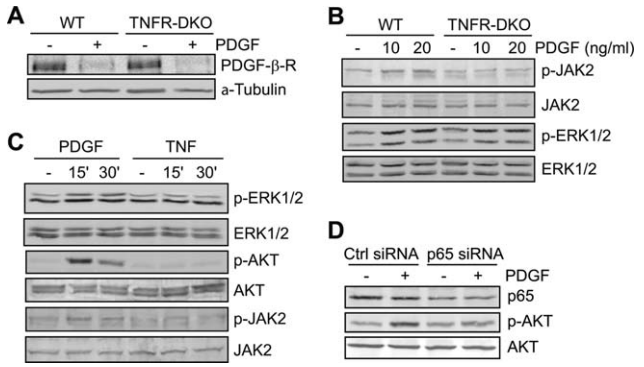

Fig. 3. PDGF-β-receptor signaling in TNF-DKO HSC. (A) PDGF-β-receptor degradation after PDGF challenge (20 ng/mL, 2 hours) and (B) JAK2 and ERK1/2 activation after PDGF challenge (15 minutes) in wild-type and TNFR-DKO HSCs. (C) ERK1/2, AKT, and JAK2 activation by PDGF (20 ng/mL) or TNF (50 ng/mL) in LX2 cells. (D) p65 expression and AKT activation by PDGF (15 minutes) in control and p65 siRNA-transfected LX2 cells.

Moreover, TNFR1-KO HSCs displayed a reduced phosphorylation of AKT in response to PDGF (Fig. 2E); however, TNFR2-KO HSCs (Fig. 2F) were able to phosphorylate AKT similarly to wild-type HSCs, thus suggesting an intricate interplay between TNFR1 and PDGF signaling. Consistent with these observations, cell proliferation in response to PDGF was impaired in TNFR1-KO, but not in TNFR2-KO, HSCs (Fig 2C).

Furthermore, we addressed downstream signaling pathways involved in the proliferation of HSCs induced by PDGF. First, we observed that PDGF receptor degradation stimulated by ligand binding was unimpaired in TNFR-DKO HSCs (Fig. 3A). Moreover, in addition to the requirement for TNFR1 for Akt phosphorylation in response to PDGF (Fig 2E), PDGF also induced the phosphorylation of ERK1/2 and JAK2 in wild-type HSC or LX2 cells (Fig. 3B,C). However, the phosphorylation of JAK2, but not ERK1/2, was impaired in TNFR-DKO HSC (Fig. 3B). Unlike ERK1/2, we did not observe p38 phosphorylation by PDGF in mouse HSC or human LX2 cells (not shown). In addition, AKT phosphorylation by PDGF was dependent on NF-κB activation, because p65 silencing by siRNA reduced PDGF-dependent AKT activation, compared to control-siRNA–transfected cells (Fig. 3D).

TNFR1 Controls MMP-9 Expression in HSCs and Human LX2 Cells. Because matrix remodeling is another critical facet of liver fibrosis and a consequence of HSC activation, we next examined the role of TNF receptors on MMP-9 expression. In the presence of 10% FBS, MMP-9 mRNA expression was reduced in TNFR-DKO HSCs (Fig. 4A). To validate the importance of TNF as a putative inducer of MMP-9, HSCs from wild-type and TNFR-DKO mice were depleted of serum up to 0.5% and incubated with TNF. This maneuver resulted in an induction of MMP-9 mRNA (Fig. 4B) and protein (Fig. 4C) in wild-type, but not in TNFR-DKO, HSCs. The induction of MMP-9 was mediated by TNFR1, as TNFR2-KO HSCs were able to activate MMP-9 mRNA (Fig. 4B). Of note, under conditions of serum limitation (0.5% FBS), the expression of MMP-9 mRNA in wild-type HSCs was similar to that of TNFR-DKO HSCs, indicating that the basal induction of MMP-9 is independent of TNF, but that its induction under growing conditions required TNF (Supporting Fig. 1). Moreover, the induction of MMP-9 by TNF in mouse HSCs was dependent on the time of activation being higher in 14-day, compared to 7-day, HSC cultures and similar to the levels observed with IL-1α or IL-1β (Fig. 4D). The participation of TNFR1 as the receptor responsible for MMP-9 induction was further validated in

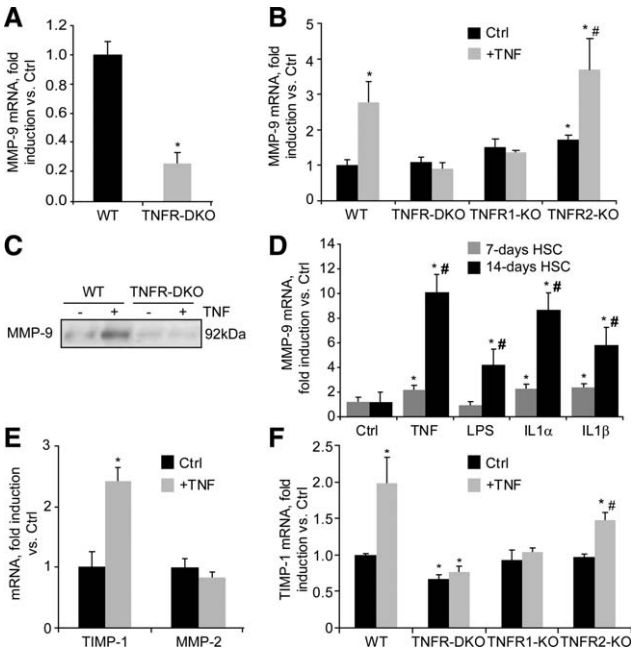

Fig. 4. TNF controls MMP-9 expression in HSCs. (A) Basal MMP-9 mRNA expression in wild-type and TNFR-DKO HSC and (B) after TNF challenge (50 ng/mL) for 24 hours in wild-type, TNFR-DKO, TNFR1-KO, and TNFR2-KO HSCs. (C) Effect of TNF (50 ng/mL, 24 hours) on MMP-9 protein expression. (D) MMP-9 mRNA expression in primary 7- and 14-day-old HSCs incubated with an equivalent concentration (50 ng/mL) of TNF, LPS, IL-1α, and IL-1β for 24 hours. (E) MMP-2 and TIMP-1 mRNA expression in wild-type HSC after TNF challenge (50 ng/mL, 24 hours). (F) TIMP-1 mRNA expression after TNF challenge (50 ng/mL) for 24 hours in wild-type (WT), TNFR-DKO, TNFR1-KO, and TNFR2-KO HSCs. Data are mean $\pm$ standard deviation; $n = 4$, $^*P \leq 0.05$ versus WT or untreated HSCs; in (B) and (F), $\#P \leq 0.05$ versus TNFR2-KO Ctrl HSCs; in (D), $\#P \leq 0.05$ versus 7-day-old treated HSCs.

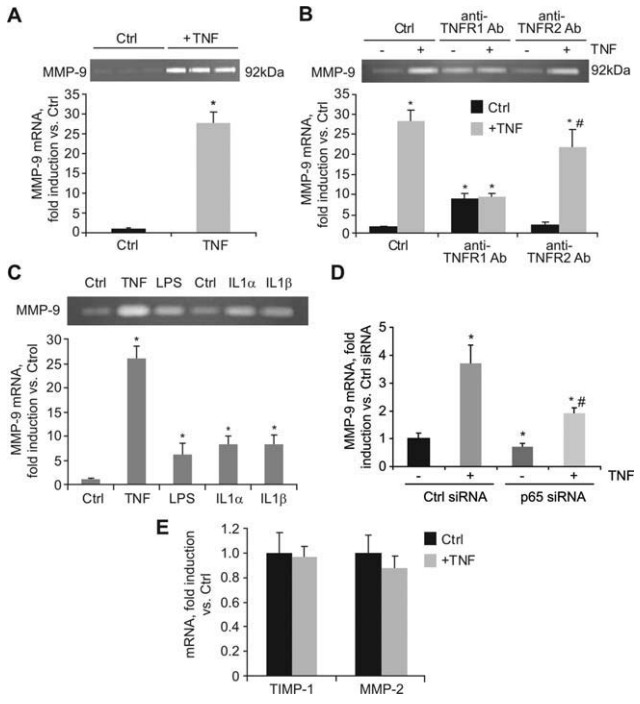

Fig. 5. TNF controls MMP-9 expression in LX2. (A) Effect of TNF (50 ng/mL, 24 hours) on MMP-9 mRNA expression and activity by zymography. (B) MMP-9 mRNA and activity after 24-hour challenge with TNF (50 ng/mL) in LX2 cells in the presence of TNFR1- or TNFR2-blocking antibodies (preincubation at 10 μg/mL, 30 minutes). (C) MMP-9 mRNA expression and activity in LX2 cells incubated with equivalent concentration (50 ng/mL) of TNF, LPS, IL-1α, and IL-1β for 24 hours. (D) MMP-9 mRNA expression in control and p65 siRNA-transfected LX2 cells after TNF challenge (50 ng/mL, 24 hours). (E) TIMP-1 and MMP-2 mRNA expression after TNF challenge (50 ng/mL, 24 hours) in LX2 cells. Data are mean $\pm$ standard deviation, $n = 3$, $^*P \leq 0.05$ versus Ctrl LX2 cells; in (B), $\#P \leq 0.05$ versus anti-TNFR2-treated control LX2 cells; in (D), $\#P \leq 0.05$ versus p65 siRNA-untreated LX2 cells.

LX2 cells. LX2 responded to TNF by inducing MMP-9 mRNA, and its activity could be clearly detected in extracellular media by zymography (Fig. 5A). In addition, by using blocking antibodies against TNFR1 and TNFR2, we could confirm that TNFR1 was the receptor responsible for MMP-9 induction by TNF at the mRNA or activity level (Fig. 5B). Intriguingly, MMP-9 expression by TNF in LX2 cells was higher than that caused by LPS or IL-1α/IL-1β (Fig. 5C), correlating with the nuclear translocation of p65 (not shown). Of note, neither in LX2 cells (Fig. 5E) nor in wild-type HSCs (Fig. 4E) was TNF able to increase the expression of another important matrix collagenase, MMP-2, thus discarding the participation of TNF signaling in MMP-2 regulation. In contrast, although TNF induced TIMP-1 mRNA in wild-type HSCs (Fig. 4E), which required TNFR1 (Fig. 4F), it failed to do so in LX2 cells (Fig. 5E). Despite the divergence observed in TIMP-1 regulation, results obtained in activated human LX2 cells emphasize the specific requirement for TNFR1-dependent signaling in the expression of matrix-remodeling factors, such as MMP-9 in HSCs.

For instance, although the individual participation of IL-1[23] or TNF[24,25] in the induction of MMP-9 has been already described in HSCs, their relative contribution to the activation of MMP-9 has not been carefully addressed, nor has the comparison of their stimulating effect on MMP-9 expression between primary mouse and human HSCs. To this aim, we challenged primary mouse HSCs as well as human LX2 cells in parallel with TNF, IL-1α, IL-1β, or LPS to analyze the extent of MMP-9 activation at the mRNA and protein level. TNF induced MMP-9 in 7-day-old primary mouse HSCs to a similar extent as IL-1, and the extent of MMP-9 expression changed with activation, because, in 14-day-old HSCs, MMP-9 expression by TNF and IL-1 was greatly enhanced, and, at this stage, cells were also responsive to LPS (Fig. 4D). In addition, TNF was a more potent inducer of MMP-9 in the human LX2 cell, as displayed also by the enhanced activity of MMP-9 in extracellular media after TNF challenge (Fig. 5C). Thus, in comparison to other known MMP-9 inducers, TNF is a relevant trigger of MMP-9 expression in primary mouse and human HSCs, and this induction is mediated by NF-κB activation, as p65 silencing in LX2 cells reduced the expression of MMP-9 induced by TNF, compared to control-siRNA transfected LX2 cells (Fig. 5D).

TNFR Deletion Reduces Early Fibrogenesis in a Mouse Model of BDL. To evaluate the causal relationship between liver damage and fibrogenesis, we examined, in parallel, the injury and fibrosis in mice with impaired TNF signaling *in vivo* using the BDL model of liver fibrogenesis. TNFR1-KO mice displayed ameliorated tissue damage, compared with that of the wild-type controls, as indicated by the reduced volume of biliary infarcts in H&E staining and serum transaminase levels (Fig. 6A,B), despite similar bilirubin levels (8.78 $\pm$ 1.25 mg/dL in wild-type versus 8.64 $\pm$ 0.96 mg/dL in TNFR1-KO mice), indicative of comparable cholestasis in both wild-type and TNFR1-KO mice. Interestingly, after BDL, TNFR1-KO mice displayed reduced levels of hepatic TNF mRNA (Fig. 6C), compared to wild-type animals. This correlated with decreased levels of MMP-9, TIMP-1 mRNA (Fig. 6D), and procollagen-α1(I) mRNA (Fig. 6E). In contrast, MMP-2 mRNA expression (Fig. 6E) was not, apparently, regulated by TNF. α-SMA was also reduced in TNFR1-KO livers, compared to the wild type (Fig. 6F), indicating decreased HSC activation *in vivo*.

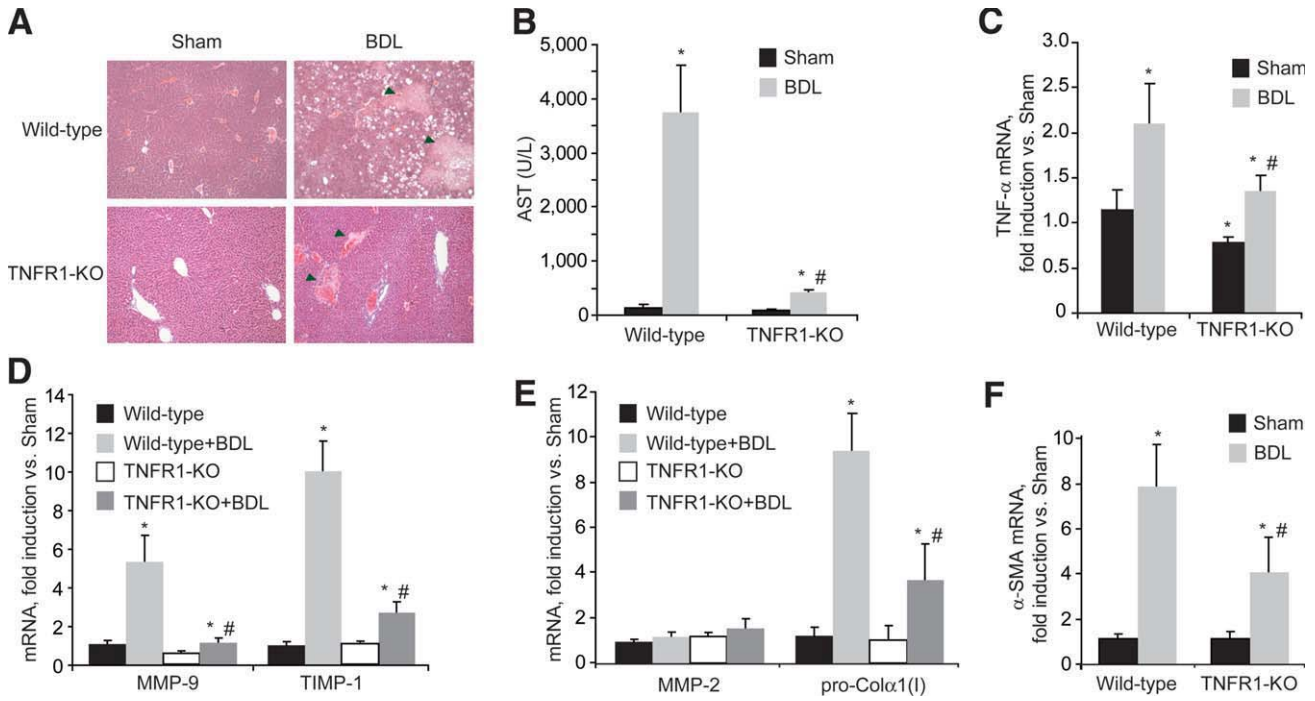

Fig. 6. Reduced liver damage and fibrosis in TNFR1-KO mice after BDL. H&E staining of liver sections (A) and serum transaminase levels (B) in wild-type and TNFR1-KO mice after BDL. TNF-α (C), MMP-9 and TIMP-1 (D), MMP-2 and pro-Colα1(I) (E), and α-SMA (F) mRNA expression in wild-type and TNFR1-KO livers after BDL. In (A), arrowheads signal bile infarcts. Data are mean ± standard error of the mean; $n = 4$-5 animals/group, $*P \leq 0.05$ versus wild-type Sham, $\#P \leq 0.05$ versus wild-type BDL.

Similar findings were observed in the TNFR-DKO mice, whereas TNFR2-KO mice behaved similarly to wild-type animals (Supporting Fig. 2). Therefore, the *in vivo* BDL model recapitulates the *in vitro* effects observed in HSCs, showing the dependence on TNFR1 signaling to induce changes in ECM remodeling during early fibrogenesis.

Discussion

TNF has been implicated in the development of many chronic liver diseases, and hepatic fibrosis is a hallmark of disease progression. Unlike its involvement in hepatocellular apoptosis and liver diseases, the role of TNF in liver fibrosis remains unclear, particularly whether TNF and its binding to specific TNFR1 or TNFR2 regulates HSC biology. Using genetic and pharmacological approaches, we show a profibrogenic role for TNF, specifically via binding to receptor R1. In particular, we used primary mouse HSCs from wild-type and mice deficient in TNFRs to analyze the role of TNF and its receptors in HSC activation and proliferation, which are critical steps in the cascade of events leading to fibrosis. Moreover, the findings were extended to human HSCs, in which TNF receptors were individually antagonized by specific neutralizing antibodies.

Our results indicate that although TNF does not directly participate in some fundamental traits of HSC transdifferentiation into a myofibroblast phenotype, such as increase in α-SMA or TGF-β expression, TNF, through TNFR1, has an important role in other important features, such as proliferation as well as MMP-9 and TIMP-1 expression. A significant difference between primary mouse and human HSCs was found in the participation of TNF in TIMP-1 induction. Although primary mouse HSCs augment TIMP-1 expression in response to TNF, we failed to observe any increase of TIMP-1 in LX2 cells under the same experimental conditions. Several conceivable possibilities could explain this differential behavior, including that TIMP-1 regulation may fundamentally differ between mouse and human HSCs. Another explanation could be the fact that LX2 cells display an almost negligible expression of TIMP-1, as compared to primary HSCs or to the parental cell line, LX1, implying that TIMP-1 expression may have been lost during its selection under low serum conditions (2% FBS).[26]

A striking finding was the decrease in proliferation observed in TNFR-DKO HSCs compared to wild-type HSCs. Mechanistically, the decreased proliferation was mediated by a defective PI3K/AKT pathway in TNFR-DKO HSC that was reproduced in TNFR1-KO, but not in TNFR2-KO, HSCs. Indeed, both TNFR1-KO

and TNFR-DKO HSCs display reduced AKT phosphorylation and proliferation in response to PDGF, a potent mitogen of HSCs, despite correct ligand binding and subsequent receptor degradation. These observations suggest that proteins or mediators necessary for PDGF signaling located upstream of AKT rely on NF-κB–dependent TNFR1 signaling, indicating a cross-talk between PDGF and TNFR1 receptors. In line with our observations, previous findings in vascular smooth muscle cells indicated a similar overlapping between TNF and PDGF necessary for cell migration and proliferation.[27] However, the identification of the NF-κB–dependent targets responsible for the reduced proliferation in response to PDGF in TNFR-DKO and TNFR1 KO HSCs remains unknown and requires further work.

In contrast to TGF-β expression, we observed a decreased basal level of procollagen-α1(I) in activated HSCs from TNFR-DKO and TNFR1-KO, compared to wild-type mice, findings that were reproduced in LX2 cells using anti-TNFR1-blocking antibody. Consistent with previous studies,[17,18] TNF addition to HSC cultures did not induce procollagen-α1(I) mRNA (data not shown), thus discarding a direct effect of TNF on procollagen-α1(I) regulation. However, the known ability of MMP-9 to activate latent TGF-β to its active form,[28] which plays an essential role in earlier stages of liver fibrogenesis when collagen production of HSCs is stimulated by TGF-β,[29] could explain why TNFR-DKO and TNFR1-KO HSCs show decreased basal levels of procollagen-α1(I) mRNA expression. In agreement, with impaired MMP-9 expression in TNFR-DKO HSCs, TGF-β would be normally produced, but not activated, by MMP-9, thus resulting in a deficient procollagen-α1(I) induction.

Unlike procollagen-α1(I), interestingly, we observed a differential role of TNF receptors in the regulation of MMPs in HSCs, in particular, the requirement of TNFR1 in the expression of MMP-9, but not MMP-2. In relation to MMP-9, it has been described, in the thioacetamide model of liver injury and fibrosis,[30] that MMP-9 colocalizes predominantly to desmin-positive cells, suggesting that HSCs are the source of MMP-9 cells *in vivo*. The importance of MMP-9 is highlighted by the observation that MMP-9–deficient mice are partially protected from liver injury and HSC activation.[30] In contrast to MMP-9, although associative studies and cell-culture findings suggest that MMP-2, a type IV collagenase up-regulated in chronic liver diseases and considered a profibrogenic mediator, promotes hepatic fibrogenesis, no *in vivo* model has definitively established a pathologic role for MMP-2 in the development and progression of liver fibrosis. In fact, recent findings, using MMP-2–deficient mice, suggest a protective, rather than pathogenic, role for MMP-2.[31]

Because the above findings indicated a selective requirement for TNFR1 in specific steps of HSC activation and proliferation, we next addressed the *in vivo* relevance for liver fibrogenesis. The data, using the BDL model of liver fibrosis, although limited in interpretation because the TNFR1-KO and TNFR-DKO mice displayed both reduced liver damage and decreased matrix deposition, suggest a correlation between TNF and MMP-9, TIMP-1, and procollagen-α1(I) mRNA expression. In contrast to the BDL model shown here, previous reports using the chronic administration of CCl_4 reported a controversial role of TNFR1 in liver fibrosis. For instance, the lack of TNFR1 inhibited procollagen-α1(I) expression and liver fibrosis after CCl_4 treatment without effect on liver injury.[11,12] However, interestingly, de Meijer et al.[13] recently reported decreased liver injury and inflammation, but increased collagen deposition, in the CCl_4 model by blocking TNF production through the inhibition of its processing via TNF-alpha-converting enzyme, as well as in TNFR-DKO mice.

Taken together, our observations in *in vitro* HSC culture and *in vivo* point to TNF not only as an inducer of hepatocellular damage, but also as a profibrogenic factor in the liver, and hence targeting TNF or its receptor, TNFR1, could be of benefit toward preserving hepatocellular integrity and prevent HSC proliferation and liver fibrosis.

Acknowledgment: The technical assistance of Susana Núñez is greatly appreciated. The authors thank Dr. Horst Bluethmann (Hoffmann-La Roche Ltd., Basel, Switzerland) for providing the knockout mice involved in this study. The work was carried out, in part, at the Esther Koplowitz Center, Barcelona, Spain.

References

1. Grell M, Douni E, Wajant H, Löhden M, Clauss M, Maxeiner B, et al. The transmembrane form of tumor necrosis factor is the prime activating ligand of the 80 kDa tumor necrosis factor receptor. Cell 1995;83:793-802.
2. Grell M, Wajant H, Zimmermann G, Scheurich P. The type 1 receptor (CD120a) is the high-affinity receptor for soluble tumor necrosis factor. Proc Natl Acad Sci U S A 1998;95:570-575.
3. Yamada Y, Fausto N. Deficient liver regeneration after carbon tetrachloride injury in mice lacking type 1 but not type 2 tumor necrosis factor receptor. Am J Pathol 1998;152:1577-1589.
4. Yamada Y, Webber EM, Kirillova I, Peschon JJ, Fausto N. Analysis of liver regeneration in mice lacking type 1 or type tumor necrosis factor receptor: requirement for type 1 but not type 2 receptor. HEPATOLOGY 1998;28:959-970.

5. Bradham CA, Plümpe J, Manns MP, Brenner DA, Trautwein C. Mechanisms of hepatic toxicity. I. TNF-induced liver injury. Am J Physiol 1998;275:G387-G392.
6. Schwabe RF, Brenner DA. Mechanisms of liver injury. I. TNF-alpha-induced liver injury: role of IKK, JNK, and ROS pathways. Am J Physiol Gastrointest Liver Physiol 2006;290:G583-G589.
7. Bataller R, Brenner DA. Liver fibrosis. J Clin Invest 2005;115:209-218.
8. Friedman SL. Mechanisms of hepatic fibrogenesis. Gastroenterology 2008;134:1655-1669.
9. Wullaert A, Heyninck K, Beyaert R. Mechanisms of crosstalk between TNF-induced NF-kappaB and JNK activation in hepatocytes. Biochem Pharmacol 2006;72:1090-1101.
10. Han D, Ybanez MD, Ahmadi S, Yeh K, Kaplowitz N. Redox regulation of tumor necrosis factor signaling. Antioxid Redox Signal 2009; 11:2245-2263.
11. Sudo K, Yamada Y, Moriwaki H, Saito K, Seishima M. Lack of tumor necrosis factor receptor type 1 inhibits liver fibrosis induced by carbon tetrachloride in mice. Cytokine 2005;29:236-244.
12. Simeonova PP, Gallucci RM, Hulderman T, Wilson R, Kommineni C, Rao M, et al. The role of tumor necrosis factor-alpha in liver toxicity, inflammation, and fibrosis induced by carbon tetrachloride. Toxicol Appl Pharmacol 2001;177:112-120.
13. de Meijer VE, Sverdlov DY, Popov Y, Le HD, Meisel JA, Nosé V, et al. Broad-spectrum matrix metalloproteinase inhibition curbs inflammation and liver injury but aggravates experimental liver fibrosis in mice. PLoS One 2010;5:e11256.
14. Hernández I, de la Torre P, Rey-Campos J, Garcia I, Sánchez JA, Muñoz R, et al. Collagen alpha1(I) gene contains an element responsive to tumor necrosis factor-alpha located in the 5′ untranslated region of its first exon. DNA Cell Biol 2000;19:341-352.
15. Hernández-Muñoz I, de la Torre P, Sánchez-Alcázar JA, García I, Santiago E, Muñoz-Yagüe MT, et al. Tumor necrosis factor alpha inhibits collagen alpha 1(I) gene expression in rat hepatic stellate cells through a G protein. Gastroenterology 1997;113:625-640.
16. Houglum K, Buck M, Kim DJ, Chojkier M. TNF-alpha inhibits liver collagen-alpha 1(I) gene expression through a tissue-specific regulatory region. Am J Physiol 1998;274:G840-G847.
17. Solis-Herruzo JA, Brenner DA, Chojkier M. Tumor necrosis factor alpha inhibits collagen gene transcription and collagen synthesis in cultured human fibroblasts. J Biol Chem 1988;263:5841-5845.
18. Varela-Rey M, Fontán-Gabás L, Blanco P, López-Zabalza MJ, Iraburu MJ. Glutathione depletion is involved in the inhibition of procollagen alpha1(I) mRNA levels caused by TNF-alpha on hepatic stellate cells. Cytokine 2007;37:212-217.
19. de Leeuw AM, McCarthy SP, Geerts A, Knook DL. Purified rat liver fat-storing cells in culture divide and contain collagen. HEPATOLOGY 1984;4:392-403.
20. Friedman SL, Rockey DC, McGuire RF, Maher JJ, Boyles JK, Yamasaki G. Isolated hepatic lipocytes and Kupffer cells from normal human liver: morphological and functional characteristics in primary culture. HEPATOLOGY 1992;15:234-243.
21. Moles A, Tarrats N, Fernández-Checa JC, Marí M. Cathepsins B and D drive hepatic stellate cell proliferation and promote their fibrogenic potential. HEPATOLOGY 2009,49:1297-1307.
22. Moles A, Tarrats N, Morales A, Domínguez M, Bataller R, Caballería J, et al. Acidic sphingomyelinase controls hepatic stellate cell activation and *in vivo* liver fibrogenesis. Am J Pathol 2010;177:1214-1224.
23. Han YP, Zhou L, Wang J, Xiong S, Garner WL, French SW, et al. Essential role of matrix metalloproteinases in interleukin-1-induced myofibroblastic activation of hepatic stellate cell in collagen. J Biol Chem 2004;279:4820-4828.
24. Migita K, Maeda Y, Abiru S, Nakamura M, Komori A, Yokoyama T, et al. Immunosuppressant FK506 inhibits matrix metalloproteinase-9 induction in TNF-alpha-stimulated human hepatic stellate cells. Life Sci 2006;78:2510-2515.
25. Zhou L, Yan C, Gieling RG, Kida Y, Garner W, Li W, et al. Tumor necrosis factor-alpha induced expression of matrix metalloproteinase-9 through p21-activated kinase-1. BMC Immunol 2009;10:15.
26. Xu L, Hui AY, Albanis E, Arthur MJ, O'Byrne SM, Blaner WS, et al. Human hepatic stellate cell lines, LX-1 and LX-2: new tools for analysis of hepatic fibrosis. Gut 2005;54:142-151.
27. Peppel K, Zhang L, Orman ES, Hagen PO, Amalfitano A, Brian L, et al. Activation of vascular smooth muscle cells by TNF and PDGF: overlapping and complementary signal transduction mechanisms. Cardiovasc Res 2005;65:674-682.
28. Yu Q, Stamenkovic I. Cell surface-localized matrix metalloproteinase-9 proteolytically activates TGF-beta and promotes tumor invasion and angiogenesis. Genes Dev 2000;14:163-176.
29. Cao Q, Mak KM, Lieber CS. Dilinoleoylphosphatidylcholine decreases acetaldehyde-induced TNF-alpha generation in Kupffer cells of ethanol-fed rats. Biochem Biophys Res Commun 2002;299:459-464.
30. Gieling RG, Wallace K, Han YP. Interleukin-1 participates in the progression from liver injury to fibrosis. Am J Physiol Gastrointest Liver Physiol 2009;296:G1324-G1331.
31. Radbill BD, Gupta R, Ramirez MC, Difeo A, Martignetti JA, Alvarez CE, et al. Loss of matrix metalloproteinase-2 amplifies murine toxin-induced liver fibrosis by upregulating collagen I expression. Dig Dis Sci 2011;56:406-416.

OBJECTIU 2

Articles derivats:

Moles A, et al. **Acid Sphingomyelinase promotes Hepatic Stellate Cell activation and liver fibrosis via Cathepsins B induction**. *Am J Pathol* 2010;177(3p1214-24.

Moles A*, Tarrats N*, et al. **Cathepsin B overexpresion due to acidic sphingomyelinase ablation promotes liver fibrosis in Niemann-Pick disease**. *J Biol Chem*. 2012;287(2p1178-88.

Resum:

- L'activitat de l'ASMasa, però no de l'esfingomielinasa neutra (NSMasap augmenta a mesura que les CEH es transdiferencien de forma paral·lela a l'augment en l'expressió α-SMA, CtsB i CtsD, indicant que l'activació *in vitro* de les CEH comporta una estimulació marcada i selectiva de l'ASMasa.

- Donat que en estudis anteriors del grup (Moles et al. 2009ps'havia relacionat la CtsB/D amb la fibrosi i per altra banda s'ha associat la CtsD amb l'ASMasa en un context de mort cel·lular (Heinrich et al. 2004p varem voler avaluar si l'augment del processat de les CtsB/D durant la transdiferenciació de les CEH associat a fibrogènesi era o no dependent de l'ASMasa. Així doncs, mitjançant la inhibició genètica (siRNAsp o farmacològica (imipraminap de l'ASMasa observàrem que el processat de la CtsB/D durant l'activació de les CEH depèn de l'ASMasa.

- La inhibició de l'ASMasa condueix a un menor processat de les CtsB/D, i redueix el potencial proliferatiu tant de les CEH primàries de ratolí com de les LX2 humanes. La inhibició específica de CtsB no modifica l'activitat de l'ASMasa, indicant que és l'ASMase qui regula l'activitat CtsB. Així doncs, tant en humans com en ratolí, la regulació de les CEH mitjançant el processament de les CtsB/D mediat per ASMasa, tindria una potencial rellevància en la fibrosi hepàtica.

- Donat que la inhibició de l'ASMasa condueix a una reducció de CtsB/D i la proliferació de les CEH, vam estudiar el procés de transdiferenciació de CEH procedents de ratolins heterozigots per l'ASMasa (ASMasa$^{+/-}$p, els quals mostren un 40% d'activitat ASMasa romanent. Les CEH d'aquests ratolins tenen una menor expressió de CtsB/D i α-SMA durant la seva activació, i una taxa de proliferació basal més baixa que els ratolins control (ASMasa$^{+/+}$p Aquests efectes eren encara més acusats després del tractament amb l'inhibidor de la CtsB.

- Basats en els resultats anteriors, s'esperaria, *in vivo,* que en estudis de fibrogènesi mitjançant lligadura del conducte biliar (LCBpels ratolins ASMasa$^{+/-}$ mostréssin una menor fibrosi que els controls, mentre que el possible efecte de la presència d'ASMase sobre el dany hepàtic seria menys predictiu. Així doncs, els animals ASMasa$^{+/-}$ amb LCB mostraven un menor dany hepàtic tant histològicament com bioquímicament (ALTp, així com una menor expressió de pro-col·lagen tipus I. L'expressió de TNF, però, era similar respecte els ratolins salvatges amb LCB. Aquests resultats indiquen la rellevància de l'expressió de l'ASMasa en el control del dany hepàtic i en la fibrogènesi en ratolins colestàsics.

- L'altre model *in vivo* utilitzat és el del CCl_4. En aquest cas però, el dany hepàtic que s'observa és similar en animals control com ASMasa$^{+/-}$. Tot i així, els ratolins ASMasa$^{+/-}$ mostraren una menor fibrosi juntament amb una reduïda expressió de pro-col·lagen tipus I, i menys presència de cèl·lules α-SMA positives. Així doncs, a diferència del model LCB, aquests resultats mostren un paper crucial de l'ASMasa en la fibrosi hepàtica, independent del dany.

- Es va voler comprovar si aquest increment de CtsB i ASMasa, observats en ratolins i en CEH, podia ser observat en alguna patologia crònica hepàtica humana. Per aquest motiu varem analitzar l'expressió de CtsB i ASMasa en pacients amb diferents estadis d'esteatohepatitis no alcohòlica (NASHpon hi havia un % molt elevat d'individus amb fibrosi hepàtica. Observàvem que els individus amb un estadi molt avançat de NASH mostraven una expressió més elevada d'ASMasa i de CtsB respecte a pacients control, mentre que els que estaven en un estadi intermedi només mostraven una expressió elevada de CtsB.

- Basant-nos en les observacions que indicaven que els ratolins heterozigots de l'ASMasa, mostraven una reducció del 60-70% de la seva activitat i de l'expressió i activitat de la CtsB, vam voler observar què passava en ratolins deficients en ASMasa (ASMasa$^{-/-}$p, model animal per a la malaltia de Niemann-Pick tipus A. Sorprenentment, tot i que l'activitat ASMasa és nul·la, l'activitat de la CtsB no es veia disminuïda sinó que augmentava d'una forma molt contundent, indicant així un possible mecanisme compensatori. En concret, vam observar que les CEH ASMasa$^{-/-}$ mostraven una major expressió i activitat de CtsB/D, així com una major taxa de proliferació i expressió de gens pro-fibrogènics com α-SMA, pro-col·lagen tipus I, o TGF-β. Així doncs, les CEH ASMasa$^{-/-}$ mostren un potencial fibrogènic augmentat que correlacionaria amb nivells elevats de CtsB/D.

- Es va voler analitzar si la regulació a l'alça de la CtsB, observada en CEH de ratolins ASMasa$^{-/-}$, era la responsable del seu elevat potencial fibrogènic. Usant l'inhibidor específic de la CtsB (Ca074-Mepvarem observar com es reduïen els nivells basals elevats de pro-col·lagen tipus I, α-SMA i la proliferació de les CEH ASMasa$^{-/-}$. Observàvem doncs, que la CtsB és la responsable de les característiques d'una potencial fibrogènesi més augmentada en les CEH ASMasa$^{-/-}$.

- Ja que en resultats previs havíem observat que els animals ASMasa$^{+/-}$ són menys sensibles a la fibrosi induïda *in vivo* degut a una menor activació de la CtsB, vam voler observar si aquesta sobreexpressió compensatòria de CtsB en els ratolins ASMasa$^{-/-}$ contribuïa a una sensibilització i per tant un increment de la fibrosi. El model usat va ser el de CCl_4 administrat durant 4 setmanes. Els ratolins ASMasa$^{-/-}$, tot i mostrar un dany hepàtic similar, mostraven una major activitat CtsB, major processat de CtsB, major grau de fibrosi, així com un número més elevat de cèl·lules α-SMA positives, i infiltració de neutròfils. Així doncs, es podia constatar que la fibrosi hepàtica està clarament augmentada en els animals ASMasa$^{-/-}$. En aquest model, la inhibició farmacològica de CtsB millorava la fibrogènesi en els animals ASMasa$^{-/-}$ tractats amb CCl_4. Els animals tractats amb inhibidor no mostraven cap millora en quan a dany hepàtic, fet que indica que la CtsB no participa en el mecanisme responsable del dany hepàtic; però es disminuïa l'expressió i processat de l'α-SMA i la CtsD, i es

reduïa de forma clara la tendència fibrogènica, les cèl·lules α-SMA positives i la infiltració de neutròfils. Aquests resultats indicaven que efectivament la CtsB juga un paper crític en la fibrogènesi *in vivo* en els animals ASMasa$^{-/-}$.

- També es va voler analitzar si l'expressió augmentada de CtsB es donava únicament al fetge dels animals ASMasa$^{-/-}$, o si per al contrari, era un efecte extensiu a altres òrgans. L'expressió i activitat de la CtsB i D estava clarament augmentada en cervell, pulmó, teixit adipós epididimal, múscul i pell. En melsa, pàncrees i intestí, no s'observava cap canvi significatiu. Cal recalcar que fetge, cervell i pulmó, on s'observa una clara inducció de CtsB, són els teixits més afectats per la NPD, que és causada per una absència/disminució d'ASMasa.

- També vam analitzar, emprant un anticòs pan-catepsina, la potencial participació d'altres catepsines diferents de CtsB o CtsD en el fenotip NPD. El patró d'expressió de les diferents catepsines eren similars entre les CEH control i les procedents d'animals ASMasa$^{-/-}$. Tot i que observem patrons diferents d'expressió entre els diferents teixits estudiats, no varem trobar diferències significatives entre els animals control i ASMasa$^{-/-}$, a excepció del pulmó, on es veia en els animals ASMasa$^{-/-}$, un increment marcat d'una catepsina, la identitat de la qual desconeixem. Aquests resultats indicaven que la participació d'altres catepsines en el fenotip NPD seria teixit específic.

- Donat que la CtsB s'ha relacionat amb mort cel·lular a través del seu alliberament del lisosoma al citosol, varem voler determinar si l'estabilitat lisosomal estava afectada en les CEH i els diferents teixits dels animals control i ASMasa$^{-/-}$. Un augment en l'expressió de la proteïna lisosomal LAMP-2 en CEH i teixits ASMasa$^{-/-}$ indicava que l'augment de CtsB en ASMasa$^{-/-}$ seria en part degut a un increment de la massa lisosomal, i no a una desestabilització dels mateixos lisosomes. La localització de CtsB al lisosoma, i no al citosol, es va validar també mitjançant microscopia confocal.

- Per últim, analitzàrem si l'autofagia, molt relacionada amb processos degeneratius i depenent de proteases lisosomals, jugava algun paper en l'activació de les CEH i la degeneració tissular observada en els ratolins ASMasa$^{-/-}$. Mitjançant la determinació del truncament de la proteïna LC3-I en LC3-II (relacionada amb la quantitat d'autofagosomes), vam veure que malgrat

que en alguns teixits de ratolins ASMasa$^{-/-}$ s'observava una major presència de LC3-II que en ratolins salvatge, no hi havia una correlació entre l'expressió de CtsB/D i la conversió de LC3-I a LC3-II , descartant per tant una contribució de l'increment de CtsB/D en els processos autofàgics en la NPD.

The American Journal of Pathology, Vol. 177, No. 3, September 2010

DOI: 10.2353/ajpath.2010.091257

Gastrointestinal, Hepatobiliary and Pancreatic Pathology

Acidic Sphingomyelinase Controls Hepatic Stellate Cell Activation and *in Vivo* Liver Fibrogenesis

Anna Moles,*† Núria Tarrats,*† Albert Morales,*† Marlene Domínguez,* Ramón Bataller,* Juan Caballería,* Carmen García-Ruiz,*† José C. Fernández-Checa,*†‡ and Montserrat Marí*†

From the Institut d'Investigacions Biomèdiques August Pi i Sunyer, Liver Unit, Hospital Clinic, Centre d'Investigació Biomèdica Esther Koplowitz, Centro de Investigación Biomédicas en Red en el Área temática de Enfermedades Hepáticas y Digestivas; Department of Cell Death and Proliferation,† Consejo Superior de Investigaciones Científicas Instituto de Investigaciones Biomédicas de Barcelona, Barcelona, Spain; and the Research Center for Alcoholic Liver and Pancreatic Diseases,‡ Keck School of Medicine of the University of Southern California, Los Angeles, California*

The mechanisms linking hepatocellular death, hepatic stellate cell (HSC) activation, and liver fibrosis are largely unknown. Here, we investigate whether acidic sphingomyelinase (ASMase), a known regulator of death receptor and stress-induced hepatocyte apoptosis, plays a role in liver fibrogenesis. We show that selective stimulation of ASMase (up to sixfold), but not neutral sphingomyelinase, occurs during the transdifferentiation/activation of primary mouse HSCs into myofibroblast-like cells, coinciding with cathepsin B (CtsB) and D (CtsD) processing. ASMase inhibition or genetic down-regulation by small interfering RNA blunted CtsB/D processing, preventing the activation and proliferation of mouse and human HSCs (LX2 cells). In accordance, HSCs from heterozygous ASMase mice exhibited decreased CtsB/D processing, as well as lower levels of α-smooth muscle actin expression and proliferation. Moreover, pharmacological CtsB inhibition reproduced the antagonism of ASMase in preventing the fibrogenic properties of HSCs, without affecting ASMase activity. Interestingly, liver fibrosis induced by bile duct ligation or carbon tetrachloride administration was reduced in heterozygous ASMase mice compared with that in wild-type animals, regardless of their sensitivity to liver injury in either model. To provide further evidence for the ASMase-CtsB pathway in hepatic fibrosis, liver samples from patients with nonalcoholic steatohepatitis were studied. CtsB and ASMase mRNA levels increased eight- and threefold, respectively, in patients compared with healthy controls. These findings illustrate a novel role of ASMase in HSC biology and liver fibrogenesis by regulating its downstream effectors CtsB/D. ***(Am J Pathol 2010, 177:1214–1224; DOI: 10.2353/ajpath.2010.091257)***

Hepatic fibrosis is a wound-healing response of the liver to chronic injury and represents a common and complex clinical challenge worldwide.[1–3] Liver fibrosis often reflects progressive liver disease caused by a variety of factors and etiologies including viral infection, cholestasis, alcoholic steatohepatitis, and nonalcoholic steatohepatitis (NASH). In developed countries, nonalcoholic fatty liver disease is associated with increasing rates of obesity and is currently one of the most common forms of chronic liver disease and a major cause of hepatic fibrosis. Nonalcoholic fatty liver disease, which encompasses a spectrum of liver diseases ranging from simple steatosis to NASH, is characterized by oxidative stress, inflammation, hepatocellular death, and fibrosis, which can further progress to cirrhosis and hepatocellular carcinoma.[4–6] Thus, the number of individuals at risk for fibrosis and end-stage liver disease is rapidly expanding.[7]

In the liver, myofibroblasts are potentially derived from a number of cellular sources including activated hepatic stellate cells (HSCs), which mediate the fibrotic compo-

Supported by the Instituto de Salud Carlos III (grants PI070193 and PI0900056); the Plan Nacional de I+D, Spain (grants SAF2006-06780, SAF2005-06245, SAF2008-02199, 2009-11417); and the Research Center for Liver and Pancreatic Diseases, National Institute on Alcohol Abuse and Alcoholism, National Institutes of Health (grant P50-AA-11999). M.M. is an Institut d'investigacions Biomèdiques August Pi i Sunyer Investigator. A.M. is a recipient of a predoctoral fellowship from the Instituto de Salud Carlos III.

M.M. and J.C.F.-C. contributed equally to this work.

Accepted for publication May 6, 2010.

None of the authors disclosed any relevant financial relationships.

Supplemental material for this article can be found on *http://ajp.amjpathol.org.*

Address reprint requests to José C. Fernandez-Checa, Ph.D., or Montserrat Marí, Ph.D., Liver Unit, Hospital Clinic, C/Villarroel 170, 08036-Barcelona, Spain. E-mail: checa229@yahoo.com and monmari@clinic.ub.es.

nent of the wound-healing response to chronic injury.[1,2,8] Under these conditions, HSCs undergo a phenotypic transformation from quiescent, nonproliferating, retinoid-storing cells, to a proliferating, matrix-producing phenotype similar to myofibroblasts responsible for the progression of liver fibrosis.[9,10] Despite increasing knowledge of the mechanisms that govern this so-called "activation," the treatment for advanced liver fibrosis is inefficient, and hence the development of novel antifibrotic targets and therapies is essential.

Membrane sphingolipids have been implicated in signal transduction cascades regulating proliferation, differentiation, and cell death.[11,12] Among sphingolipids, ceramide has attracted considerable attention, given its central role in sphingolipid metabolism. Cellular ceramide levels increase in response to a variety of stimuli and agents from chemotherapy[13] to death ligands,[14–17] radiation,[18] or viral/bacterial infections,[19,20] because of the hydrolysis of sphingomyelin mainly by two specific phosphodiesterases named sphingomyelinases, a plasma membrane-bound neutral sphingomyelinase (NSMase) and an acidic SMase (ASMase).[21–24] In particular, ASMase is expressed by almost any cell type and is mainly located at the endosomal/lysosomal compartment, although it has also been found at the plasma membrane in specific microdomains, where it serves as a signaling platform by cell surface receptors such as Fas.[14–17] The placement of ASMase at the crossroad of vesicular trafficking and cellular signaling suggests that ASMase exerts important functions in signal transduction pathways. For instance, tumor necrosis factor (TNF) is a prominent prototype of an ASMase-activating cytokine that is central to the regulation of both the innate and the adaptive immune system as well as cell death.[25,26] Although ASMase has been recognized to play a key role in the pathophysiology of different common diseases,[27] its specific contribution to liver fibrosis has not been examined previously.

Moreover, the participation of cathepsin D (CtsD) as a target of ASMase-generated ceramide in endolysosomal compartments[28,29] and the observation that cathepsin B (CtsB)-deficient hepatocytes are resistant to TNF-dependent cell death[30] imply a functional relationship between ASMase and cathepsins, at least, in cell death regulation. However, this specific link has not been previously addressed in HSC biology and liver fibrosis. Because we have just uncovered a new function of CtsB and CtsD in mediating HSC activation and liver fibrosis,[31] our aim was to investigate the role of ASMase in hepatic fibrogenesis. In this study, we tested whether ASMase contributes to the activation of mouse HSCs *in vitro* and to the development of fibrosis *in vivo* after bile duct ligation (BDL) or chronic carbon tetrachloride (CCl_4) injection. Here, we show that ASMase activity is induced during the transdifferentiation of HSCs into myofibroblasts, whereas HSC activation and proliferation are reduced by genetic or pharmacological antagonism of ASMase. Interestingly, heterozygous ASMase mice were resistant to BDL and chronic CCl_4 administration-induced liver fibrosis compared with wild-type mice, even though their sensitivity to liver injury was markedly different with reduced liver damage in $ASMase^{+/-}$ mice after BDL but not after CCl_4 administration. In addition, patients with NASH displayed enhanced levels of both CtsB and ASMase mRNA, underscoring the role of the ASMase-cathepsins axis in liver pathology and its relevance for future therapeutic approaches.

Materials and Methods

Reagents

The following reagents were from Invitrogen (Paisley, UK): Dulbecco's modified Eagle's medium, trypsin-EDTA, penicillin-streptomycin, TRIzol, fetal bovine serum, HistoGrip, Opti-MEM, and Lipofectamine LTX with PLUS. All tissue culture ware was from Nunc (Roskilde, Denmark). The DAKO Biotin Blocking System, peroxidase substrate (diaminobenzidine), peroxidase buffer, and hematoxylin were from DAKO (Glostrup, Denmark). Aquatex was from Merck (Darmstadt, Germany). The ABC kit was from Vectastain (Burlingame, CA). Platelet-derived growth factor (PDGF)-BB was from PeproTech EC (London, UK). Proteinase inhibitors were from Roche (Madrid, Spain). The iScript One-Step RT-PCR kit with SYBR Green was from Bio-Rad (Hercules, CA). ECL Western Blotting Substrate was from Pierce (Thermo Fisher Scientific, Rockford, IL). Imipramine, amitriptyline, and Ca074Me were from Sigma-Aldrich (St. Louis, MO), and unless otherwise stated all other reagents were also from Sigma-Aldrich.

Antibodies

We used the following primary antibodies: rabbit polyclonal anti-cathepsin B from Upstate (Millipore, Billerica, MA), goat polyclonal anti-cathepsin D from Santa Cruz Biotechnology (Heidelberg, Germany), and monoclonal antibodies anti-α-smooth muscle actin (SMA) and anti-β-actin from Sigma-Aldrich. Rabbit polyclonal anti-α-SMA and rabbit polyclonal anti-myeloperoxidase were from Abcam (Cambridge, UK). ECL-labeled anti-mouse, anti-rabbit, and anti-goat antibodies were from Sigma-Aldrich.

Mice and HSC Isolation

Wild-type, heterozygous, and ASMase knockout mice (male, 8 to 10 weeks old, littermates) (C57BL/6 strain) were obtained by propagation of heterozygous breeding pairs (a generous gift from R. Kolesnick, Memorial Sloan-Kettering Cancer Center, New York, NY, and E. Gulbins, University of Duisburg-Essen, Essen, Germany) and genotyped as described previously.[26] All animals received humane care according to the criteria outlined in the *Guide for the Care and Use of Laboratory Animals*, published by the National Institutes of Health.[32] HSCs were isolated by perfusion with collagenase-pronase and cultured as described previously.[31] Cells were cultured in Dulbecco's modified Eagle's medium complemented with 10% fetal bovine serum and antibiotics at 37°C in a humidified atmosphere of 95% air and 5% CO_2.

In Vivo *Liver Fibrogenesis*

To perform BDL, ASMase$^{+/+}$ and ASMase$^{+/-}$ mice were anesthetized by isoflurane inhalation. Under anesthesia, the peritoneal cavity was opened and the common bile duct was double-ligated with 5-0 sutures and cut between the ligatures. Controls underwent a sham operation that consisted of exposure but not ligation of the common bile duct. Animals were sacrificed 4 days after BDL, and liver and serum samples were collected for analyses. In another set of experiments, ASMase$^{+/+}$ and ASMase$^{+/-}$ mice were treated with CCl_4 diluted in corn oil at a dose of 0.5 μl of CCl_4/g b.wt. by intraperitoneal injection twice a week, for 6 weeks. Control animals received vehicle alone.

In Vitro *Small Interfering RNA Transfection*

To silence ASMase expression, specific predesigned siRNAs for mouse[33] were used for transfection using Lipofectamine LTX with PLUS following the manufacture's instruction as described previously.[31] Cells were transfected 5 days after isolation and usually assayed 48 hours after small interfering (si) RNAs transfection.

ASMase and NSMase Activities

ASMase and NSMase activities from tissue or HSC lysates were determined using a fluorescent sphingomyelin analog (NBD-C6-sphingomyelin). Samples were incubated for 60 minutes at 37°C in incubation buffer containing 10 μmol/L NBD-C6-sphingomyelin (250 mmol/L sodium acetate and 0.1% Triton X-100, pH:5.0, for ASMase analysis, and 20 mmol/L HEPES, 1 mmol/L $MgCl_2$, and 0.1% Triton X-100, pH 7.4, for NSMase). Lipids were extracted, dried under N_2, and separated by thin-layer chromatography (chloroform-methanol-20% NH_4OH, 70:30:5, v/v). NBD-ceramide was visualized under UV light, and images were acquired and analyzed using a Gel Doc XR System with Quantity One software (Bio-Rad).

Real Time RT-PCR and Primer Sequences

Total RNA from HSCs, mouse liver tissues, or LX2 cells was isolated with TRIzol reagent. Real-time RT-PCR was performed with an iScript One-Step RT-PCR Kit with SYBR Green following the manufacturer's instructions. The primers sequences used were the following: mouse α-SMA, forward 5′-ACTACTGCCGAGCGTGAGAT-3′ and reverse 5′-AAGGTAGACAGCGAAGCCAA-3′ (GenBank accession no. NM_007392); mouse transforming growth factor-β, forward 5′-GTCAGACATTCGGGAAGCAG-3′ and reverse 5′-GCGTATCAGTGGGGGTCA-3′ (GenBank accession no. NM_011577); mouse β-actin, forward 5′-GACGGCCAGGTCATCACTAT-3′and reverse 5′-CGGATGTCAACGTCACACTT-3′ (GenBank accession no. NM_007393); mouse collagen type 1α1 (Col1A1), forward 5′-ACTTCAGCTTCCTGCCTCAG-3′ and reverse 5′-TGACTCAGGCTCTTGAGGGT-3′ (GenBank accession no. NM_007742); mouse TNF-α, forward 5′-CTGAACTTCGGGGTGATCGGT-3′ and reverse 5′-ACGTGGGCTACAGGCTTGTCA-3′ (GenBank accession no. NM_013693); mouse 2′,5′ oligoadenylate synthetase 1, forward 5′-GACCTGCTGAAGGAGGTGAA-3′ and reverse 5′-GGTACGCCCACTGATGAGAT-3′ (GenBank accession no. AF466822); human β-actin, forward 5′-GATGAGATTGGCATGGCTTT-3′ and reverse 5′-GAGAAGTGGGGTGGCTT-3′ (GenBank accession no. NM_001101); and human α-SMA, forward 5′-CCGACCGAATGCAGAAGG-3′ and reverse 5′-ACAGAGTATTTGCGCTCCGGA-3′ (GenBank accession no. NM_001613).

CtsB Activity

CtsB activity was assayed fluorimetrically with *Z*-Arg-Arg-7-amido-4-methylcoumarin hydrochloride (60 μmol/L) at pH 7.4 and 37°C as described previously.[31]

[^{3}H]Thymidine Incorporation

Proliferation was estimated as the amount of [^{3}H]thymidine incorporated into trichloroacetic acid-precipitable material as described previously.[31]

SDS-Polyacrylamide Gel Electrophoresis and Immunoblot Analysis

Lysates were prepared in radioimmunoprecipitation assay buffer (50 mmol/L Tris-HCl, pH 7.4, 150 mmol/L NaCl, 1% Nonidet P-40, 1 mmol/L Na_3VO_4, 1 mmol/L EDTA, 0.25% sodium deoxycholate, 0.1% SDS, and 1% Triton X-100 plus proteinase inhibitors). Protein concentration was determined by the Bradford assay, and samples containing 10 to 30 μg were separated by 8 to 10% SDS-polyacrylamide gel electrophoresis. Proteins were transferred to nitrocellulose membranes. After membranes were blocked in 8% nonfat milk in 20 mmol/L Tris-HCl, 150 mmol/L NaCl, and 1% Tween 20 for 1 hour at room temperature, the membranes were incubated with the primary antibody overnight and developed with the ECL-peroxidase system.

Determination of Hydroxyproline in Liver Tissue

Hepatic hydroxyproline content was determined as described by Jamall et al.[34] In brief, tissue samples were hydrolyzed in 6 mol/L HCl overnight at 100°C and purified 4-hydroxy-L-proline standards for 20 minutes at 120°C. Free hydroxyproline content from each hydrolysate was oxidized with Chloramine-T. The addition of Ehrlich reagent resulted in the formation of a chromophore that was read at 550 nm. Data were normalized to liver wet weight.

Immunohistochemical Staining

Paraffin molds containing liver sections were cut into 5-μm sections and mounted on HistoGrip-coated slides. The sections were deparaffinized in xylene and dehydrated in a graded alcohol series. When necessary, endogenous peroxidase (3% H_2O_2) and endogenous avidin

and biotin were blocked. Slides were incubated with primary antibody overnight in a wet chamber at 4°C. After a rinse with 1× PBS, the slides were incubated with a biotinylated antibody for 45 minutes in a wet chamber and developed with an ABC Kit with peroxidase substrate (diaminobenzidine) and peroxidase buffer. After the slides were rinsed with tap water, they were counterstained with hematoxylin and mounted with Aquatex.

H&E and Sirius Red Staining

Livers were fixed, and sections of 7-μm were routinely stained with H&E or with a 0.1% Sirius Red-picric solution following standard procedures. Bile-infarcted areas (the percentage of infarct area per high power field) were also quantified using digital image analysis software (ImageJ).

Human NASH Cohort

Patients with either borderline NASH (n = 14) or definite NASH (n = 18), according to the Kleiner classification,[35] sent to the hospital for bariatric surgery were included in the study. Patients underwent gastric bypass by laparoscopy and during the surgery procedure a liver biopsy was obtained using a Tru-Cut needle. Normal livers were obtained from optimal cadaveric liver donors (n = 3) or resection of liver metastases (n = 2). All controls had normal serum aminotransferase levels and normal liver histology. These subjects did not have a past history of liver disease, alcohol abuse, or metabolic syndrome. The study was approved by the ethics committee of the Hospital Clinic, and all patients gave informed consent.

Hepatic Gene Expression Analysis in Human Samples

Liver biopsy specimens were submerged in an RNA stabilization solution (RNAlater, Ambion, Applied Biosystems, Austin, TX) and stored at −20°C until RNA extraction. Total RNA was extracted with TRIzol. Five hundred micrograms of total RNA were retrotranscribed with a high-capacity complementary DNA Archive Kit (Applied Biosystems). The genes selected were distributed into 384-well TaqMan Low Density Array cards, and samples were analyzed in quadruplicate using an ABI PRISM 7900 (Applied Biosystems). Predesigned TaqMan assays for target genes from Applied Biosystems were used (CtsB, Hs00157194_m1; ASMase, Hs00609415_m1; and 18S, Hs99999901_s1). Expression levels of target genes were normalized to expression of 18S rRNA (endogenous gene). Gene expression values were calculated based on the $\Delta\Delta C_t$ method.[36] The results are expressed as $2^{-\Delta\Delta C_t}$ referred as fold in relation to mean normal livers.

Statistical Analysis

All images display representative data from at least three independent observations. Statistical analyses were performed using Microsoft Excel software. The statistical significance of differences was determined using the unpaired, nonparametric Student's t-test.

Results

In Vitro *Activation of Mouse Primary HSCs Parallels ASMase Stimulation*

The culture of primary freshly isolated HSCs on plastic is known to cause transdifferentiation from a quiescent to a proliferating phenotype characterized by the activation of matrix-producing genes, which is the standard approach to analyze the activation of HSCs into myofibroblast-like cells.[2,8,9] Because this transdifferentiation is a central event in liver fibrogenesis, we first studied whether this process is accompanied by changes in ASMase activity. Thus, freshly prepared mouse primary HSCs were isolated to analyze ASMase and NSMase activity at different time points during transdifferentiation in culture. As shown in Figure 1A, ASMase activity, but not NSMase activity, increased more than fivefold from day 2 to day 9 of culture. In addition, the ASMase activity observed in primary mouse HSCs at day 9 was similar to the ASMase activity of LX2 cells (620 ± 85 vs. 583 ± 63 arbitrary units/mg of protein), an immortalized human HSC cell line similar to human activated HSCs.[37] This increase in ASMase activity paralleled the expression of α-SMA, a reliable marker of the phenotypic transformation of HSCs into myofibroblast-like cells,[2] which coincided with the levels of mature forms of CtsB and CtsD (Figure 1B). Thus, these findings indicate that *in vitro* activation of HSCs results in marked and selective stimulation of ASMase.

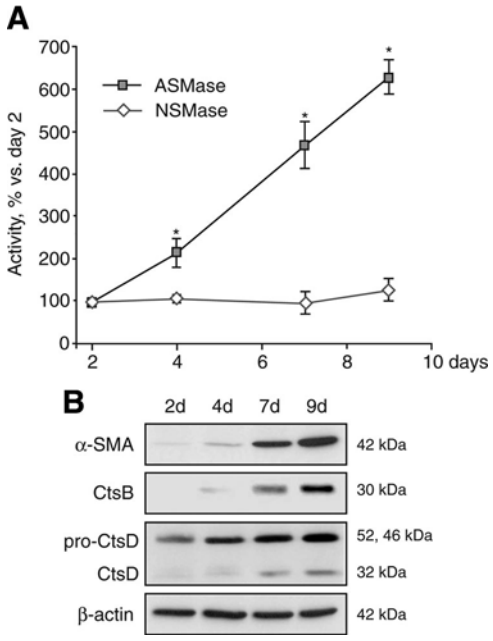

Figure 1. ASMase activity increases concordantly with CtsB and CtsD expression during HSC activation. **A:** Time-course of ASMase and NSMase activity during mouse HSC activation in culture. **B:** Time-course of α-SMA, CtsB, and CtsD expression in primary mouse HSCs in *in vitro* culture from day two to day nine. Data are means ± SD; n = 3. *$P \leq 0.05$ versus day 2 HSCs.

Pharmacological ASMase Inhibition or Genetic Silencing Blunts CtsB/D Processing and HSC Activation

Given our previous results positioning CtsB/D as key players in liver fibrosis[31] and because a functional relationship between ASMase and cathepsins has been established only in cell death regulation,[28,29] we decided to evaluate whether the increased processing of CtsB and/or CtsD observed during HSC activation and recently associated with liver fibrogenesis,[31] was dependent on ASMase. Therefore, ASMase was antagonized by two approaches, pharmacological inhibition and genetic down-regulation by siRNAs. Imipramine and amitriptyline are weak bases that induce the detachment of ASMase from the intralysosomal membrane, resulting in its subsequent functional inactivation.[38] As shown in Figure 2A, both imipramine treatment and ASMase silencing by siRNA resulted in a reduction in ASMase activity by 85 ± 4 and 48 ± 12%, respectively, without inducing an interferon response (not shown). The decline in ASMase activity, either by pharmacological inhibition or genetic silencing, resulted in decreased expression of CtsB/D processed forms (Figure 2, B and C). Moreover, the expression of α-SMA was also reduced under these conditions (Figure 2, B and D), indicating an attenuation of the fibrogenic properties of HSCs after ASMase antagonism. The expression of Col1A1 or transforming growth factor-β, however, was not significantly altered after ASMase inhibition or silencing (not shown), discarding the theory of direct participation of ASMase in either of these two pathways. On the other hand, complete CtsB inhibition, using Ca074Me, was able to significantly decrease transforming growth factor-β expression (not shown), consistent with our previous observations.[31] In addition, pharmacological inhibition of ASMase dramatically prevented HSC proliferation (Figure 2E). Even though cathepsins have previously been implicated in the degradation of PDGFβR,[39,40] we have not observed any alteration in the basal levels of PDGFβR with inhibition of either ASMase or CstB (not shown). In line with this result, we have previously reported that although CtsB inhibition did not affect PDGFβR levels, it impaired AKT phosphorylation after PDGF challenge, thus regulating HSC proliferation.[31] To analyze the hierarchy between ASMase and cathepsins, we evaluated the effect of CtsB inhibition on ASMase levels. CtsB inhibition did not alter ASMase activity (Figure 2F) but was able to significantly blunt HSC proliferation (Figure 2E). Therefore, our results suggest that CtsB and CtsD processing depend on and are downstream of ASMase during the activation of HSCs into myofibroblasts.

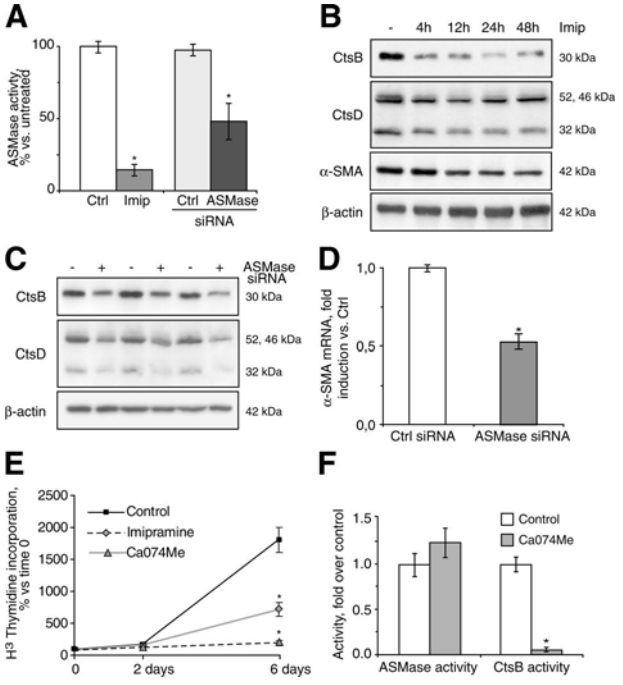

Figure 2. ASMase inhibition or siRNA transfection reduces HSC activation and proliferation. **A:** ASMase activity after inhibition with imipramine (Imip, 25 μmol/L) for 24 hours or ASMase siRNA silencing for 48 hours, in cultured 7-days old mouse HSCs. CtsB and CtsD protein expression (**B**) and α-SMA mRNA levels (**D**) after ASMase siRNA silencing for 48 hours, in cultured 7-days old mouse HSCs. **C:** Time course of CtsB, CtsD, and α-SMA expression after ASMase inhibition (Imip, 25 μmol/L) in 7-day-old HSCs. **E:** Time course of HSC proliferation in the presence of ASMase (Imip, 25 μmol/L) or CtsB inhibitor (Ca074Me, 10 μmol/L) in 7-day-old HSCs. **F:** ASMase and CtsB activity on inhibition of CtsB with Ca074Me (10 μmol/L, 24 hours) in 7-day-old HSCs. Data are means ± SD; $n = 4$. $^*P \leq 0.05$ versus control HSCs. Ctrl, control.

ASMase Inhibition Attenuates the Proliferation of Human HSCs

To examine the relevance of the preceding findings in human fibrogenesis, we also evaluated the effect of ASMase inhibition in the human LX2 cell line.[37] As shown in Figure 3A, ASMase inhibition by either imipramine or amitriptyline down-regulated the processing of CtsB and CtsD forms (Figure 3B), resulting in a striking decrease of α-SMA expression at the protein and mRNA levels (Figure 3, B and

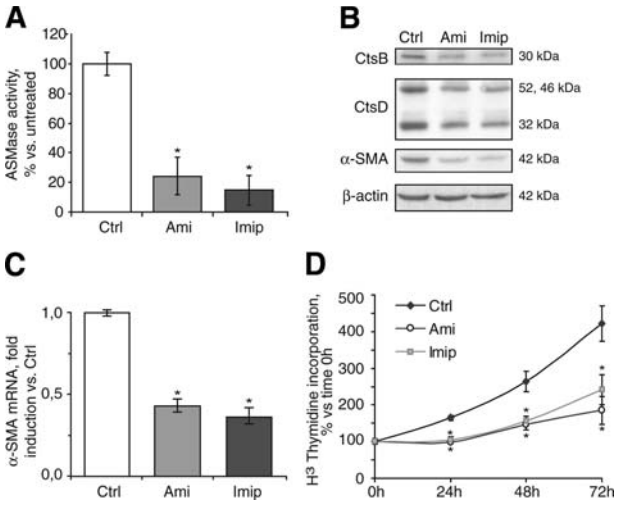

Figure 3. ASMase inhibition decreases CtsB, CtsD, and α-SMA expression as well as proliferation in the human LX2 cell line. **A:** ASMase activity after inhibition with imipramine (Imip, 25 μmol/L) or amitriptyline (Ami, 25 μmol/L) for 24 hours in LX2 cells. CtsB, CtsD, and α-SMA protein expression (**B**) and α-SMA mRNA levels (**C**) in LX2 cells after ASMase inhibition with imipramine (25 μmol/L) or amitriptyline (25 μmol/L) for 24 hours. **D:** Time course of HSC proliferation in LX2 cells in the presence ASMase inhibitors (imipramine, 25 μmol/L; amitriptyline, 25 μmol/L) for up to 72 hours. Data are means ± SD; $n = 3$. $^*P \leq 0.05$ versus control LX2 cells. Ctrl, control.

C), followed by a reduction in LX2 proliferation (Figure 3D). Thus, in humans and rodents, the regulation of HSC activation and proliferation by ASMase-mediated CtsB/D processing may be of potential relevance in liver fibrosis.

HSCs from Heterozygous ASMase Mice Exhibit Decreased ASMase Activity, CtsB/D Processing, and Proliferation

Because pharmacological inhibition or siRNA-mediated reduction in ASMase expression decreased CtsB/D levels and HSC proliferation, we next evaluated the *in vivo* transdifferentiation process using HSCs from mice with a genetic reduction in ASMase. Indeed, HSCs from heterozygous ASMase mice displayed a 60 to 70% decrease in ASMase activity (Figure 4A). ASMase$^{+/-}$ HSCs exhibited low CtsB/CtsD and α-SMA expression during *in vitro* activation (Figure 4B) compared with wild-type HSCs, consistent with the preceding data on ASMase antagonism (either pharmacological or by siRNA down-regulation). Of note, the normal proliferation rate of heterozygous ASMase$^{+/-}$ HSCs was slower than that of wild-type HSCs (Figure 4C). Moreover, CtsB inhibition, using the specific CtsB inhibitor Ca074Me, down-regulated both the proliferation (Figure 4C) and activation (Figure 4D) of wild-type and heterozygous ASMase HSCs. These findings further strengthened the evidence for a role of ASMase in the regulation of CtsB/D processing, which is critical for HSC activation and proliferation.

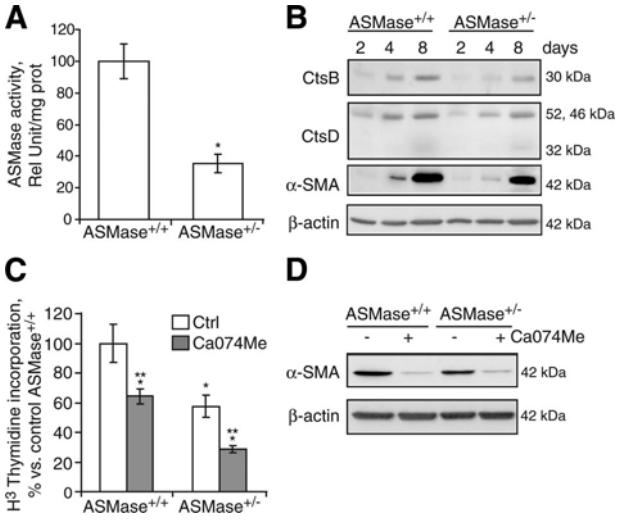

Figure 4. Heterozygous ASMase$^{+/-}$ HSCs exhibit decreased expression of CtsB, CtsD, and α-SMA, and reduced proliferation in culture. **A:** ASMase activity in cultured 7-day-old wild-type or heterozygous ASMase$^{+/-}$ HSCs. **B:** Time course of CtsB, CtsD, and α-SMA protein expression in wild-type and heterozygous ASMase$^{+/-}$ HSCs. Proliferation rate (**C**) and α-SMA protein levels (**D**) after CtsB inhibition (Ca074Me, 10 μmol/L, 24 hours) in wild-type or heterozygous ASMase$^{+/-}$ 7-day-old HSCs. In **A** data are means ± SD; $n = 4$. *$P \leq 0.01$ versus ASMase$^{+/+}$ HSCs. In **C** data are means ± SD; $n = 3$. *$P \leq 0.05$ versus ASMase$^{+/+}$ control HSCs; **$P \leq 0.05$ versus respective controls (Ctrl). Rel Unit, relative units.

Decreased Liver Damage and Fibrosis in Heterozygous ASMase After Bile Duct Ligation

In view of the earlier findings indicating reduced fibrogenic potential of HSCs from heterozygous ASMase mice, we next assessed the *in vivo* susceptibility of wild-type and heterozygous ASMase mice to liver fibrosis. BDL is a well established model of liver fibrosis that is associated with intrahepatic cholestasis and bile acid accumulation. Because cholestasis is also known to induce hepatocyte damage, we used BDL in ASMase$^{+/-}$ mice to examine the contribution of ASMase in BDL-mediated hepatic damage, HSC activation, and liver fibrosis. Based on our preceding findings, we would expect lower liver fibrosis after BDL in heterozygous ASMase mice compared with wild-type mice. However, for liver or hepatocyte damage, the anticipated effect of BDL on hepatocyte injury remained less predictable, based on recent findings reporting a critical role for Kupffer cell-derived ASMase in AKT activation of hepatocytes that is required for the survival and regenerative responses after BDL.[41]

Total hepatic extracts from heterozygous ASMase mice displayed a significant reduction in ASMase activity (50 to 60% decrease) compared with wild-type livers, in line with our observations during *in vitro* HSC activation (Figure 4A). Serum alanine aminotransferase (ALT), as an indicator of liver damage, was markedly increased in wild-type mice after BDL for 4 days. However, unexpectedly, ALT levels were significantly reduced in heterozygous ASMase BDL mice compared with wild-type BDL mice (Figure 5A). These observations were further validated by terminal deoxynucleotidyl transferase dUTP nick-end labeling staining of liver sections, revealing severe parenchymal damage after BDL in wild-type but not in heterozygous ASMase livers (Supplemental Figure 1, see *http://ajp.amjpathol.org*), thus indicating a novel role for ASMase in cholestasis-induced hepatocellular death. To analyze the fibrogenic process, levels of hydroxyproline (Figure 5B), a major component of collagen, and Col1A1 mRNA (Figure 5C) were analyzed. Both parameters were significantly enhanced in wild-type BDL livers but reduced in heterozygous ASMase BDL livers. Bile infarcts are confluent foci of degenerated hepatocytes due to bile acid toxicity and are a prominent feature of liver injury in the BDL mouse. The number of bile infarcts in the liver was quantified by conventional H&E staining. Numerous bile infarcts per high power field area were observed in the wild-type BDL model; however, the occurrence of bile infarcts was scarce in heterozygous BDL livers (Figure 5D). Histopathological examination of liver tissue (Figure 5E) demonstrated cholestatic hepatitis, with widespread incidence of bile infarcts and hepatocellular damage in wild-type BDL mice. In contrast, heterozygous ASMase mice displayed minor liver injury. Moreover, when the appearance of collagen was analyzed by Sirius Red staining, the presence of collagen fibers was only observed in wild-type BDL mice but not in ASMase$^{+/-}$ mice (Figure 5E). This enhanced liver damage and the presence of bile infarcts in wild-type BDL mice occurred despite expression of TNF in heterozy-

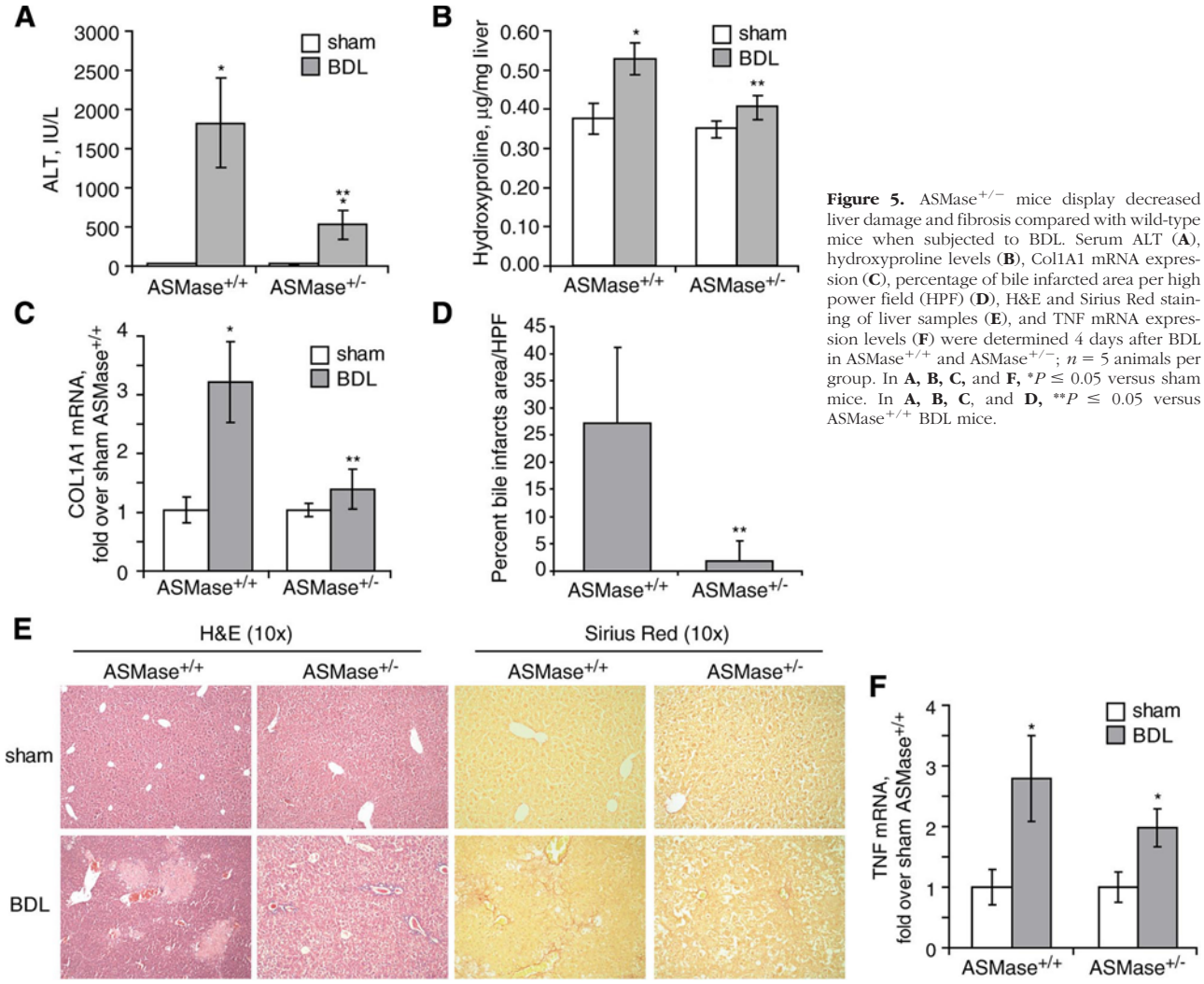

Figure 5. ASMase$^{+/-}$ mice display decreased liver damage and fibrosis compared with wild-type mice when subjected to BDL. Serum ALT (**A**), hydroxyproline levels (**B**), Col1A1 mRNA expression (**C**), percentage of bile infarcted area per high power field (HPF) (**D**), H&E and Sirius Red staining of liver samples (**E**), and TNF mRNA expression levels (**F**) were determined 4 days after BDL in ASMase$^{+/+}$ and ASMase$^{+/-}$; $n = 5$ animals per group. In **A, B, C,** and **F,** $^{*}P \leq 0.05$ versus sham mice. In **A, B, C**, and **D,** $^{**}P \leq 0.05$ versus ASMase$^{+/+}$ BDL mice.

gous ASMase BDL mice similar to that in wild-type mice (Figure 5F). Moreover, the total pool of bile acids in liver extracts after BDL did not differ between wild-type and heterozygous ASMase (not shown), indicating that the reduction in liver fibrosis is not a consequence of lower cholestasis. These findings underscore the relevance of ASMase expression in controlling both hepatocellular damage and liver fibrosis in mice during cholestasis.

Similar Liver Damage but Reduced Fibrosis in Heterozygous ASMase Mice after CCl_4 Administration

We next assessed the contribution of ASMase in an experimental model that includes significant hepatocellular injury followed by fibrosis, using the *in vivo* model of CCl_4 administration, a well established model of liver injury and liver fibrosis. CCl_4 administered twice a week for 6 weeks to ASMase$^{+/+}$ and ASMase$^{+/-}$ mice increased serum ALT to a similar level in wild-type and heterozygous ASMase mice (Figure 6A). Hepatocellular damage was also assessed by terminal deoxynucleotidyl transferase dUTP nick-end labeling staining of liver sections, revealing comparable injury in wild-type and ASMase$^{+/-}$ livers (Supplemental Figure 1, see *http://ajp.amjpathol.org*). However, regardless of the extent of liver damage, ASMase$^{+/-}$ mice exhibited significantly decreased liver fibrosis, detected by hydroxyproline levels (Figure 6B), Col1A1 mRNA expression (Figure 6C), immunostaining of α-SMA-positive cells (Figure 6D), and Sirius Red staining (Figure 6E). Thus, unlike the BDL model, these findings underscore a hepatocellular damage-independent role of ASMase in liver fibrosis.

Increased Expression of ASMase and CtsB in Livers from Patients with NASH

Finally, to explore whether the observed effects in HSCs and mice may be of potential relevance in human disease, we analyzed the mRNA expression of ASMase and CtsB in patients with NASH at different stages. As shown in Figure 7A, ASMase mRNA expression was significantly increased in a group of 18 patients with NASH with a Kleiner score of 5 to 6, indicative of definitive NASH[35] based on the assessment of the range of histological features of human NASH. However, in patients with a score of 3 to 4 and classified as having borderline NASH

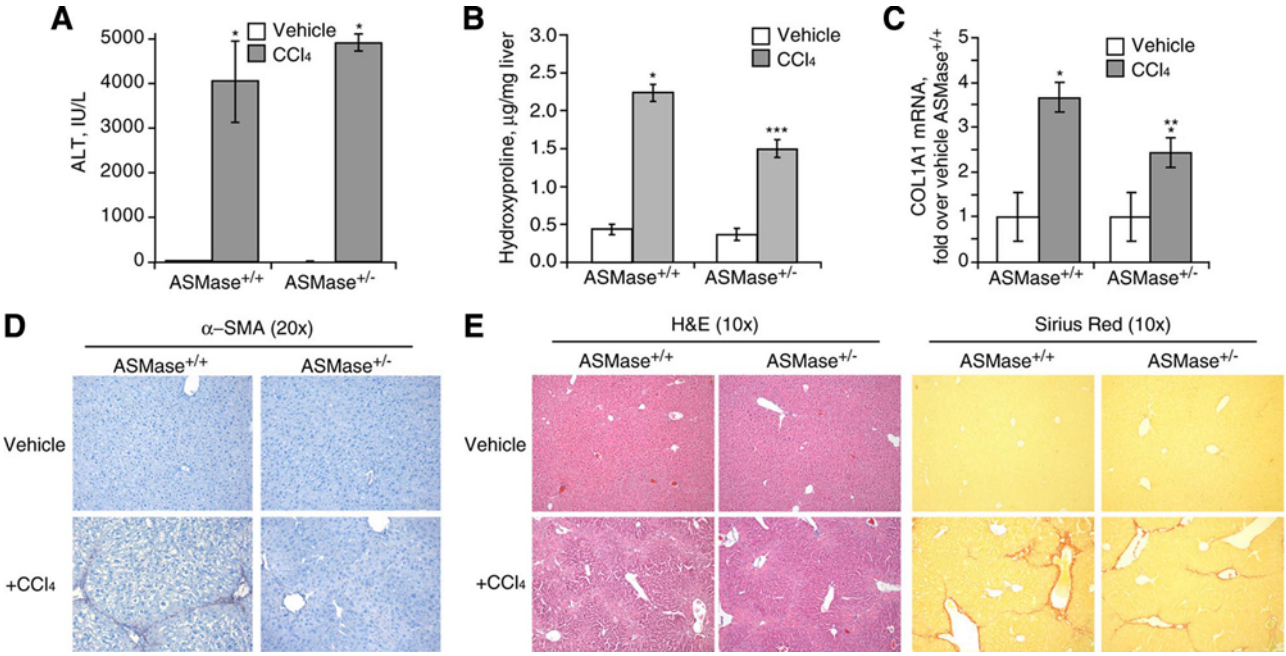

Figure 6. ASMase$^{+/-}$ mice display similar liver damage but decreased fibrosis after CCl_4 injection. Six weeks after initial CCl4 challenge, we determined serum ALT (**A**), hydroxyproline levels (**B**), Col1A1 mRNA expression (**C**), α-SMA immunostaining (**D**), and H&E and Sirius Red staining of liver samples (**E**) from ASMase$^{+/+}$ and ASMase$^{+/-}$ mice. Data are means ± SEM; $n = 5$ animals per group. In **A, B,** and **C,** $^{*}P \leq 0.05$ versus vehicle-treated mice. In **B** and **C,** $^{**}P \leq 0.05$ versus ASMase$^{+/+}$ + CCl_4-treated mice.

($n = 14$), mean mRNA expression of ASMase was increased compared with that of control patients, but it did not reach statistical significance. Of note, both groups of patients with NASH exhibited significantly enhanced CtsB mRNA expression, with a higher mean value observed in those patients who were classified as having definitive NASH (Figure 7B). In addition, although laboratory test abnormalities may be suggestive of NASH, histological evaluation remains the only way to accurately stage NASH. Even though the Kleiner activity score does not include histological evaluation of fibrosis, 71% (10 of 14) and 91.44% (17 of 18) of our patients with borderline or definite NASH, respectively, had some degree of hepatic fibrosis, none of them reaching the cirrhosis stage.

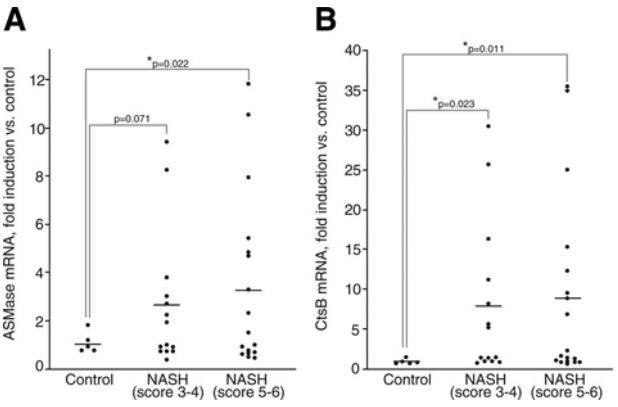

Figure 7. ASMase and CtsB expression are increased in patients with NASH. Liver samples from control or NASH subjects were processed for RNA isolation to determine the expression of ASMase mRNA (**A**) and CtsB mRNA (**B**). Patients with NASH were separated in two groups: those with a score of 3 to 4 or borderline NASH, and those with a score of 5 to 6 or definite NASH, according to the Kleiner classification. *P* values are indicated in the graph.

Moreover, the presence of fibrosis is an unequivocal indicator of progressive liver disease. In fact, despite the classification established by our pathologists, the clinical data of the patients with borderline or definite NASH, summarized in Table 1, did not reveal major significant differences among groups. In all, our findings indicate that the elevation of ASMase and CtsB levels may be of relevance in patients with NASH, including those at an initial stage of the disease. As a caveat, the only information we have available regarding CtsB and ASMase in these sets of patients is their mRNA expression, and hence we cannot directly determine that this mRNA increase is exclusively due to fibrosis. Other features of NASH, such as hepatocellular apoptosis, could contribute to this outcome because both CtsB and ASMase have also been associated with apoptosis.[12,25,27,29,30] Moreover, although in the CCl_4 model of liver fibrosis we have previously observed that the expression of CtsB was confined to activated HSCs and not in parenchymal cells,[31] we cannot reach such a conclusion in the present human cohort, which will need further study. Therefore, the present level of analyses suggests that certain patients with histological NASH have abnormal expression of hepatic ASMase and CtsB mRNA.

Discussion

Using *in vitro* HSCs and *in vivo* models of liver fibrosis, we describe a previously unknown role for ASMase in HSC activation and liver fibrosis and establish a causal relationship between ASMase and cathepsins in HSC biology. Up-regulation of ASMase has been described in

Table 1. Clinical Data of Patients with Borderline or Definite NASH

	Borderline NASH (n = 14)	Definite NASH (n = 18)	P
Age (years)	44.07 ± 3.31	49.5 ± 2.16	NS
Female (%)	42.86	66.66	NS
BMI (kg/m^2)	47.56 ± 1.94	50.49 ± 1.86	NS
Waist circumference (cm)	142.19 ± 4.17	138.08 ± 5.01	NS
Diabetes (%)	35.71	50	NS
Hypertension (%)	64.28	77.77	NS
Metabolic syndrome	71.43	88.88	NS
Glucose (mg/dl)	121 ± 12	133 ± 13	NS
HOMA	12.82 ± 2.82	11.93 ± 1.55	NS
Cholesterol (mg/dl)	184.57 ± 8.56	203.39 ± 7.87	NS
Triglycerides (mg/dl)	137.85 ± 11.34	147 ± 15.68	NS
GGT (U/L)	38 ± 4	51 ± 9	0.047
ALT (U/L)	42 ± 5	62 ± 7	NS
AST (U/L)	33 ± 3	41 ± 4	0.002
Bilirubin (mg/dl)	0.57 ± 0.06	0.58 ± 0.05	NS
Platelet count ($\times 10^9$)	296 ± 15	297 ± 17	NS
Fibrosis, stage 1 to 3 (%)	71	91.44	NS

Data are means ± SE or %.
NS, not significant; HOMA, homeostasis model assessment; GGT, γ-glutamyl transferase; ALT, alanine transferase; AST, aspartate aminotransferase.

similar contexts such as differentiation of monocytes to macrophages[42] and in drug-induced differentiation of leukemia cells.[43] Although the participation of ceramide generated by ASMase in multiple signaling cellular processes of physiological or pathological impact, such as radiation-induced apoptosis,[44] Wilson disease,[45] fulminant hepatitis,[25] cystic fibrosis,[46] *Pseudomonas aeruginosa* infection,[19] or emphysema,[47] and in other common diseases[27] has been reported, the role of ASMase in HSC activation and liver fibrogenesis had not been fully characterized so far. Recent observations suggest that the activation of rat HSCs by hydrophobic bile acids is mediated by NAPDH oxidases in an ASMase- and protein kinase Cζ-dependent manner.[48] However, the contribution of ASMase per se to the activation of HSCs and liver fibrosis was not specifically addressed. Our results indicate that pharmacological inhibition or silencing of ASMase decreases the profibrogenic phenotype of HSCs, further supporting the participation of ASMase in HSC transdifferentiation. Moreover, the involvement of ASMase in HSC activation and proliferation was also validated in LX2 cells, a well established human HSC cell line, indicating that the regulation of HSC activation by ASMase may have potential relevance in human liver fibrosis.

Most previous studies linked ASMase-derived ceramide to cell death, even though the direct targets of ASMase-derived ceramide are still poorly defined.[12] For instance, in liver injury, ASMase activation has been shown to promote hepatocyte apoptosis mediated by TNF[25,26] or hepatic ischemia-reperfusion[33] or in Wilson's disease.[45] Our findings add another facet of ASMase in liver pathobiology: ASMase promotes HSC activation and liver fibrosis by regulating CtsB/D processing. Although cathepsins and possibly other acidic proteases participate in self-sustained processing events,[31] our data indicate that ASMase is essential for CtsB/D processing, but not *vice versa*, suggesting that ASMase is upstream of both CtsB and CtsD.

After the encouraging results observed with antagonism of ASMase by pharmacological inhibition or siRNA silencing, we used a genetic model of ASMase deficiency. Surprisingly, complete loss of ASMase activity in the ASMase knockout mouse reflected by undetectable activity of ASMase resulted in an enhanced basal level of CtsB and CtsD processing (not shown) compared with that of either wild-type or ASMase$^{+/-}$ mice (which exhibit a partial reduction in ASMase as shown in Figure 4A). Because we observed that ASMase is critical for the proteolytic processing of both CtsB and CtsD, these findings with the knockout mice indicate that the total loss of ASMase leads to a compensatory gain of function of cathepsins, which in turn, exacerbates *in vivo* fibrosis after carbon tetrachloride administration (not shown). These observations are intriguing and merit further assessment. Total loss of ASMase is pathological and serves as a model for Niemann-Pick type A disease. Although Niemann-Pick type A disease is mainly characterized by rapid neurodegeneration, these patients also often exhibit liver deterioration, with some patients dying of liver failure within 3 years before the onset of the neurological symptoms.[49] Interestingly, introducing a partially functional gene (~8% residual ASMase activity) in mice onto the complete ASMase knockout background prevented the neurological phenotype, and the mice exhibited a normal lifespan.[50] Hence, these observations provide evidence that very low levels of ASMase activity are sufficient to eliminate the pathological state induced by complete ASMase deficiency, illustrating the paradoxical role of ASMase in pathophysiology.[49]

In sharp contrast with the observations with ASMase knockout mice, our data with heterozygous ASMase clearly indicate a vital role for ASMase in the regulation of HSC activation and proliferation *in vitro* as well as liver fibrogenesis *in vivo* by modulating the processing of CtsB and CtsD. Although the role of ASMase in *in vivo* liver fibrosis induced by BDL and CCl_4 is consistent with our *in vitro* observations, the impact of ASMase on hepatocyte

damage caused by cholestasis is unexpected and deserves further comment. The extent of liver damage caused by BDL, a model of liver injury mediated predominantly by accumulation of toxic bile acids, was extensive in wild-type mice, accompanied by inflammatory cells infiltration, features that were markedly reduced in heterozygous ASMase mice. These findings point to a novel role of ASMase in cholestasis-mediated hepatocellular injury, which deserves further study to determine the underlying mechanisms. Recently, Osawa et al,[41] assessed the specific role of ASMase in Kupffer cells during BDL-induced cholestasis. Somewhat contrary to our observations, silencing ASMase in Kupffer cells but not in hepatocytes impaired BDL-mediated AKT activation in hepatocytes, which was essential for cell survival and liver regeneration. On the other hand, deoxycholic acid has been reported to activate c-Jun NH_2-terminal kinase, a stress-activated kinase that regulates cell death, by a mechanism involving the ASMase/Fas receptor.[51] Thus, although it was out of the scope of the study, our observations point to a novel role for ASMase in BDL-induced hepatocyte injury.

Paralleling the resistance of heterozygous ASMase mice to hepatocyte damage caused by BDL, collagen synthesis and liver fibrosis were significantly reduced, in line with the notion that hepatocellular damage is an important trigger of HSC activation and hence fibrosis fostered in previous studies.[52] In contrast, in the experimental model of liver fibrosis by chronic CCl_4 administration, heterozygous ASMase mice display liver damage similar to that of wild-type mice but reduced fibrosis, thus strengthening the evidence for a critical contribution of ASMase in HSC activation, independent of hepatocellular damage.

Overall, our findings indicate a dual function of ASMase in liver fibrogenesis with a direct role primarily determined by the regulation of HSC activation/proliferation via CtsB/D processing and an indirect role by modulating hepatocyte susceptibility to apoptosis induced by cholestasis and perhaps other forms of liver injury. In view of our findings indicating that ASMase is upstream of CtsB in HSCs and the critical role of CtsB in BDL-induced hepatocyte apoptosis,[52] the functional relationship between ASMase and CtsB in the hepatocellular susceptibility to BDL deserves further investigation. Given the role of ASMase in regulating hepatocellular injury shown in previous studies[25,26] and liver fibrosis in the present study, this enzyme may be an attractive target for chronic liver diseases. Therefore, a therapy based on ASMase antagonism may induce a dual beneficial effect, on the one hand by limiting ASMase activity in hepatocytes and thus protecting them from hepatocellular damage, and on the other hand by interfering with HSC activation and reducing liver fibrosis.

Finally, our findings indicate that patients with NASH exhibit increased expression of ASMase and CtsB mRNA levels compared with healthy controls. However, we cannot rule out the contribution of other features of NASH apart from fibrosis, such as apoptosis, to this outcome. Therefore, further work is needed to identify the cell population of enhanced CtsB and ASMase expression and mechanisms responsible for these events in human livers and validate whether the increase in ASMase/CtsB mRNA occurs in liver fibrosis of different etiology such as chronic viral hepatitis.

Acknowledgment

The technical assistance of Susana Nuñez is highly appreciated.

References

1. Iredale JP: Models of liver fibrosis: exploring the dynamic nature of inflammation and repair in a solid organ. J Clin Invest 2007, 117:539–548
2. Friedman SL: Hepatic stellate cells: protean, multifunctional, and enigmatic cells of the liver. Physiol Rev 2008, 88:125–172
3. Tsukada S, Parsons CJ, Rippe RA: Mechanisms of liver fibrosis. Clin Chim Acta 2006, 364:33–60
4. Brunt EM: Nonalcoholic steatohepatitis. Semin Liver Dis 2004, 24:3–20
5. Bugianesi E, Leone N, Vanni E: Expanding the natural history of nonalcoholic steatohepatitis: from cryptogenic cirrhosis to hepatocellular carcinoma. Gastroenterology 2002, 123:134–140
6. Clark JM, Diehl AM: Nonalcoholic fatty liver disease: an underrecognized cause of cryptogenic cirrhosis. JAMA 2003, 289:3000–3004
7. Erickson SK: Nonalcoholic fatty liver disease. J Lipid Res 2009, 50:S412–S416
8. Bataller R, Brenner DA: Liver fibrosis. J Clin Invest 2005, 115:209–218
9. Gressner AM: Transdifferentiation of hepatic stellate cells (Ito cells) to myofibroblasts: a key event in hepatic fibrogenesis. Kidney Int 1996, 54:S39–S45
10. Kisseleva T, Brenner DA: Hepatic stellate cells and the reversal of fibrosis. J Gastroenterol Hepatol 2006, 21:S84–S87
11. Hannun YA, Obeid LM: Principles of bioactive lipid signalling: lessons from sphingolipids. Nat Rev Mol Cell Biol 2008, 9:139–150
12. Morales A, Lee H, Goñi FM, Kolesnick R, Fernández-Checa JC: Sphingolipids and cell death. Apoptosis 2007, 12:923–939
13. Liu YY, Yu JY, Yin D, Patwardhan GA, Gupta V, Hirabayashi Y, Holleran WM, Giuliano AE, Jazwinski SM, Gouaze-Andersson V, Consoli DP, Cabot MC: A role for ceramide in driving cancer cell resistance to doxorubicin. FASEB J 2008, 22:2541–2551
14. Grassmé H, Jekle A, Riehle A, Schwarz H, Berger J, Sandhoff K, Kolesnick R, Gulbins E: CD95 signaling via ceramide-rich membrane rafts. J Biol Chem 2001, 276:20589–20596
15. Grassmé H, Cremesti A, Kolesnick R, Gulbins E: Ceramide-mediated clustering is required for CD95-DISC formation. Oncogene 2003, 22:5457–5470
16. Krönke M: Biophysics of ceramide signaling: interaction with proteins and phase transition of membranes. Chem Phys Lipids 1999, 101:109–121
17. Schuchman EH, Suchi M, Takahashi T, Sandhoff K, Desnick RJ: Human acid sphingomyelinase. Isolation, nucleotide sequence and expression of the full-length and alternatively spliced cDNAs. J Biol Chem 1991, 266:8531–8539
18. Smith EL, Schuchman EH: Acid sphingomyelinase overexpression enhances the antineoplastic effects of irradiation in vitro and in vivo. Mol Ther 2008, 16:1565–1571
19. Grassmé H, Jendrossek V, Riehle A, von Kürthy G, Berger J, Schwarz H, Weller M, Kolesnick R, Gulbins E: Host defense against Pseudomonas aeruginosa requires ceramide-rich membrane rafts. Nat Med 2003, 9:322–330
20. Becker KA, Gellhaus A, Winterhager E, Gulbins E: Ceramide-enriched membrane domains in infectious biology and development. Subcell Biochem 2008, 49:523–538
21. Schütze S, Potthoff K, Machleidt T, Berkovic D, Wiegmann K, Krönke M: TNF activates NF-κB by phosphatidylcholine-specific phospholipase C-induced "acidic" sphingomyelin breakdown. Cell 1992, 71:765–776
22. Wiegmann K, Schütze S, Machleidt T, Witte D, Krönke M: Functional dichotomy of neutral and acidic sphingomyelinases in tumor necrosis factor signaling. Cell 1994, 78:1005–1015

23. Cifone MG, Roncaioli P, De Maria R, Camarda G, Santoni A, Ruberti G, Testi R: Multiple pathways originate at the Fas/APO-1 (CD95) receptor: sequential involvement of phosphatidylcholine-specific phospholipase C and acidic sphingomyelinase in the propagation of the apoptotic signal. EMBO J 1995, 14:5859–5868
24. Liu P, Anderson RG: Compartmentalized production of ceramide at the cell surface. J Biol Chem 1995, 270:27179–27185
25. García-Ruiz C, Colell A, Marí M, Morales A, Calvo M, Enrich C, Fernández-Checa JC: Defective TNF-α-mediated hepatocellular apoptosis and liver damage in acidic sphingomyelinase knockout mice. J Clin Invest 2003, 111:197–208
26. Marí M, Colell A, Morales A, Pañeda C, Varela-Nieto I, García-Ruiz C, Fernández-Checa JC: Acidic sphingomyelinase downregulates the liver-specific methionine adenosyltransferase 1A, contributing to tumor necrosis factor-induced lethal hepatitis. J Clin Invest 2004, 113:895–904
27. Smith EL, Schuchman EH: The unexpected role of acid sphingomyelinase in cell death and the pathophysiology of common diseases. FASEB J 2008, 22:3419–3431
28. Heinrich M, Wickel M, Schneider-Brachert W, Sandberg C, Gahr J, Schwandner R, Weber T, Saftig P, Peters C, Brunner J, Krönke M, Schütze S: Cathepsin D targeted by acid sphingomyelinase-derived ceramide. EMBO J 1999, 8:5252–5263
29. Heinrich M, Neumeyer J, Jakob M, Hallas C, Tchikov V, Winoto-Morbach S, Wickel M, Schneider-Brachert W, Trauzold A, Hethke A, Schütze S: Cathepsin D links TNF-induced acid sphingomyelinase to Bid-mediated caspase-9 and -3 activation. Cell Death Differ 2004, 11:550–563
30. Guicciardi ME, Deussing J, Miyoshi H, Bronk SF, Svingen PA, Peters C, Kaufmann SH, Gores GJ: Cathepsin B contributes to TNF-α-mediated hepatocyte apoptosis by promoting mitochondrial release of cytochrome c. J Clin Invest 2000, 106:1127–1137
31. Moles A, Tarrats N, Fernández-Checa JC, Marí M: Cathepsins B and D drive hepatic stellate cell proliferation and promote their fibrogenic potential. Hepatology 2009, 49:1297–1307
32. Institute of Laboratory Animal Resources: Guide for the Care and Use of Laboratory Animals, 7th ed. Washington, DC, Institute of Laboratory Animal Resources, Commission on Life Sciences, National Research Council, 1996
33. Llacuna L, Marí M, Garcia-Ruiz C, Fernández-Checa JC, Morales A: Critical role of acidic sphingomyelinase in murine hepatic ischemia-reperfusion injury. Hepatology 2006, 44:561–572
34. Jamall IS, Finelli VN, Que Hee SS: A simple method to determine nanogram levels of 4-hydroxyproline in biological tissues. Anal Biochem 1981, 112:70–75
35. Kleiner DE, Brunt EM, Van Natta M, Behling C, Contos MJ, Cummings OW, Ferrell LD, Liu YC, Torbenson MS, Unalp-Arida A, Yeh M, McCullough AJ, Sanyal AJ: Nonalcoholic Steatohepatitis Clinical Research Network. Design and validation of a histological scoring system for nonalcoholic fatty liver disease. Hepatology 2005, 41:1313–1321
36. Livak KJ, Schmittgen TD: Analysis of relative gene expression data using real-time quantitative PCR and the $2^{-\Delta\Delta C_t}$. Method Methods 2001, 5:402–408
37. Xu L, Hui AY, Albanis E, Arthur MJ, O'Byrne SM, Blaner WS, Mukherjee P, Friedman SL, Eng FJ: Human hepatic stellate cell lines. LX-1 and LX-2: new tools for analysis of hepatic fibrosis. Gut 2005, 54:142–151
38. Kornhuber J, Tripal P, Reichel M, Terfloth L, Bleich S, Wiltfang J, Gulbins E: Identification of new functional inhibitors of acid sphingomyelinase using a structure-property-activity relation model. J Med Chem 2008, 51:219–237
39. Takashima T, Kawada N, Maeda N, Okuyama H, Uyama N, Seki S, Arakawa T: Pepstatin A attenuates the inhibitory effect of N-acetyl-L-cysteine on proliferation of hepatic myofibroblasts (stellate cells). Eur J Pharmacol 2002, 451:265–270
40. Okuyama H, Shimahara Y, Kawada N, Seki S, Kristensen DB, Yoshizato K, Uyama N, Yamaoka Y: Regulation of cell growth by redox-mediated extracellular proteolysis of platelet-derived growth factor receptor β. J Biol Chem 2001, 276:28274–28280
41. Osawa Y, Seki E, Adachi M, Suetsugu A, Ito H, Moriwaki H, Seishima M, Nagaki M: Role of acid sphingomyelinase of Kupffer cells in cholestatic liver injury in mice. Hepatology 2010, 51:237–845
42. Langmann T, Buechler C, Ries S, Schaeffler A, Aslanidis C, Schuierer M, Weiler M, Sandhoff K, de Jong PJ, Schmitz G: Transcription factors Sp1 and AP-2 mediate induction of acid sphingomyelinase during monocytic differentiation. J Lipid Res 1999, 40:870–880
43. Murate T, Suzuki M, Hattori M, Takagi A, Kojima T, Tanizawa T, Asano H, Hotta T, Saito H, Yoshida S, Tamiya-Koizumi K: Up-regulation of acid sphingomyelinase during retinoic acid-induced myeloid differentiation of NB4, a human acute promyelocytic leukemia cell line. J Biol Chem 2002, 277:9936–9943
44. Santana P, Peña LA, Haimovitz-Friedman A, Martin S, Green D, McLoughlin M, Cordon-Cardo C, Schuchman EH, Fuks Z, Kolesnick R: Acid sphingomyelinase-deficient human lymphoblasts and mice are defective in radiation-induced apoptosis. Cell 1996, 86:189–199
45. Lang PA, Schenck M, Nicolay JP, Becker JU, Kempe DS, Lupescu A, Koka S, Eisele K, Klarl BA, Rübben H, Schmid KW, Mann K, Hildenbrand S, Hefter H, Huber SM, Wieder T, Erhardt A, Häussinger D, Gulbins E, Lang F: Liver cell death and anemia in Wilson disease involve acid sphingomyelinase and ceramide. Nat Med 2007, 13:164–170
46. Teichgräber V, Ulrich M, Endlich N, Riethmüller J, Wilker B, De Oliveira-Munding CC, van Heeckeren AM, Barr ML, von Kürthy G, Schmid KW, Weller M, Tümmler B, Lang F, Grassme H, Döring G, Gulbins E: Ceramide accumulation mediates inflammation, cell death and infection susceptibility in cystic fibrosis. Nat Med 2008, 14:382–391
47. Petrache I, Natarajan V, Zhen L, Medler TR, Richter AT, Cho C, Hubbard WC, Berdyshev EV, Tuder RM: Ceramide upregulation causes pulmonary cell apoptosis and emphysema-like disease in mice. Nat Med 2005, 11:491–498
48. Sommerfeld A, Reinehr R, Haussinger D: Bile acid-induced EGFR activation in quiescent rat hepatic stellate cells can trigger both, proliferation and apoptosis. J Biol Chem 2009, 284:22173–22183
49. Schuchman EH: The pathogenesis and treatment of acid sphingomyelinase-deficient Niemann-Pick disease. J Inherit Metab Dis 2007, 30:654–663
50. Marathe S, Miranda SR, Devlin C, Johns A, Kuriakose G, Williams KJ, Schuchman EH, Tabas I: Creation of a mouse model for non-neurological (type B) Niemann-Pick disease by stable, low level expression of lysosomal sphingomyelinase in the absence of secretory sphingomyelinase: relationship between brain intra-lysosomal enzyme activity and central nervous system function. Hum Mol Genet 2000, 9:1967–1976
51. Gupta S, Natarajan R, Payne SG, Studer EJ, Spiegel S, Dent P, Hylemon PB: Deoxycholic acid activates the c-Jun N-terminal kinase pathway via FAS receptor activation in primary hepatocytes. Role of acidic sphingomyelinase-mediated ceramide generation in FAS receptor activation. J Biol Chem 2004, 279:5821–5828
52. Canbay A, Guicciardi ME, Higuchi H, Feldstein A, Bronk SF, Rydzewski R, Taniai M, Gores GJ: Cathepsin B inactivation attenuates hepatic injury and fibrosis during cholestasis. J Clin Invest 2003, 112:152–159

THE JOURNAL OF BIOLOGICAL CHEMISTRY VOL. 287, NO. 2, pp. 1178–1188, January 6, 2012

Cathepsin B Overexpression Due to Acid Sphingomyelinase Ablation Promotes Liver Fibrosis in Niemann-Pick Disease*

Received for publication, June 15, 2011, and in revised form, November 1, 2011 Published, JBC Papers in Press, November 18, 2011, DOI 10.1074/jbc.M111.272393

Anna Moles[‡1], **Núria Tarrats**[‡1], **José C. Fernández-Checa**[‡§2,3], **and Montserrat Marí**[‡2,4]

From the [‡]*Institut d'Investigacions Biomèdiques August Pi i Sunyer, Liver Unit-Hospital Clínic, Centro de Investigación Biomédica en Red en el Área Temática de Entermedades Hepáticas y Digestivas, and Department of Cell Death and Proliferation, Instituto de Investigaciones Biomédicas de Barcelona, Consejo Superior de Investigaciones Científicas, 08036 Barcelona, Spain and the* [§]*Research Center for Alcoholic Liver and Pancreatic Diseases, Keck School of Medicine, University of Southern California, Los Angeles, California 90089*

Background: The mechanism of liver fibrosis in Niemann-Pick disease (NPD) is unknown.
Results: The loss of ASMase stimulates cathepsin B (CtsB) activation promoting liver fibrosis.
Conclusion: CtsB contributes to the hepatic phenotype of NPD.
Significance: CtsB may be a novel therapeutic target to treat liver disease in NPD.

Niemann-Pick disease (NPD) is a lysosomal storage disease caused by the loss of acid sphingomyelinase (ASMase) that features neurodegeneration and liver disease. Because ASMase-knock-out mice models NPD and our previous findings revealed that ASMase activates cathepsins B/D (CtsB/D), our aim was to investigate the expression and processing of CtsB/D in hepatic stellate cells (HSCs) from ASMase-null mice and their role in liver fibrosis. Surprisingly, HSCs from ASMase-knock-out mice exhibit increased basal level and activity of CtsB as well as its *in vitro* processing in culture, paralleling the enhanced expression of fibrogenic markers α-smooth muscle actin (α-SMA), TGF-β, and pro-collagen-α1(I) (Col1A1). Moreover, pharmacological inhibition of CtsB blunted the expression of α-SMA and Col1A1 and proliferation of HSCs from ASMase-knock-out mice. Consistent with the enhanced activation of CtsB in HSCs from ASMase-null mice, the *in vivo* liver fibrosis induced by chronic treatment with CCl_4 increased in ASMase-null compared with wild-type mice, an effect that was reduced upon CtsB inhibition. In addition to liver, the enhanced proteolytic processing of CtsB was also observed in brain and lung of ASMase-knock-out mice, suggesting that the overexpression of CtsB may underlie the phenotype of NPD. Thus, these findings reveal a functional relationship between ASMase and CtsB and that the ablation of ASMase leads to the enhanced processing and activation of CtsB. Therefore, targeting CtsB may be of relevance in the treatment of liver fibrosis in patients with NPD.

Acid sphingomyelinase (ASMase[5]; EC 3.2.1.14) is a member of an enzyme family that catalyzes the breakdown of sphingomyelin into ceramide. ASMase works optimally at acidic pH and is located mainly in the endo/lysosomal compartments (1). Besides its important participation as key structural component of biological membranes, ceramide is recognized as a critical second messenger that regulates many cell functions (2, 3). In particular, ceramide generation by ASMase is rapid and transient and plays a proapoptotic role in response to many different stimuli (2, 3). ASMase derives from a proinactive form whose proteolytic processing within the C terminus leads to the maturation of an endosomal/lysosomal Zn^{2+}-independent form and a Zn^{2+}-dependent secretory isoenzyme (4).

Niemann-Pick disease (NPD) is a rare lysosomal storage disorder caused by recessive mutations on the *SPMD1* gene encoding ASMase (5, 6). NPD type A and B, the most common subtypes of this disease, share features such as the accumulation of sphingomyelin, cholesterol, glycosphingolipids, and bis-(monoacylglycerol) phosphate in the visceral organs such as liver, spleen, and lung. The subsequent formation of foam cells is the main cause of hepatosplenomegaly, pulmonary insufficiency, and cardiovascular disease (6). NPD type A patients typically exhibit almost a total loss of ASMase activity and suffer neurological degeneration that reduces their lifespan to about 3 years of age. NPD type B patients, however, frequently survive into adulthood and exhibit a milder phenotype with little or no neurodegeneration depending on the remaining percentage of ASMase activity (7). Despite the generation of the ASMase-knock-out mice as an animal model of NPD type A exhibiting neurological degeneration, hepatosplenomegaly, and lung dysfunction (8, 9), little progress has been made in NPD treatment.

Cathepsins are a family of lysosomal proteases whose participation in different pathologies such as liver fibrosis (10), ath-

* The work was supported, in whole or in part, by Grant P50-AA-11999 from the Research Center for Liver and Pancreatic Diseases, National Institute on Alcohol Abuse and Alcoholism. This work was carried out in part at the Esther Koplowitz Center in Barcelona, and it was also supported by Grants PI10/02114 (Instituto de Salud Carlos III), 2009-11417 (Plan Nacional de I+D), Spain; and the and Fundació La Marató de TV3.

[1] Both authors contributed equally to this work.
[2] Both authors share senior authorship.
[3] To whom correspondence may be addressed: Liver Unit, Hospital Clinic, C/Villarroel 170, 08036 Barcelona, Spain. Tel.: 34-93-227-5709; E-mail: checa229@yahoo.com.
[4] To whom correspondence may be addressed: Liver Unit, Hospital Clinic, C/Villarroel 170, 08036 Barcelona, Spain. Tel.: 34-93-227-5709; E-mail: monmari@clinic.ub.es.

[5] The abbreviations used are: ASMase, acid sphingomyelinase; α-SMA, α-smooth muscle actin; CCl_4, carbon tetrachloride; Col1A1, pro-collagen-α1(I); CtsB, cathepsin B; CtsD, cathepsin D; EWAT, epididymal white adipose tissue; HSC, hepatic stellate cell; NPD, Niemann-Pick disease.

erosclerosis (11), Alzheimer disease (12), and cancer (13, 14) has been reported in the past years. In particular, cathepsin B (CtsB) and cathepsin D (CtsD) have been implicated in signaling pathways of apoptosis (15, 16) and liver fibrosis (17). Moreover, recent studies have revealed that ASMase controls the proteolytic processing of CtsB/D, and hence ASMase down-regulation impairs CtsB/D processing resulting in decreased hepatic stellate cell (HSC) activation *in vitro* and lower *in vivo* fibrogenesis (17). However, because many cathepsins are proteolytically processed by other members of the family and due to the hierarchical relationship between ASMase and CtsB/D (17), we postulated that the complete loss of ASMase may lead to an adaptive overexpression of CtsB/D. To test this hypothesis we addressed the regulation of CtsB/D in ASMase-knock-out mice and examined the activation of HSCs *in vitro* and liver fibrosis *in vivo* as a potential contributory mechanism for enhanced liver disease observed in many NPD patients (18–21). Moreover, because the NPD phenotype is not restricted to liver, we addressed the regulation of CtsB/D in other commonly affected organs of ASMase-knock-out mice. Our findings revealed an increased proteolytic processing of CtsB/D in HSC from ASMase-null mice and that the pharmacological inhibition of CtsB prevents *in vitro* HSC activation and proliferation. Consequently, ASMase-knock-out mice exhibit increased *in vivo* liver fibrosis induced by CCl_4 challenge, which is reduced upon CtsB inhibition. Similar findings regarding enhanced basal levels and increased processing of CtSB/D were observed in brain and lung from ASMase-knock-out mice. Thus, these findings imply that the therapeutic targeting of CtsB may be of relevance in the treatment of liver fibrosis in patients with NPD.

EXPERIMENTAL PROCEDURES

Reagents—DMEM, trypsin-EDTA, penicillin-streptomycin, TRIzol, FBS, HistoGrip, and Opti-MEM, were from Invitrogen. All tissue cultureware was from Nunc. The DAKO Biotin Blocking System, peroxidase substrate (DAB), peroxidase buffer, and hematoxylin were from DAKO (Glostrup, Denmark). Aquatex was from Merck. The Vectastain ABC kit was from Vector Laboratories (Burlingame, CA). PDGF-BB was from PeProtechEC (London, UK). Proteinase inhibitors were from Roche Applied Science. iScript™ One-Step reverse transcription (RT)-PCR kit with SYBR® Green was from Bio-Rad. ECL Western blotting substrate was from Pierce. Ca074Me was from Sigma-Aldrich, and, unless otherwise stated, all other reagents were also from Sigma-Aldrich.

Antibodies—We used the following primary antibodies: rabbit polyclonal anti-cathepsin B (catalog 06-480) and rabbit polyclonal anti-Col1A1 (catalog AB765P) were from Millipore. Goat polyclonal anti-cathepsin D (catalog sc-6486) and mouse monoclonal pan-cathepsin (catalog sc-365614) were from Santa Cruz Biotechnology. Rabbit polyclonal anti-α-SMA (catalog ab5694), rabbit polyclonal anti-myeloperoxidase (catalog ab15484), and rat monoclonal anti-lysosomal associated membrane protein 2 (LAMP2) (catalog ab13524) were from Abcam. mAb anti-α-SMA (catalog A2547), mAb anti-β-actin (catalog A1978), and ECL-peroxidase labeled anti-mouse (catalog A9044), anti-rabbit (catalog A0545), and anti-goat (catalog A5420) were from Sigma-Aldrich. Anti-rat (catalog 819520) was from Invitrogen. Rabbit polyclonal anti-Hsp70 was from Enzo LifeSciences, Farmingdale, NY). Rabbit polyclonal anti-LC3B (catalog 2775) was from Cell Signaling Technology. Alexa Fluor 488 goat anti-rat (catalog A11006), Alexa Fluor 594 rabbit anti-goat (catalog A11080), and Alexa Fluor 647 goat ant-rabbit (catalog A21245) were from Invitrogen. Biotinylated labeled anti-rabbit was from BD Biosciences.

Animals and HSC Isolation—Wild-type and ASMase-knock-out mice (male, 8–10-week-old littermates) (C57BL/6 strain) were obtained by propagation of heterozygous breeding pairs (a generous gift from R. Kolesnick, Memorial Sloan-Kettering Cancer Center, New York and E. Gulbins, University of Duisburg-Essen, Germany) and genotyped as described previously (22). All animals received humane care according to the criteria outlined in the *Guide for the Care and Use of Laboratory Animals* published by the National Institutes of Health. HSCs were isolated by perfusion with collagenase-Pronase and cultured as described previously (10). Culture purity, assessed routinely by retinoid autofluorescence at 350 nm, was >95%. Lack of staining for F4/80 confirmed the absence of Kupffer cells. Cells were cultured in DMEM supplemented with 10% FBS and antibiotics at 37 °C in a humidified atmosphere of 95% air and 5% CO_2.

In Vivo Liver Fibrogenesis—Wild-type or ASMase KO mice were treated with CCl_4 at a dose of 5 μl (10% CCl_4 in corn oil)/g of body weight, by intraperitoneal injection twice a week for 4 weeks. Control animals received corn oil alone. Ca074Me (Sigma-Aldrich) was administered 30 min before CCl_4, for the last 3 week of the study. Ca074Me was given intraperitoneally in a dosage according to CtsB expression in liver (0.25–1.0 mg/mouse).

ASMase Activity—ASMase activity from cellular extracts was determined using a fluorescent sphingomyelin analog (NBD C6-sphingomyelin). Samples were incubated for 60 min at 37 °C in incubation buffer containing 10 μmol/liter NBD C6-sphingomyelin (250 mmol/liter sodium acetate, 0.1% Triton X-100, pH 5.0). Lipids were extracted, dried under N_2, and separated by TLC (chloroform:ethanol: 20% NH_4OH; 70:30:5, v/v). NBD-ceramide was visualized under UV light, and images were acquired and analyzed using a Gel Doc XR System with Quantity One software (Bio-Rad). Furthermore, ASMase activity in tissue lysates was performed as described (17).

CtsB and CtsD Activities—CtsB activity was assayed fluorometrically with Z-Arg-Arg-7-amido-4-methylcoumarin hydrochloride (60 μmol/liter) at pH 7.4 and 37 °C as described previously (10). CtsD was assayed using a Cathepsin D Activity Assay kit (catalog ab65302; Abcam) following the manufacturer's instructions. Results were expressed as cathepsin activity (slope of fluorescence emission after 40 min) per milligram of protein.

SDS-PAGE and Immunoblot Analysis—Cell lysates were prepared in radioimmune precipitation assay buffer (50 mmol/liter Tris-HCl, pH 8, 150 mmol/liter NaCl, 1% Nonidet P-40, 0.1% SDS, 1% Triton X-100 plus proteinase inhibitors). Protein concentration was determined by the Bradford assay, and samples containing 10–30 μg were separated by 8–10% SDS-PAGE.

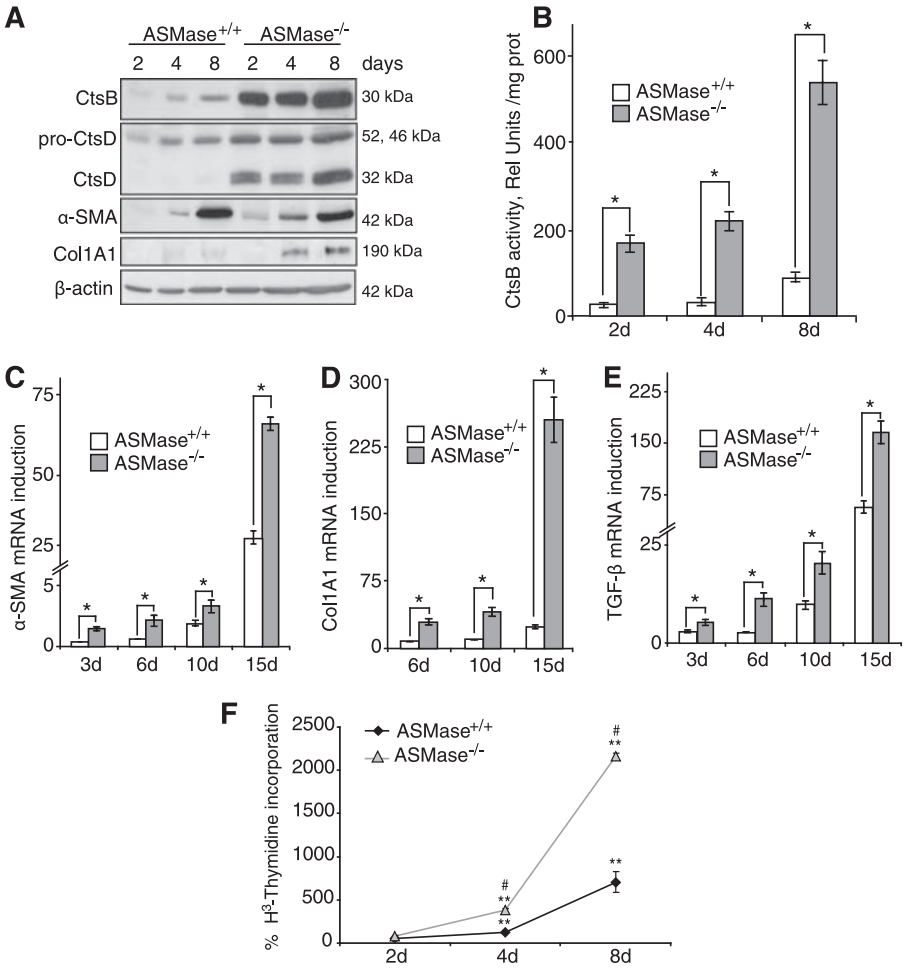

FIGURE 1. **Enhanced fibrogenic potential of ASMase$^{-/-}$ HSC.** *A*, time course of CtsB, CtsD, α-SMA, and Col1A1 protein expression. *B*, time course of CtsB activity in ASMase$^{+/+}$ and ASMase$^{-/-}$ HSCs. *C–E*, time course of α-SMA (*C*), Col1A1 (*D*), and TGF-β (*E*) mRNA levels in ASMase$^{-/-}$ HSCs compared with ASMase$^{+/+}$ HSCs. *F*, percentage of proliferation from day 2 to day 8 of culture in ASMase$^{+/+}$ and ASMase$^{-/-}$ HSCs. Data are mean ± S.D. (*error bars*), $n = 4$. *, $p \leq 0.01$ *versus* same time point ASMase$^{+/+}$ HSCs; **, $p \leq 0.05$ *versus* control day 2 HSCs; #, $p \leq 0.05$ *versus* ASMase$^{+/+}$ HSCs.

Proteins were transferred to nitrocellulose membranes. After membranes were blocked in 8% nonfat milk or 5% BSA in 20 mmol/liter Tris-HCl, 150 mmol/liter NaCl, and 0.05% Tween 20 for 1 h at room temperature, the membranes were incubated overnight at 4 °C with different primary antibodies and developed with the ECL-peroxidase system.

HSC Proliferation—Proliferation was estimated as the amount of [^{3}H]thymidine incorporated into TCA-precipitable material as described previously (17).

Hydroxyproline Content—Hepatic hydroxyproline content was determined by the method of Jamall *et al.* (23), as described previously (10). Data were normalized to wet liver weight.

RNA Isolation and Real Time RT-PCR of Mouse Samples—Total RNA was isolated from HSCs with TRIzol reagent. Real-time RT-PCR was performed with an iScript™ One-Step reverse transcription-PCR kit with SYBR® Green following the manufacturer's instructions. The primers sequences used were: mouse α-SMA forward, 5′-ACTACTGCCGAGCGTGAGAT-3′ and reverse, 5′-AAGGTAGACAGCGAAGCCAA-3′ (GenBank accession number NM_007392); mouse TGF-β forward, 5′-GTCAGACATTCGGGAAGCAG-3′ and reverse, 5′-GCGTATCAGTGGGGGTCA-3′ (GenBank accession number NM_011577); mouse Col1A1 forward, 5′-ACTTCACTTCCTGCCTCAG-3′ and reverse, 5′-TGACTCAGGCTCTTGAGGGT-3′ (GenBank accession number NM_007742); mouse β-actin forward, 5′-GACGGCCAGGTCATCACTAT-3′ and reverse, 5′-CGGATGTCAACGTCACACTT-3′ (GenBank accession number NM_007393).

Immunohistochemical Staining—Paraffin molds containing liver sections were cut into 5-μm sections and mounted on HistoGrip-coated slides. The sections were deparaffinized in xylene and dehydrated in graded alcohol series. Endogenous peroxidase (3% H_2O_2) and avidin and biotin were blocked. Slides were incubated with primary antibody overnight in a wet chamber at 4 °C. After rinsing with PBS 1×, the slides were incubated with a biotinylated antibody for 45 min in a wet chamber and developed with the ABC kit with peroxidase substrate (DAB) and peroxidase buffer. After rinsing the slides with tap water they were counterstained with hematoxylin and mounted with Aquatex.

H&E and Sirius Red Staining—Livers were fixed, included in paraffin, and sections of 7 μm were routinely stained with H&E, periodic acid-Schiff, Nissl staining, or with a 0.1% Sirius Red-picric solution following standard procedures.

Statistical Analyses—All images display representative data from at least three independent observations. The experiments

were repeated at least three times. The statistical significance of differences was performed using the unpaired, nonparametric Student's *t* test.

RESULTS

HSCs from ASMase Knock-out Mice Exhibit Increased CtsB/D Processing and Fibrogenic Potential—Given the functional relationship between ASMase and cathepsins recently reported in liver fibrosis (17), we analyzed the expression of CtsB and CtsD in HSCs from ASMase$^{-/-}$ mice. HSCs were isolated and cultured in plastic to follow their activation process *in vitro* from quiescent HSCs to myofibroblasts like cells responsible for the fiber deposition. As shown in Fig. 1*A* we observed an up-regulation of CtsB and CtsD expression and processing compared with wild-type HSCs. In particular, CtsB expression was remarkably induced, as shown by the enhanced activity of CtsB in ASMase$^{-/-}$ HSCs compared with wild-type HSCs (Fig. 1*B*). Kinetic analyses revealed enhanced expression of CtsB/D at the early phase in the activation of HSC (Fig. 1, *A* and *B*). Genetic deficiency of ASMase also resulted in elevated expression of the activation markers α-SMA and Col1A1 at the protein (Fig. 1*A*) and mRNA level (Fig. 1, *C* and *D*), which was further accompanied by overexpression of other markers of HSC activation such as transforming growth factor-β (TGF-β) (Fig. 1*E*). Considering the difference in -fold increase of mRNA levels for α-SMA and Col1A1, the corresponding increase at the protein level at day 8 of culture was more apparent for Col1A1 than for α-SMA. In parallel with these observations, the proliferation rate of HSC from day 2 after isolation to day 8 of culture was significantly increased in ASMase$^{-/-}$ HSCs compared with wild-type HSCs (Fig. 1*F*). Thus, HSCs from ASMase$^{-/-}$ mice exhibit increased fibrogenic potential, which correlated with enhanced CtsB/D levels and processing.

CtsB Inhibition Diminishes Activation of ASMase-knock-out HSCs—According to our observations in the knock-out mice, complete absence of ASMase up-regulates CtsB and CtsD. Because in previous studies we have already disclosed the importance of CtsB in liver fibrosis and that the use of a selective CtsB inhibitor (Ca074Me) reduced HSC activation in an experimental liver fibrosis model (10), we decided to test whether the up-regulation of CtsB observed in ASMase$^{-/-}$ HSCs plays a causal role in their enhanced fibrogenic potential, evaluating the effect of inhibiting CtsB using the specific inhibitor Ca074Me. In analyzing the expression of α-SMA and Col1A1 in 7-day-old HSC cultures, we observed an increased expression of these markers of HSC transdifferentiation that was prevented after Ca074Me treatment, both in wild-type and ASMase$^{-/-}$ HSCs (Fig. 2*A*). Moreover, proliferation was also significantly diminished under these conditions, even in ASMase$^{-/-}$ HSCs (Fig. 2*B*). As previously observed in wild-type HSCs (10), AKT phosphorylation induced by PDGF was enhanced in HSC from ASMase-knock-out mice and blocked by Ca074Me (data not shown). Ca074Me did not cause any noticeable cell death or toxicity at the doses and time utilized. Hence, these results suggest that CtsB is responsible for the enhanced fibrogenic features observed in ASMase-knock-out HSCs.

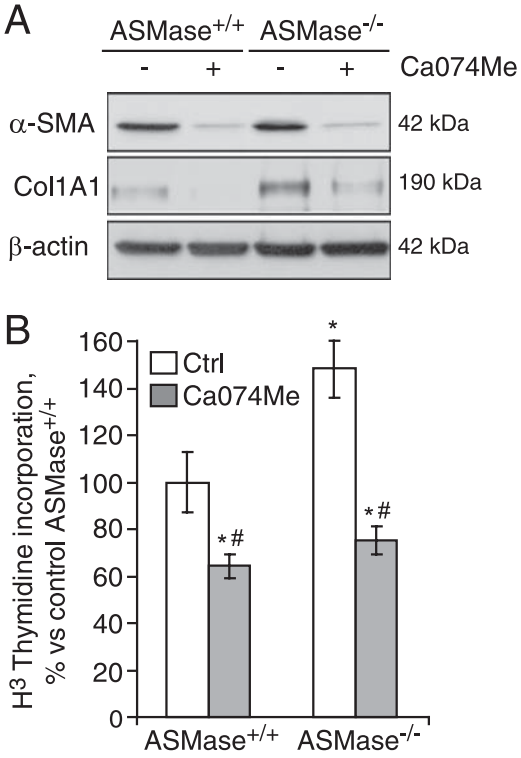

FIGURE 2. **CtsB inhibition decreases the fibrogenic potential of HSCs.** *A*, α-SMA and Col1A1 protein levels, and *B*, proliferation rate after CtsB inhibition with Ca074Me (20 μmol/liter, 48 h, added every 24 h from day 5 to day 7), in ASMase$^{+/+}$ and ASMase$^{-/-}$ HSCs. Data are mean ± S.D. (*error bars*), $n = 3$. *, $p \leq 0.05$ *versus* ASMase$^{+/+}$ control HSC; #, $p \leq 0.05$ *versus* respective controls.

ASMase-knock-out Mice Exhibit Increased Liver Fibrosis in Response to CCl_4 Due to CtsB Overexpression—Our previous studies indicated that heterozygous ASMase mice are less sensitive to *in vivo* liver fibrosis due to impaired CtsB activation. However, the preceding findings indicate that the complete loss of ASMase leads to increased CtsB expression, which is known to contribute to liver fibrosis and is a marker of disease progression in NASH patients (17). Therefore, to analyze whether CtsB overexpression sensitizes to liver fibrosis we decided to administer CCl_4 to ASMase$^{-/-}$ and wild-type mice. We chose CCl_4 instead of bile duct ligation because the degree of liver damage is independent of ASMase (17). CCl_4 challenge for 4 weeks increased serum alanine transaminase levels in wild-type and ASMase deficient mice to a similar extent (Fig. 3*A*). As shown in Fig. 3*B*, basal levels of CtsB activity were increased in ASMase$^{-/-}$ livers and were further enhanced upon induction of liver fibrosis with CCl_4 only in ASMase-deficient livers. In addition, enhanced levels of CtsD were also detected in ASMase-deficient livers that were further increased after CCl_4 challenge (Fig. 3*C*). Moreover, in CCl_4-treated animals enhanced levels of CtsB and CtsD correlated with an elevated α-SMA expression, as shown by Western blot analysis (Fig. 3*C*) and immunohistochemistry (Fig. 3*E*), indicating that ASMase-deficient animals have increased number of activated HSCs. Analysis of the hydroxyproline content in the liver revealed a significant increase in collagen accumulation in ASMase-deficient animals compared with wild-type animals after CCl_4 administration (Fig. 3*D*), which correlated with the increased

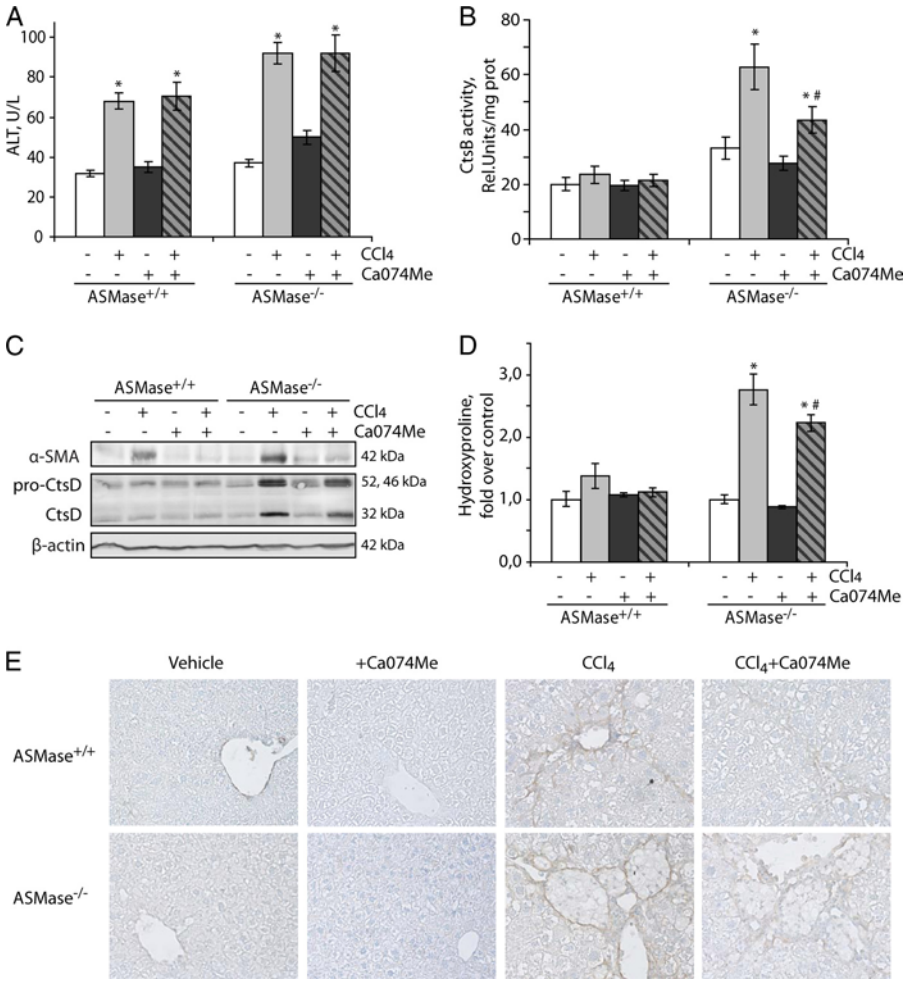

FIGURE 3. **Enhanced liver fibrosis in ASMase$^{-/-}$ mice after CCl_4 administration was ameliorated after CtsB inhibition.** *A–D*, serum alanine transaminase (*ALT*) levels (*A*), CtsB activity (*B*), CtsD and α-SMA protein expression (*C*), and hydroxyproline levels in liver homogenate (*D*). *E*, α-SMA immunostaining of liver section at ×40 magnification. Data are mean ± S.E. (*error bars*), $n = 6$ animals/group. *, $p \leq 0.05$ *versus* vehicle-treated mice; #, $p \leq 0.05$ *versus* CCl_4 ASMase$^{-/-}$-treated mice.

detection of collagen fibers in the livers of ASMase$^{-/-}$ mice that received CCl_4, as detected by Sirius Red staining (Fig. 4*A*). The Sirius Red staining, as well as the α-SMA expression, observed in the ASMase$^{-/-}$ livers did not follow the typical pattern along the collagen fibers but displayed a characteristic arrangement surrounding foam cells, lipid-accumulating macrophages also known as Niemann-Pick cells. This atypical distribution was observed only in ASMase-deficient livers that received CCl_4; this particular cell type, however, was not observed in ASMase$^{-/-}$ animals receiving only vehicle (Fig. 4*A*). On histological examination we observed mild sinusoidal dilatation, by H&E staining (Fig. 4*B*), and moderate neutrophilic infiltration, as detected by myeloperoxidase immunostaining (Fig. 4*C*) in wild-type livers upon CCl_4 challenge. These parameters were exacerbated in ASMase$^{-/-}$ animals that presented noticeable infiltration of neutrophils especially adjacent to foam cells, clearly visible by H&E staining. Collectively, these results indicate that liver fibrosis is significantly increased in ASMase-KO mice.

CtsB Inhibition Reduces in Vivo Liver Fibrosis in ASMase-null Mice—Given the above findings, and because CtsB inhibition has been proven useful in reversing liver fibrosis in wild-type mice (10), we next asked whether CtsB inhibition could be of relevance in ameliorating liver fibrogenesis in ASMase$^{-/-}$ livers *in vivo* following CCl_4 administration. To this aim, CCl_4 was first administered twice a week for 1 week, followed by CCl_4 and Ca074Me administration for 3 additional weeks. CtsB inhibition by itself did not alter any of the parameters studied in control animals (Figs. 3 and 4). As described previously (10), Ca074Me treatment did not significantly affect the increase in alanine transaminase levels observed after CCl_4 challenge, suggesting that CtsB did not participate in the mechanisms responsible for liver damage (Fig. 3*A*). However, *in vivo* Ca074Me administration significantly reduced the increase in CtsB activity (~30%) induced by CCl_4 in ASMase$^{-/-}$ mice (Fig. 3*B*). Higher doses of Ca074Me failed to inhibit CtsB activity in ASMase$^{-/-}$ mice further (data not shown). CtsB inhibition by Ca074Me reduced the increased expression of α-SMA and CtsD (Fig. 3*C*) as well as the presence of α-SMA-positive cells after CCl_4 challenge in ASMase$^{-/-}$ livers (Fig. 3*D*). Moreover, as shown in Fig. 3*E*, determination of the hydroxyproline content in the liver revealed a significant decrease in collagen accumulation in CCl_4-treated mice that received Ca074Me, compared with mice challenged with CCl_4 alone. This result was

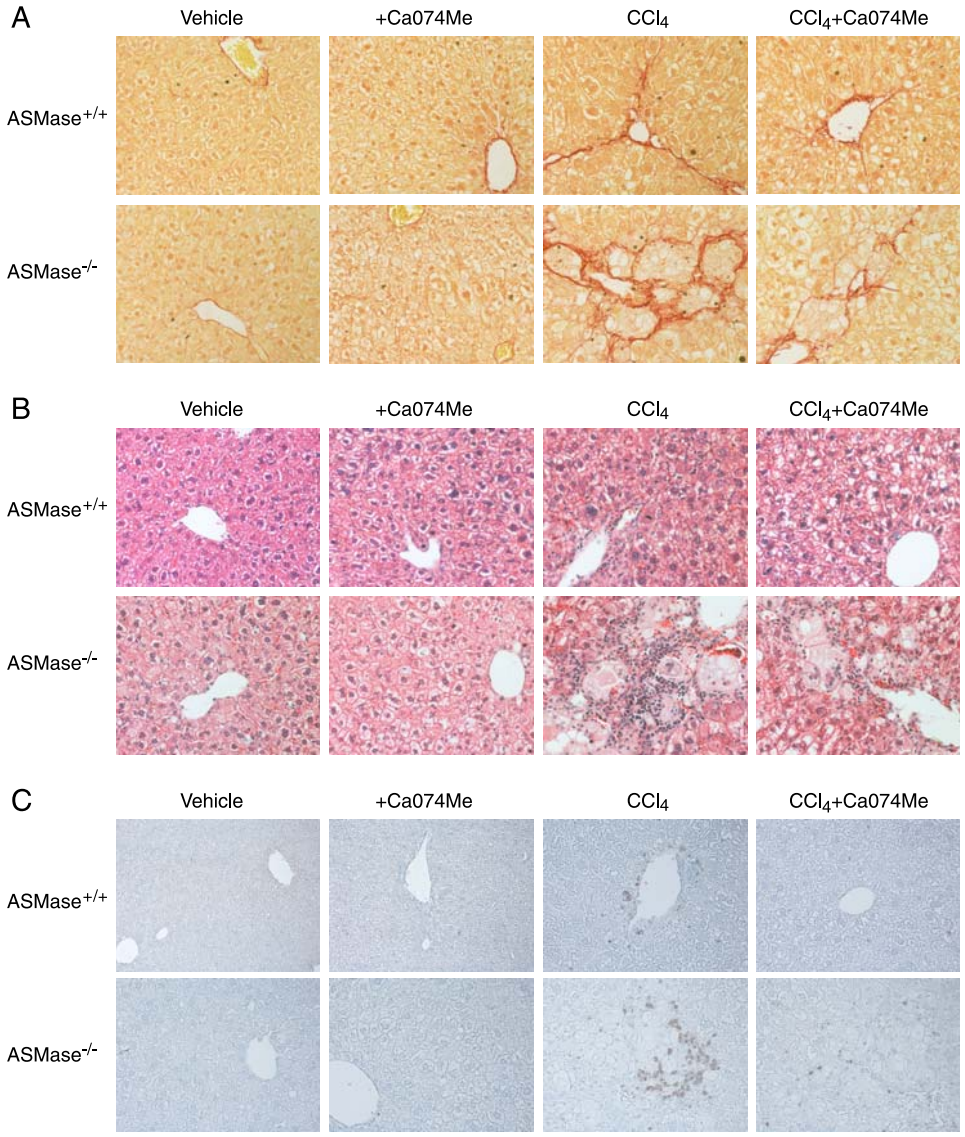

FIGURE 4. **Fiber deposition, presence of foam cells, and inflammation were decreased in ASMase$^{-/-}$ livers after CtsB inhibition.** *A*, Sirius Red staining of collagen fibers. *B* and *C*, H&E (*B*) and myeloperoxidase (*C*) staining of liver sections after the corresponding treatments. All images were taken at ×40 magnification.

further confirmed by the detection of collagen fibers by Sirius Red staining (Fig. 4*A*) in CCl_4-treated animals compared with those treated with CtsB inhibitor. Additionally, CtsB inhibition in CCl_4-treated animals moderately decreased the incidence of foam cells in the liver (Fig. 4*B*) and the number of myeloperoxidase-positive cells (Fig. 4*C*) Thus, these findings indicate that CtsB plays a critical role in *in vivo* liver fibrogenesis in ASMase-deficient livers.

CtsB and D Increase in Extrahepatic Organs in ASMase-knock-out Mice—To analyze whether the increase of CtsB and CtsD was an isolated feature of the liver from the ASMase$^{-/-}$ mice or was a general phenotypic characteristic in other organs, 21-week-old animals were killed, and different organs were harvested. CtsB (Fig. 5*A*) and CtsD (Fig. 5*B*) protein expression and activity increased in several organs affected by the accumulation of foam cells in NPD: brain, lung, liver, muscle, epididymal white adipose tissue (EWAT), and skin. However, there were no changes in spleen, pancreas, and intestine in those mice. When exploring the magnitude of ASMase and CtsB activities in the tissues of wild-type animals we did not observe any direct correlation between the extent of activation of these two enzymes in view of the fact that tissues with the lowest ASMase activity, such as spleen and muscle, displayed, respectively, the highest and the lowest CtsB activities among the tissues examined (Fig. 5*C*).

To analyze whether the increase in CtsB was also detectable in younger animals with a weak NPD phenotype, 10–12-week-old mice were studied. Accumulation of foam cells was already detectable in histological sections of lung and liver, as well as a decrease in the number of Purkinje cells in the cerebellum (Fig. 6*A*), both characteristic of the neurovisceral phenotype of the NPD. No changes were appreciated in spleen sections (data not shown). Interestingly, when enzymatic activity was measured in these almost asymptomatic young animals, CtsB was already significantly increased in the lung and liver tissue from the ASMase-knock-out mice (Fig. 6*B*), even

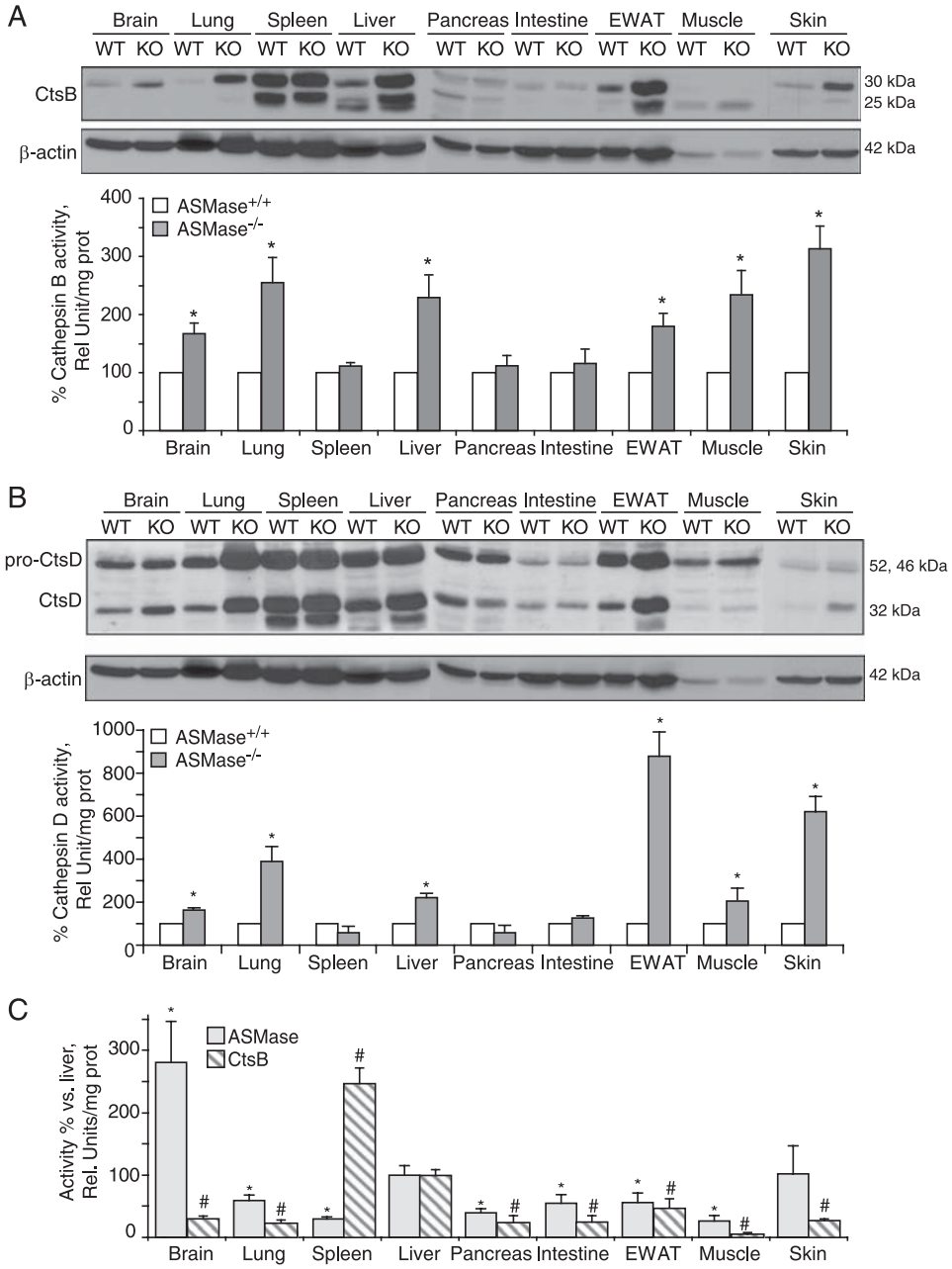

FIGURE 5. **CtsB and CtsD increase in the organs affected by the NPD phenotype.** *A* and *B*, CtsB (*A*) and CtsD (*B*) protein expression and activity in total lysates of brain, lung, spleen, liver, pancreas, intestine, EWAT, muscle, and skin of 21-week-old ASMase$^{-/-}$ and ASMase$^{+/+}$ mice. *C*, ASMase and CtsB activities in the same tissues of ASMase$^{+/+}$ mice. In *A* and *B*, data are mean ± S.D. (*error bars*), $n = 6$; *, $p \leq 0.05$ *versus* ASMase$^{+/+}$. In *C*, $n = 4$; *, $p \leq 0.05$ *versus* ASMase activity in liver; #, $p \leq 0.05$ *versus* CtsB activity in liver of ASMase$^{+/+}$ mice.

despite the weak accumulation of foam cells in these tissues, which represents an early feature of the NPD phenotype. In contrast, no changes in CtsB activity were detected in brain and spleen at this age.

Role of Other Cathepsins, Lysosomal Stability, and Autophagy—To address the potential participation of other cathepsins in the NPD phenotype, we used a pan-cathepsin antibody with specificity toward several cathepsins other than CtsB/CtsD. As seen (Fig. 7*A*) the pattern of pan-cathepsin expression between ASMase$^{+/+}$ and ASMase$^{-/-}$ HSCs was similar. Moreover, although there were different patterns of expression among tissues, there were no major differences between ASMase$^{+/+}$ and ASMase$^{-/-}$ mice (Fig. 7*B*), except the observed enhanced pan-cathepsin expression in lung from ASMase$^{-/-}$ mice. Consequently, it is feasible that the participation of other cathepsins in NPD phenotype may be tissue-specific.

Given that an increase in cathepsins in the lysosome can lead to lysosomal membrane permeabilization and subsequent release of cathepsins leading to apoptosis (24), we next analyzed whether lysosomal stability was affected and whether CtsB and CtsD were localized in the lysosomes of ASMase$^{-/-}$ HSC. As shown in Fig. 7*A*, LAMP2 expression, known to correlate with lysosomal stability (25), was increased during HSC activation in ASMase$^{-/-}$ HSCs compared with ASMase$^{+/+}$ HSCs at all time points analyzed, suggesting that in addition to increased CtsB and CtsD expression there seems to be enhanced lysosomal

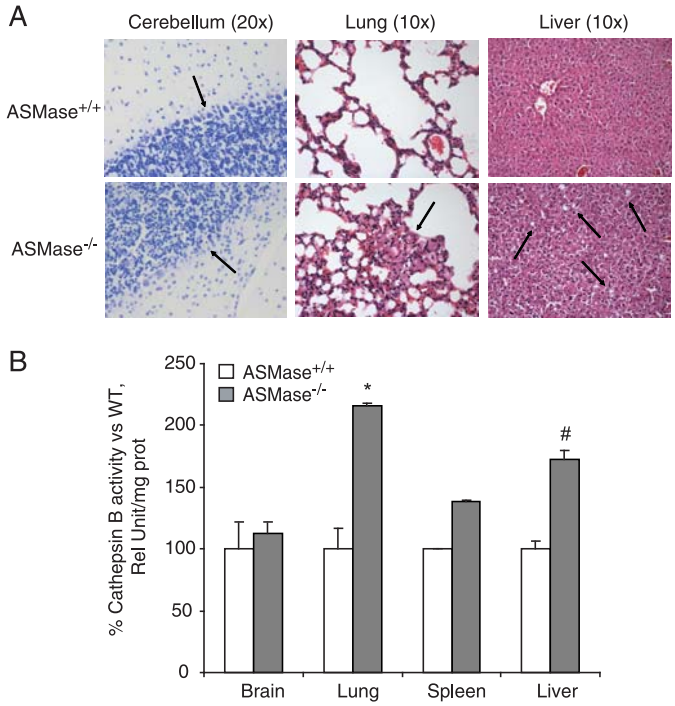

FIGURE 6. **CtsB is increased in 10–12-week-old animals with weak NPD phenotype.** *A*, Nissl staining in cerebellum histological sections and H&E staining of lung and liver sections. The *arrows* indicate the Purkinje cell population in cerebellum, population decreased in ASMase$^{-/-}$ mice, and the presence of foam cells in lung and liver in ASMase$^{-/-}$ mice. *B*, CtsB activity in total lysates of brain, lung, spleen, and liver of 10–12-week-old ASMase$^{-/-}$ and ASMase$^{+/+}$ mice. Data are mean ± S.D. (*error bars*), $n = 3$; *, $p \leq 0.01$ *versus* ASMase$^{+/+}$; #, $p \leq 0.05$ *versus* ASMase$^{+/+}$.

mass. LAMP2 expression was also enhanced in various tissues of ASMase$^{-/-}$ mice, particularly lung, liver, and spleen (Fig. 7*B*). In agreement with these findings, immunofluorescence analyses of HSCs from wild-type and ASMase-null mice indicated co-localization of both CtsB and CtsD with LAMP2, a lysosomal marker (Fig. 7*C*) and revealed increased LAMP2 staining in ASMase$^{-/-}$ HSCs compared with ASMase$^{+/+}$ HSCs. However, no increase was observed in the expression of Hsp70, a chaperone known to facilitate ASMase activity and stabilize lysosomes (26), neither in HSCs (Fig. 7*A*) nor in the different tissues analyzed (Fig. 7*B*). Thus, these findings suggest that the increased CtsB expression in ASMase$^{-/-}$ HSCs may be due to lysosomal enlargement.

Because autophagy is a catabolic process involving the degradation of cellular constituents through lysosomal digestion, we asked whether it played a role in HSC activation and tissue degeneration in NPD. To address this point, we monitored LC3 expression in the different tissues of wild-type and ASMase$^{-/-}$ mice. As shown in Fig. 7*B*, the amount of LC3-I varied among tissues but remained constant between ASMase$^{+/+}$ and ASMase$^{-/-}$ animals. There was, however, more expression of LC3-II in lung, intestine, EWAT, and skin of ASMase$^{-/-}$ mice compared with ASMase$^{+/+}$ mice. In addition, no expression of LC3-II was observed during HSC activation (Fig. 7*A*). Therefore, no direct relationship was found between CtsB or CtsD expression (Fig. 5) and LC3-I conversion to LC3-II in the NPD mouse model.

DISCUSSION

NPD is a rare lysosomal disorder caused by the loss of ASMase. Patients with NPD exhibit neurodegeneration, lung dysfunction, hepatosplenomegaly, and liver disease. Although all lysosomal storage diseases are characterized by the intralysosomal accumulation of unmetabolized substrates, acting as a primary cause of the disease, the extensive range of disease symptoms indicates that many secondary biochemical and cellular pathways can contribute to the plethora of phenotypes reported (27). Currently, there is no treatment for NPD patients, and the degree of pathology depends on the extent of ASMase loss. In the present study we extend our initial observations between ASMase and CtsB/D in HSC and liver fibrosis, which occurs in a large percentage of NPD patients (6). Heterozygous ASMase mice, which exhibit a residual 30–40% ASMase activity, are protected against *in vivo* liver fibrosis due to a decreased CtsB/D activation (17). Moreover, pharmacological ASMase inhibition (by 70–80%) decreased CtsB/D activation and the fibrogenic potential and proliferation of murine and human HSC. Quite surprisingly, we observe here that the genetic ablation of ASMase leads to a paradoxical increased basal level and activity of CtsB, which confers increased fibrogenic potential and proliferation on HSCs from ASMase-null mice leading to enhanced liver fibrosis.

Consistent with findings in death ligand-induced apoptosis (15), our previous studies disclosed a hierarchical functional relationship between ASMase and CtsB of relevance in liver fibrosis (17). Unlike the pharmacological inhibition of ASMase, which impaired CtsB/D maturation and hence HSC activation, the inhibition of CtsB did not affect ASMase activity during *in vitro* HSC activation, indicating that ASMase is required for and upstream of CtsB/D proteolytic processing and that the gradual down-regulation of ASMase, as in the heterozygous ASMase mice, results in impaired CtsB/D processing and activation. Although genetic CtsD silencing did reduce HSC proliferation and α-SMA expression in line with the effects observed with CtsB silencing, it did not affect HSC migration (10). Moreover, unlike CtsD, the expression of CtsB appears to be more restricted to activated HSC (10), suggesting that CtsB rather than CtsD may be a better target to address its role in liver fibrosis in NPD (10). Although the present findings support a critical role for CtsB in hepatic fibrosis in NPD, we cannot rule out a potential contribution of other cathepsins, including CtsD.

Due to the critical role of CtsB in liver fibrosis (10), the proportional direct relationship between the down-regulation of ASMase and CtsB dictates a low susceptibility of the ASMase$^{+/-}$ mice to liver fibrosis (17). However, unexpectedly, the loss of ASMase below a critical threshold toward the total deficiency of ASMase, as in the ASMase-knock-out mice, results in an adaptive increase in the basal levels of some cathepsins and enhanced proteolytic processing during HSC activation *in vitro* that sensitizes ASMase-null mice to *in vivo* fibrosis. The unexpected rebound relationship between the loss of ASMase and activation of CtsB may be of particular relevance to type A but not type B NPD patients, which exhibit a residual ASMase activity. Pharmacological inhibition of CtsB decreases

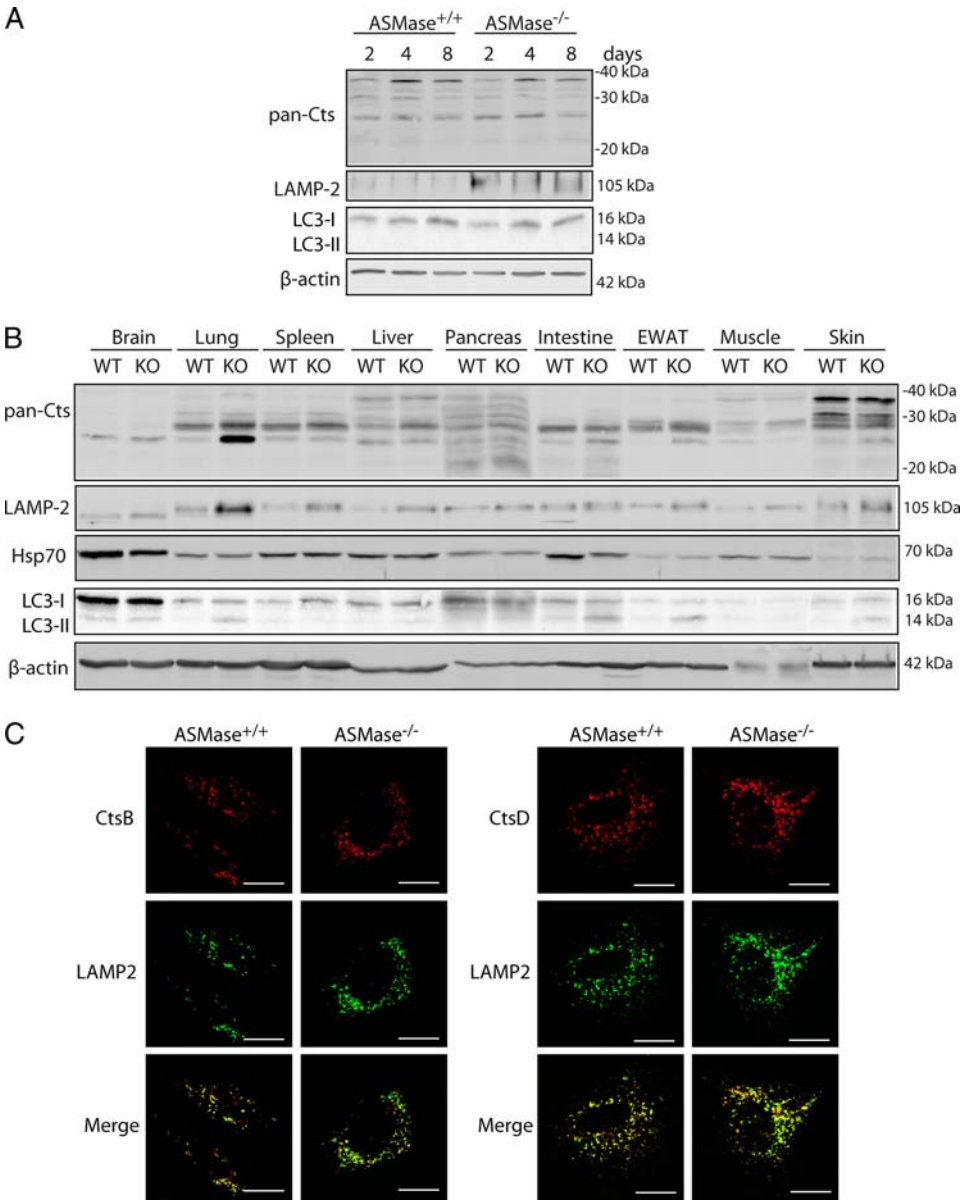

FIGURE 7. **Analysis of other cathepsins, lysosomal stability, and autophagy in the NPD mouse model.** *A*, time course of pan-cathepsin, LAMP2, and LC3 expression in ASMase$^{+/+}$ and ASMase$^{-/-}$ HSCs. *B*, pan-cathepsin, LAMP2, Hsp70, and LC3 expression in total lysates of brain, lung, spleen, liver, pancreas, intestine, EWAT, muscle, and skin of 21-weeks old ASMase$^{-/-}$ and ASMase$^{+/+}$ mice. (*C*) Confocal imaging of 7 day-old ASMase$^{+/+}$ and ASMase$^{-/-}$ HSCs displaying CtsB and CtsD co-localization with a lysosomal marker (LAMP2). *Scale bars*, 10 μm.

the *in vitro* activation of HSC from ASMase-null mice and *in vivo* liver fibrosis, thus suggesting that targeting CtsB may be a novel treatment for the underlying liver fibrosis in NPD patients.

Similar to the NPD phenotype, patients with Niemann-Pick type C1 (NPC1) disease caused by mutation in NPC1, an endosomal/lysosomal protein that regulates intracellular cholesterol trafficking, exhibit similar biochemical changes including free cholesterol, sphingolipids, and bis-(monoacylglycerol) phosphate accumulation in intracellular compartments, including lysosomes and mitochondria from affected organs including brain and liver (28, 29). Interestingly, similar to the findings presented in the current study, Amritraj *et al.* described increased CtsB/D activity in neurons from the cerebellum of NPC1$^{-/-}$ mouse brain (30). Consistent with the lack of neuronal degeneration in the hippocampus of NPC1$^{-/-}$ mouse, CtsB activation was not observed in this particular neuron population, thus establishing a correlation between increased CtsB activity and selective neurological dysfunction in NPC1 disease. Our findings indicate that CtsB and CtsD enhanced expression in the ASMase$^{-/-}$ mice are accompanied by an increase in lysosomal mass, but are probably not related to autophagy. Of note, although Hsp70 has been found to correlate not only with lysosomal stability but also to reverse NPD associated lysosomal pathology (31), we did not observe up-regulation of Hsp70 in ASMase$^{-/-}$ tissues. In line with our observations, studies in fibroblasts of NPC1 patients or after treatment of normal fibroblasts with U18666A, a drug that reproduces the NPC1 phenotype by increasing free cholesterol accumulation in lysosomes, indicate that enhanced lysosomal cholesterol

stimulates CtsD and LAMP2 expression, resulting in increased lysosomal stability and resistance to apoptosis (32). Moreover, these results were also independent of Hsp70 expression or autophagy. Of interest, secondary to ASMase deficiency there may be several associated changes in different tissues of ASMase-null mice, including sphingolipids and cholesterol (33). However, unlike these data reported in 5-month-old ASMase-null mice, our findings did not reveal any change in the hepatic cholesterol levels in 8–10-week-old ASMase-knock-out mice (data not shown), suggesting that the increase of hepatic cholesterol in the NPD mouse model may be age-related and that cholesterol plays a minor role in the increased susceptibility of ASMase-null mice to hepatic fibrosis. Moreover, the protection against liver fibrosis afforded after CtsB inhibition appears to be independent on cholesterol changes.

Our findings imply that liver fibrosis of NPD type A patients could be corrected by targeting a secondary associated enzyme, namely that the genetic cause of NPD type A liver disease due to the lack of ASMase, can be overcome by the inhibition of the adaptive increase in CtsB processing. Consistent with this concept, it has been shown that the phenotype defects observed in NPC1 disease, including free cholesterol accumulation and impaired transferring receptor recycling, could be corrected by overexpressing ASMase, whose expression is also decreased in NPC1 disease (34).

An important feature of the present study is that the up-regulation of CtsB due to the lack of ASMase is not restricted to liver, but also observed in other affected organs, such as brain and lung, in an age-dependent mechanism. Of relevance to the neurological phenotype, there seems to be a threshold for ASMase activity below which these symptoms arise. For instance, it has been shown using mutation-specific mouse models that as little as 8% ASMase activity can completely prevent the occurrence of neurological disease (35). In addition, whereas the residual ASMase activity of ~5% results in NPD type B, a further reduction to ~1–2% or less induces the severe type A phenotype (36). These observations highlight the fact that although low levels of ASMase activity are sufficient to maintain intact neurological function, the absence of this activity has devastating consequences in the brain (37).

Collectively, our results point to a new role for ASMase-CtsB axis in NPD. In addition to its known function as a proapoptotic intermediate in TNF- or Fas-induced cell death (15, 38), ASMase plays a critical role in regulating cathepsin processing and hence in modulating the diverse phenotypes of NPD, including liver disease and neurological manifestations of the disease. Thus, targeting the increase in CtsB secondary to the loss of ASMase may be of relevance to NPD, particularly for the fibrosis and liver disease phenotype of the disease.

Acknowledgment—We thank Susana Núñez for technical assistance.

REFERENCES

1. Jenkins, R. W., Canals, D., and Hannun, Y. A. (2009) Roles and regulation of secretory and lysosomal acid sphingomyelinase. *Cell. Signal.* **21,** 836–846
2. Morales, A., Lee, H., Goñi, F. M., Kolesnick, R., and Fernandez-Checa, J. C. (2007) Sphingolipids and cell death. *Apoptosis* **12,** 923–939
3. Smith, E. L., and Schuchman, E. H. (2008) The unexpected role of acid sphingomyelinase in cell death and the pathophysiology of common diseases. *FASEB J.* **22,** 3419–3431
4. Jenkins, R. W., Idkowiak-Baldys, J., Simbari, F., Canals, D., Roddy, P., Riner, C. D., Clarke, C. J., and Hannun, Y. A. (2011) A novel mechanism of lysosomal acid sphingomyelinase maturation: requirement for carboxyl-terminal proteolytic processing. *J. Biol. Chem.* **286,** 3777–3788
5. Schneider, P. B., and Kennedy, E. P. (1967) Sphingomyelinase in normal human spleens and in spleens from subjects with Niemann-Pick disease. *J. Lipid Res.* **8,** 202–209
6. Schuchman, E. H. (2010) Acid sphingomyelinase, cell membranes and human disease: lessons from Niemann-Pick disease. *FEBS Lett.* **584,** 1895–1900
7. Schuchman, E. H. (2009) The pathogenesis and treatment of acid sphingomyelinase-deficient Niemann-Pick disease. *Int. J. Clin. Pharmacol. Ther.* **47,** S48–57
8. Horinouchi, K., Erlich, S., Perl, D. P., Ferlinz, K., Bisgaier, C. L., Sandhoff, K., Desnick, R. J., Stewart, C. L., and Schuchman, E. H. (1995) Acid sphingomyelinase deficient mice: a model of types A and B Niemann-Pick disease. *Nat. Genet.* **10,** 288–293
9. Otterbach, B., and Stoffel, W. (1995) Acid sphingomyelinase-deficient mice mimic the neurovisceral form of human lysosomal storage disease (Niemann-Pick disease). *Cell* **81,** 1053–1061
10. Moles, A., Tarrats, N., Fernández-Checa, J. C., and Marí, M. (2009) Cathepsins B and D drive hepatic stellate cell proliferation and promote their fibrogenic potential. *Hepatology* **49,** 1297–1307
11. Lutgens, S. P., Cleutjens, K. B., Daemen, M. J., and Heeneman, S. (2007) Cathepsin cysteine proteases in cardiovascular disease. *FASEB J.* **21,** 3029–3041
12. Haque, A., Banik, N. L., and Ray, S. K. (2008) New insights into the roles of endolysosomal cathepsins in the pathogenesis of Alzheimer's disease: cathepsin inhibitors as potential therapeutics. *CNS Neurol. Disord. Drug Targets* **7,** 270–277
13. Vasiljeva, O., Reinheckel, T., Peters, C., Turk, D., Turk, V., and Turk, B. (2007) Emerging roles of cysteine cathepsins in disease and their potential as drug targets. *Curr. Pharm. Des.* **13,** 387–403
14. Leto, G., Tumminello, F. M., Pizzolanti, G., Montalto, G., Soresi, M., Ruggeri, I., and Gebbia, N. (1996) Cathepsin D serum mass concentrations in patients with hepatocellular carcinoma and/or liver cirrhosis. *Eur. J. Clin. Chem. Clin. Biochem.* **34,** 555–560
15. Heinrich, M., Neumeyer, J., Jakob, M., Hallas, C., Tchikov, V., Winoto-Morbach, S., Wickel, M., Schneider-Brachert, W., Trauzold, A., Hethke, A., and Schütze, S. (2004) Cathepsin D links TNF-induced acid sphingomyelinase to Bid-mediated caspase-9 and -3 activation. *Cell Death Differ.* **11,** 550–563
16. Guicciardi, M. E., Deussing, J., Miyoshi, H., Bronk, S. F., Svingen, P. A., Peters, C., Kaufmann, S. H., and Gores, G. J. (2000) Cathepsin B contributes to TNF-α-mediated hepatocyte apoptosis by promoting mitochondrial release of cytochrome *c*. *J. Clin. Invest.* **106,** 1127–1137
17. Moles, A., Tarrats, N., Morales, A., Domínguez, M., Bataller, R., Caballería, J., García-Ruiz, C., Fernández-Checa, J. C., and Marí, M. (2010) Acidic sphingomyelinase controls hepatic stellate cell activation and *in vivo* liver fibrogenesis. *Am. J. Pathol.* **177,** 1214–1224
18. Labrune, P., Bedossa, P., Huguet, P., Roset, F., Vanier, M. T., and Odievre, M. (1991) Fatal liver failure in two children with Niemann-Pick disease type B. *J. Pediatr. Gastroenterol. Nutr.* **13,** 104–109
19. Tassoni, J. P., Jr., Fawaz, K. A., and Johnston, D. E. (1991) Cirrhosis and portal hypertension in a patient with adult Niemann-Pick disease. *Gastroenterology* **100,** 567–569
20. Fotoulaki, M., Schuchman, E. H., Simonaro, C. M., Augoustides-Savvopoulou, P., Michelakakis, H., Panagopoulou, P., Varlamis, G., and Nousia-Arvanitakis, S. (2007) Acid sphingomyelinase-deficient Niemann-Pick disease: novel findings in a Greek child. *J. Inherit. Metab. Dis.* **30,** 986
21. Takahashi, T., Akiyama, K., Tomihara, M., Tokudome, T., Nishinomiya, F., Tazawa, Y., Horinouchi, K., Sakiyama, T., and Takada, G. (1997) Heterogeneity of liver disorder in type B Niemann-Pick disease. *Hum. Pathol.* **28,** 385–388
22. Marí, M., Colell, A., Morales, A., Pañeda, C., Varela-Nieto, I., García-Ruiz,

C., and Fernández-Checa, J. C. (2004) Acidic sphingomyelinase down-regulates the liver-specific methionine adenosyltransferase 1A, contributing to tumor necrosis factor-induced lethal hepatitis. *J. Clin. Invest.* **113,** 895–904
23. Jamall, I. S., Finelli, V. N., and Que Hee, S. S. (1981) A simple method to determine nanogram levels of 4-hydroxyproline in biological tissues. *Anal. Biochem.* **112,** 70–75
24. Johansson, A. C., Appelqvist, H., Nilsson, C., Kågedal, K., Roberg, K., and Ollinger, K. (2010) Regulation of apoptosis-associated lysosomal membrane permeabilization. *Apoptosis* **15,** 527–540
25. Fehrenbacher, N., Bastholm, L., Kirkegaard-Sørensen, T., Rafn, B., Bøttzauw, T., Nielsen, C., Weber, E., Shirasawa, S., Kallunki, T., and Jäättelä, M. (2008) Sensitization to the lysosomal cell death pathway by oncogene-induced down-regulation of lysosome-associated membrane proteins 1 and 2. *Cancer Res.* **68,** 6623–6633
26. Petersen, N. H., Kirkegaard, T, Olsen, O. D., and Jäättelä, M. (2010) Connecting Hsp70, sphingolipid metabolism and lysosomal stability. *Cell Cycle* **9,** 2305–2309
27. Futerman, A. H., and van Meer, G. (2004) The cell biology of lysosomal storage disorders. *Nat. Rev. Mol. Cell Biol.* **5,** 554–565
28. Marí, M., Caballero, F., Colell, A., Morales, A., Caballeria, J., Fernandez, A., Enrich, C., Fernandez-Checa, J. C., and García-Ruiz, C. (2006) Mitochondrial free cholesterol loading sensitizes to TNF- and Fas-mediated steatohepatitis. *Cell Metab.* **4,** 185–198
29. Yu, W., Gong, J. S., Ko, M., Garver, W. S., Yanagisawa, K., and Michikawa, M. (2005) Altered cholesterol metabolism in Niemann-Pick type C1 mouse brains affects mitochondrial function. *J. Biol. Chem.* **280,** 11731–11739
30. Amritraj, A., Peake, K., Kodam, A., Salio, C., Merighi, A., Vance, J. E., and Kar, S. (2009) Increased activity and altered subcellular distribution of lysosomal enzymes determine neuronal vulnerability in Niemann-Pick type C1-deficient mice. *Am. J. Pathol.* **175,** 2540–2556
31. Kirkegaard, T., Roth, A. G., Petersen, N. H., Mahalka, A. K., Olsen, O. D., Moilanen, I., Zylicz, A., Knudsen, J., Sandhoff, K., Arenz, C., Kinnunen, P. K., Nylandsted, J., and Jäättelä, M. (2010) Hsp70 stabilizes lysosomes and reverts Niemann-Pick disease-associated lysosomal pathology. *Nature* **463,** 549–553
32. Appelqvist, H., Nilsson, C., Garner, B., Brown, A. J., Kågedal, K., and Ollinger, K. (2011) Attenuation of the lysosomal death pathway by lysosomal cholesterol accumulation. *Am. J. Pathol.* **178,** 629–639
33. Prinetti, A., Prioni, S., Chiricozzi, E., Schuchman, E. H., Chigorno, V., and Sonnino, S. (2011) Secondary alterations of sphingolipid metabolism in lysosomal storage diseases. *Neurochem. Res.* **36,** 1654–1668
34. Devlin, C., Pipalia, N. H., Liao, X., Schuchman, E. H., Maxfield, F. R., and Tabas, I. (2010) Improvement in lipid and protein trafficking in Niemann-Pick C1 cells by correction of a secondary enzyme defect. *Traffic* **11,** 601–615
35. Jones, I., He, X., Katouzian, F., Darroch, P. I., and Schuchman, E. H. (2008) Characterization of common SMPD1 mutations causing types A and B Niemann-Pick disease and generation of mutation-specific mouse models. *Mol. Genet. Metab.* **95,** 152–162
36. Graber, D., Salvayre, R., and Levade, T. (1994) Accurate differentiation of neuronopathic and nonneuronopathic forms of Niemann-Pick disease by evaluation of the effective residual lysosomal sphingomyelinase activity in intact cells. *J. Neurochem.* **63,** 1060–1068
37. Ledesma, M. D., Prinetti, A., Sonnino, S., and Schuchman, E. H. (2011) Brain pathology in Niemann-Pick disease type A: insights from the acid sphingomyelinase knockout mice. *J. Neurochem.* **116,** 779–788
38. García-Ruiz, C., Colell, A., Marí, M., Morales, A., Calvo, M., Enrich, C., and Fernández-Checa, J. C. (2003) Defective TNF-α-mediated hepatocellular apoptosis and liver damage in acidic sphingomyelinase knockout mice. *J. Clin. Invest.* **111,** 197–208